LA-6083-T
Thesis

UC-4
Reporting Date: September 1975
Issued: October 1975

Oxygen Potential of Uranium-Plutonium Oxide as Determined by Controlled-Atmosphere Thermogravimetry

by

Gerald C. Swanson*

*Hanford Engineering Development Laboratory, Richland, WA 99352

los alamos
scientific laboratory
of the University of California
LOS ALAMOS, NEW MEXICO 87545

An Affirmative Action/Equal Opportunity Employer

UNITED STATES
ENERGY RESEARCH AND DEVELOPMENT ADMINISTRATION
CONTRACT W-7405-ENG. 36

This report is derived from a dissertation submitted to the Graduate School, University of New Mexico, Albuquerque, NM, in partial fulfillment of the requirements for the Degree of Doctor of Philosophy in Chemistry.

This report represents the independent work of the author and has not been edited by the Technical Information staff.

The work was supported by the Reactor Research and Development Division, US Energy Research and Development Administration.

Printed in the United States of America. Available from
National Technical Information Service
U.S. Department of Commerce
5285 Port Royal Road
Springfield, VA 22151
Price: Printed Copy $5.45 Microfiche $2.25

TABLE OF CONTENTS

LIST OF FIGURES

LIST OF FIGURES-cont.

LIST OF TABLES

OXYGEN POTENTIAL OF URANIUM-PLUTONIUM DIOXIDE AS DETERMINED BY CONTROLLED-ATMOSPHERE THERMOGRAVIMETRY*

Gerald C. Swanson

ABSTRACT

The oxygen-to-metal atom ratio, or O/M, of solid solution uranium-plutonium oxide reactor fuel is a measure of the concentration of crystal defects in the oxide which affect many fuel properties, particularly, fuel oxygen potential. Measurement of the oxygen potential of solid solution uranium-plutonium oxide, O/M reference material at O/M ratios near 2.000 provides baseline O/M values for thermogravimetric and gas equilibration methods of O/M analysis.

The oxygen potential of the atmosphere within a modified commercial thermobalance has been controlled by the ratio of H_2O and H_2 added to a He carrier gas. The balance modifications include enclosure of the sample chamber within a glovebox for handling plutonium, redirection of gas flow to ensure sample equilibration, and digital recording of data on paper tape for off-line computer analysis. The H_2O is added to the He as H_2 and O_2 recombined at a Pt catalyst following production by H_2O electrolysis and drying by a liquid nitrogen trap. Hydrogen is metered into the He either as pure H_2 or as He-H_2 premixed gas. Fabrication of a high-temperature oxygen electrode, employing an electro-active tip of oxygen-deficient solid-state electrolyte, intended to confirm gaseous oxygen

potentials is described.

Uranium oxide and plutonium oxide O/M reference materials were prepared by in situ oxidation of high purity metals in the thermobalance. A solid solution uranium-plutonium oxide O/M reference material was prepared by alloying the uranium and plutonium metals in a yttrium oxide crucible at 1200°C and oxidizing with moist He at 250°C. The individual and solid solution oxides were isothermally equilibrated with controlled oxygen potentials between 800°C and 1300°C and the equilibrated O/M ratios calculated with corrections for impurities and buoyancy effects.

Oxygen potential-O/M relationships measured for the individual oxides compare well with literature values. The relationships measured for the solid solution oxide were biased due to weight gain of the yttrium oxide. When corrected, the oxygen potential change occured at the expected O/M= 2.000. The solid solution shows a much larger oxygen potential change at O/M=2.000 than calculated for the sum of the uranium and plutonium oxide relationships. The defect structure of the hypostoichiometric solid solution oxide appears to be fully ionized oxygen vacancies for the O/M range 1.994 to 2.000. The high-temperature oxygen electrode produced a stable, but non-theoretical, EMF when exposed to controlled oxygen potentials, but the data was not applied to the O/M equilibration studies.

Use of a reference oxygen potential of -100 kcal/mol to produce an O/M of 2.000 is confirmed by these results. However, because of the lengthy equilibration times required for all oxides, use of the O/M reference materials rather than a reference oxygen potential is recommended for O/M analysis methods calibrations.

INTRODUCTION

The United States is rapidly depleting its fossil fuel and recoverable fissionable uranium resources. To utilize the energy potentially available in the fertile isotopes ^{232}Th and ^{238}U and reserve fossil fuel resources as a supply of feedstock chemicals, the Energy Research and Development Administration's (Erda's) development of breeder reactors is being accelerated. Breeder reactors use the neutrons produced by fission to convert fertile isotopes to fissionable isotopes. Fertile isotopes comprise the majority of recoverable actinide resources, and because breeder reactors produce more fissionable fuel than they "burn", such fertile isotopes represent an extensive energy supply.

The two major breeder cycles are ^{232}Th - ^{233}U and ^{238}U - ^{239}Pu cycles. Breeder reactors utilizing fertile ^{232}Th and fissionable ^{233}U include the High Temperature Gas-cooled Reactor (HTGR) and the Molten Salt Breeder Reactor (MSBR). The principle reactor utilizing the ^{238}U - ^{239}Pu breeding cycle is the Liquid Metal cooled Fast Breeder Reactor (LMFBR), which utilizes a mixed uranium-plutonium oxide fuel.

Breeder reactors use extremely energetic neutron fluxes to convert fertile to fissionable isotopes. The high temperatures associated with such energetic fluxes require high-melting, stable fuels for the reactor core. Uranium-plutonium oxide has been chosen as the prime candidate fuel for the LMFBR because it is a high-melting ceramic material and a large body of knowledge exists about its ceramic properties.

An important characteristic of uranium-plutonium oxide is the extensive defect structure which readily occurs within its crystal lattice. A measure of the defect concentration is the deviation of the oxide stoichiometry or oxygen-to-metal atom ratio (O/M) from 2.000. For the mixed uranium-plutonium oxide fuel of the LMFBR, the O/M ratio can vary widely around the nominal value.[1] The O/M is of concern because the defect structure which it measures affects many important fuel operating parameters including thermal conductivity,[2] melting point,[3] heat rating,[4] migration of fission products, and cladding-fuel interactions.[5] The oxygen partial pressure (Po_2)

and oxygen potential ($\Delta\overline{G}_{O_2}$) of the fuel both measure the oxidizing character of the fuel and are both directly related to the defect concentration, temperature, and to a lesser extent impurity content of the fuel. Correlation of O/M and oxygen potential allows theoretical interpretation of the fuel defect structures.

Analytical methods developed to determine either O/M or oxygen potential of uranium-plutonium oxide are usually correlated by measurements on standard materials or through use of standard conditions. Development of O/M and oxygen potential measurements and standards for UO_2, PuO_2, and $(U,Pu)O_2$ are briefly surveyed.

Measurement of O/M and Oxygen Potential of Uranium Oxide

Uranium oxide displays several stable phases between UO_2 and U_3O_8, and a hypo-stoichiometric UO_{2-x} phase ($x \leq 0.3$) stable at temperatures over 1200°C.[6] Each phase is capable of significant departure from nominal stoichiometry without phase change. Essentially every procedure for determination of O/M in uranium oxide is based upon some measurement of the extent of departure of the oxide from either UO_2 or U_3O_8.

Florence[7] has provided an excellent review of the methods of determining O/M and $\Delta\overline{G}_{O_2}$ of uranium oxide, classifying the methods generally as wet chemical or dry methods. The wet chemical methods generally involve measurement of excess U(VI) in the U(IV) matrix by use of polarography,[8] controlled potential coulometry,[9] or titrimetric methods[10] following dissolution in a non-oxidizing acid. In principle such methods are absolute as the U(VI) measured is a direct measure of the oxygen in excess of UO_2. However, extreme caution must be used to prevent air oxidation of the sample either before or after dissolution. The wet chemical methods do not require an O/M standard although appropriate uranium standards are employed to assure the accuracy of the U measurements.

Dry measurements include thermogravimetric, gas equilibration, electrochemical, and metallurgical techniques. In the thermogravimetric techniques the uranium oxide is oxidized or reduced to a known O/M, and the weight change between initial and final states is used to

calculate O/M. The classical thermogravimetric determination of O/M for uranium oxide is ignition to U_3O_8.[11-16] However, the product of ignition shows variable O/M influenced by factors such as history of the oxide[11] and moisture levels.[12] Brouns and Mills showed that even pure metal used as a starting material attained an O/M of 2.667 with a reproducibility of only ±0.005 on ignition in air at 1000°C.[13] O/M has also been determined by reduction of a hyperstoichiometric oxide to $UO_{2.00}$ and either gravimetrically measuring the weight change of the oxide[17,18] or gravimetrically or gasometrically measuring the H_2O [19] or CO_2 [19-22] evolved in the reduction. The reducing agents used are H_2,[17-19] CO,[17,19,20,22] or C[21] at temperatures from 800°C to 1000°C. Each of these different sets of reductants and temperatures is claimed to reduce the O/M to 2.00 exactly.

Other methods used to determine O/M are direct measurement of the oxygen content of the oxide by inert gas fusion[23,24] or reaction with BrF_3 to liberate the oxygen.[25] Both methods suffer from insufficient precision for use in accurate O/M determinations.

Several studies of the oxygen potential of uranium oxide using high-temperature electrochemical cells have been reported.[26-32] These cells employ a solid-state electrolyte responsive to oxygen partial pressure or oxygen potential of the oxide in contact with the electrolyte. The studies attempt to relate the oxygen potential of the uranium oxide to the O/M as a function of temperature. In one study,[29] uranium oxides with large departures from stoichiometry were prepared by mixing and annealing "stoichiometric" UO_2 and U_3O_8, without analytical verification of starting material stoichiometry. In several studies[26,27,30,32] the O/M is referred to nominal UO_2 prepared by CO or H_2 reduction at 800 to 850°C. In only one study[28] is the O/M referred to a wet chemical determination of the stoichiometry.

Several other methods suggested for determination of O/M of uranium oxide are spectrophotometry of the solid uranium oxide,[33,34] magnetic susceptability measurements,[35] electrical conductivity measurements,[36] and neutron diffraction studies.[37]

Several studies of the oxygen potential of uranium oxide have been made using gas equilibration techniques with concurrent or subsequent determination of equilibrated O/M values.[38-43]

Similar studies have also been made using X-ray crystallographic, metallographic, and mass spectrometric methods to determine the oxide phase composition.[44,45]

Many studies of the O/M or oxygen potential of uranium oxide have used as a reference point the composition of the oxide in equilibrium with a 10:1 CO/CO_2 gas mixture at 800 to 850°C.[17,19,20,22,26,27,30,38,39,42,43] The basic assumption is that these conditions have been shown to produce an O/M of exactly 2.000. Drummond and Sinclair[17] stated the circumstances which led to use of a 10:1 CO/CO_2 gas mixture as a reference condition, "workers...proposed the establishment of a reference point close to the stoichiometric composition by reduction...under defined conditions of temperature and atmosphere. Reduction...in a CO/CO_2 mixture at 800°C was suggested. All oxygen-to-metal ratios calculated from this reference point would have the correct relative order and be close to the absolute value." Drummond and Sinclair found, however, that reduction in H_2 at temperatures as high as 1150 °C was necessary to produce $UO_{2.000}$ from hyperstoichiometric uranium dioxide prepared from high purity U metal. The O/M of uranium oxide equilibrated with 10:1 CO/CO_2 at 800 to 850°C (an oxygen potential of -100 kcal/mol) has not been established.

Measurement of O/M and Oxygen Potential of Plutonium Oxide

Plutonium dioxide is single phase over the O/M range 1.61 to 2.00 above 600°C.[46] For the analysis of O/M of hypostoichiometric PuO_2 the classical procedure is ignition to PuO_2 at 1050 to 1100°C in air.[47] Despite an extensive study of ignition of various plutonium compounds which showed that ignition in air at 1250°C frequently produced hyperstoichiometric oxides,[48] one laboratory persists with ignition in air at 850°C.[49]

Several methods developed for analysis of O/M in UO_2 or $(U,Pu)O_2$ have been adopted for PuO_2.[18,20,24,50,51] The methods involve oxidation in air and reduction at 1000°C in H_2,[18] direct equilibration with a H_2O/H_2 atmosphere at 850°C,[50] direct measurement of the oxygen content of the oxide,[24,51] and oxidation of the oxide with a controlled excess of O_2 with calculation of O/M from the CO_2 produced by a subsequent CO reduction.[20]

Oxygen potential of plutonium dioxide has been measured by solid-state electrochemical cells[52-54] and gas tensimetric and mass spectrometric techniques.[55-58] In these measurements the O/M's were referred either to equilibration in 10:1 CO/CO_2[20,52-55] or to an oxidation to a nominal O/M of 2.00 in air.[55,56,58] The O/M produced by either reference state is not well defined.

Measurement of O/M and Oxygen Potential of Solid Solution Uranium-Plutonium Oxides

The solid solution of uranium-plutonium oxide, abbreviated MO_2, displays an O/M ranging from extremely hypo- to extremely hyperstoichiometric, depending on the percent plutonium in the oxide. Measurements of O/M or $\Delta\overline{G}_{O_2}$ for MO_2 are referred to conditions believed to produce stoichiometric dioxide. Methods of O/M measurement in MO_2 have been reviewed by Lyon,[59] Dahlby et.al.,[18] McGowan et.al.,[60] and Gurumurthy.[61] Only one wet chemical method has been proposed to determine O/M in MO_2.[62] In this method, the sample is partially dissolved in non-oxidizing H_3PO_4 and the U(VI), total U, Pu(IV), and total Pu are determined by controlled potential coulometry. The O/M is calculated from the average valence departure from +4. The method is extremely sensitive to air oxidation, and since only partial dissolution of the sample is achieved only true solid-solution samples may be analyzed. A gravimetric study of air oxidation of MO_2 to a mixture of U_3O_8 and PuO_2 has been reported.[63] Oxidation at 750°C produced a product of varying composition unless Pu content was <10%.

Many thermogravimetric procedures have been developed to determine O/M of MO_2, all using conditions claimed to produce a stoichiometric dioxide.[17,18,20,22,49,50,59,64-68] The gas compositions and temperatures claimed to produce $MO_{2.000}$ include: 10:1 CO/CO_2 at 800 to 900°C;[20,22,49] controlled H_2/H_2O at 800°C;[50] reduction in H_2 at 800°C,[59,65] 850°C,[67] 900°C,[68] 1000°C,[18] 1150°C,[17] and 1200°C;[66] and reduction in CO at 800°C.[65] Drummond and Sinclair,[17] Dahlby et.al.,[18] McNiely and Chikalla,[50] and Metz et.al.[64] used mixtures of UO_2 and PuO_2 prepared from the respective metals as references. Maurice and Bujis[49] referred their studies to uranium oxide for which O/M was determined chemically, and plutonium oxide for which O/M was determined by air oxidation. MacDougall et.al.[34] reported the determination of O/M in MO_2 by carbon reduction of the oxide and titrimetric determination of uranium and plutonium.

Several studies of the oxygen potential of MO_2 as a function of O/M and temperature have been reported.[52,69-72] Oxygen responsive, solid-state electrochemical cells,[52,71] gas equilibration techniques,[69,70] and an electron microprobe technique[72] have been used to determine oxygen potential. Two reviews of the $\Delta\bar{G}o_2$ data are also available,[46,74] as well as discussions of the effects of the oxygen potential on reactor fuel characteristics.[52,73] With the exception of a thermodynamic phase-structure study referred to metallographic data,[59] all studies of $\Delta\bar{G}o_2$ versus O/M are referred to an assumed O/M of 2.000. Conditions used to produce the reference O/M include: equilibration with 10:1 CO/CO_2 at 800°C[52] and at 850°C[70,71] and equilibration to an H_2/H_2O gas ratio setting $\Delta\bar{G}o_2$ to −100 kcal/mol at 800°C.[69] The electron microprobe study by Johnson et.al.[72] measured the fission product molybdenum in a MO_2 fuel pellet following irradiation, and calculated $\Delta\bar{G}o_2$ from the ratio of Mo as metallic inclusions to Mo oxides in the matrix. The calculated oxygen potential gradient is extremely dependent on the temperature profile assumed for the pellet cross section.

Two continuing studies of the thermodynamics of mixed oxide fuels and the thermodynamic effects on reactor fuel properties are being performed at the Argonne National Laboratory[75] and the Vallecitos Nuclear Center of the General Electric Company.[76]

In an effort to clarify the differences in the product O/M produced by three different thermogravimetric methods, Urie et.al.[77] comparatively studied the three methods. They include: oxidation in air at 1000°C, reduction in He-6% H_2 at 1000°C for six hours; equilibration with a −100 kcal/mol oxygen potential atmosphere at 800°C; and oxidation in air at 750°C, reduction in He-6% H_2 to constant weight at 750°C. When the three methods were simultaneously applied to a large batch of sintered mixed oxide pellets, the O/M's determined for the pellets by the three methods agreed to within a difference in O/M of ±0.003. Dahlby et.al.[18] found, however, that application of the three conditions to blended UO_2 and PuO_2 powders gave differences in product O/M's of ±0.016. These results suggest that the only presently available standard for MO_2, a mixture of UO_2 and PuO_2 prepared from the respective highly pure metals, reacts differently in O/M determinations than solid-solution mixed oxide.

Summary

Although the relation of oxygen potential to O/M has been extensively studied for UO_2, PuO_2, and MO_2; none of these studies has definitively determined the oxygen potential of these oxides at a measured O/M of 2.000. The validity of use of mixed UO_2 and PuO_2 as a standard for solid solution mixed oxide has also not been shown. The purpose of this research is to prepare a solid solution MO_2 standard for O/M determinations, to determine the oxygen potential at O/M = 2.000 for UO_2, PuO_2, and MO_2; and provide baseline data for interpretation of previous studies.

A commercial themobalance has been modified to allow use of plutonium, a gas manifold has been constructed to precisely control gaseous oxygen potentials within the thermobalance, a solid-state oxygen electrode has been designed to measure gaseous oxygen potentials in the thermobalance, and UO_2, PuO_2, and MO_2 O/M standards have been prepared from highly pure U and Pu metals. The oxygen potentials of the three oxides at and near stoichiometry have been correlated to the conditions in reported O/M determination methods to define the respective oxide product stoichiometries.

THEORETICAL

Thermodynamics of Chemical Reactions

The free energy of a system, G, is given by the equation: G= H-TS; where G is the Gibb's free energy H is the enthalpy, S the entropy, and T the absolute temperature of the system. Since the change in free energy, or ΔG, is the measure of the driving force for a chemical reaction, a system at equilibrium has $\Delta G=0$.

The partial molar free energy of a constituent of a system is a measure of the energy change of the system when one mole of the constituent is added to such a large quantity of the system that the composition, temperature, and pressure of the system remain unchanged. For the "i"th component of a system, the partial molar free energy is $(\partial G/\partial n_i)_{T,P,n} = \bar{G}n_i$. The partial molar free energy is the same as the chemical potential, μ_i.

The free energy of an ideal system composed of n components is a function of the chemical potential and mole fraction, n_i, of each component:

$$G = \mu_1 n_1 + \mu_2 n_2 + \mu_3 n_3 + \cdots + \mu_i n_i . \qquad (1)$$

For an open system at constant temperature and pressure the free energy change of the system, dG, is given by:

$$dG = \mu_1 dn_1 + \mu_2 dn_2 + \mu_3 dn_3 + \cdots + \mu_i dn_i . \qquad (2)$$

and at equilibrium

$$dG = 0 = \Sigma \mu_i dn_i . \qquad (3)$$

this latter relation can be shown to be equivalent to

$$dG = 0 = \Sigma d\mu_i n_i \qquad (4)$$

which is another form of the Gibbs-Duhem relationship.

In a chemical reaction:

$$aA + bB \rightleftharpoons cC + dD \tag{5}$$

the free energy change is given by the difference between the total free energy of the final state and the total free energy of the initial state,

$$dG = (c\mu_C + d\mu_D) - (a\mu_A + b\mu_B) . \tag{6}$$

The chemical potential, μ_i, of the "i"th constituent of a mixture is given by,

$$\mu_i = \mu_i^\circ + RT \ln a_i \tag{7}$$

where μ_i° is the chemical potential at a chosen standard state of unit activity and a_i is the activity of the "i"th component in the mixture. For reaction (5) at equilibrium

$$dG = (c\mu_C^\circ + d\mu_D^\circ) - (a\mu_A^\circ + b\mu_B^\circ) + RT \ln [(a_C)^c(a_D)^d/(a_A)^a(a_B)^b] \tag{8}$$

let,

$$\Delta G^\circ = (c\mu_C^\circ + d\mu_D^\circ) - (a\mu_A^\circ + b\mu_B^\circ) \tag{9}$$

and recognize at equilibrium the activities of A, B, C, and D are constant.

therefore:

$$K = [(a_C)^c(a_D)^d/(a_A)^a(a_B)^b] . \tag{10}$$

Since the reaction is at equilibrium dG = 0, and

$$dG = \Delta G^\circ + RT \ln K . \tag{11}$$

$$\Delta G^\circ = -RT \ln K . \tag{12}$$

Oxide Defect Structures

The nonstoichiometry of UO_2, PuO_2, and $(U,Pu)O_2$ are indicative of defect structures within nominally perfect crystal structures. The treatment of such defects used by Kofstad[46] using the notation of Kroger and Vink[79] will be considered.

The perfect MO_2 crystal (M= U, Pu, or solid-solution U+Pu) contains metal ions and oxide ions occupying normal metal and oxygen sites within the crystal. A metal ion occupying a normal metal site is indicated by M_M, where M is the symbol for the ion or defect and the subscript represents the site within the crystal lattice. Thus, an oxide ion occupying a normal oxygen site is designated by O_O. Valence charges of the ions are designated by symbols denoting departure from the valence charge within the perfect crystal. A valence defect which is negative compared to the perfect crystal is denoted by a "prime"('), a defect positive compared to the perfect crystal is denoted by a "dot" (·), and non-departure from the perfect crystal charge is denoted by a superscript "x" (^{x}). A metal ion on a metal site, which is negative compared to the normal site charge, is denoted M_M', an example would be a Pu^{+3} ion on a normal Pu^{+4} site in PuO_{2-x}. Similarly, a U^{+6} ion on a normal U^{+4}site would be designated $M_M^{\cdot\cdot}$. In addition to normal sites and ions there are vacancies which can occur on a normal site (V) and there are interstitial sites (i). A non-exhaustive list of defects which can appear in an MO_2 crystal, ignoring impurities and valence defects, include: M_M, a metal ion on a metal site; O_O, an oxide ion on an oxygen site; V_M a vacancy at a metal site; M_i, a metal ion on an interstitial site; V_O, a vacancy at an oxygen site; and O_i, an interstitial oxide ion. Besides the electron (valence) defects which occur at crystal defects, intrinsic defects occur by ionization of valence electrons to the conduction band leaving an electron hole in the valence band and denoted respectively by n and p.

In oxidation of UO_2 to UO_{2+x}, it is generally agreed that the predominating resultant defect is interstitial oxygen ions (O_i'').[38,46] The relationship of oxygen interstitials to P_{O_2}, the oxygen partial pressure, may be derived from mass action considerations as follows.

$$M_M + O_O + 1/2\ O_2 \leftrightarrows M_M + O_O + O_i^X \tag{13}$$

$$O_i^X \leftrightarrows O_i^{\cdot} + p \tag{14}$$

$$O_i^{\cdot} \leftrightarrows O_i^{\cdot\cdot} + p \tag{15}$$

The mass action relations for equations (13) to (15) are written as follows:

$$K_1 = [M_M][O_O][O_i^X]/[M_M][O_O]\ Po_2^{1/2} = [O_i^X]/Po_2^{1/2} \tag{13a}$$

$$K_a = [O_i^{\cdot}][p]/[O_i] \tag{14a}$$

$$K_b = [O_i^{\cdot\cdot}][p]/[O_i^{\cdot}] \tag{15a}$$

Assuming electroneutrality, that $|O_i''| \gg |O_i'|$, and therefore, $2|O_i''| = |p|$. Equations (13a), (14a), (15a), and the latter relationship lead to:

$$[O_i^{\cdot\cdot}] = (K_b K_a K_1/4)^{1/3}\ Po_2^{1/6} \tag{16}$$

Thus the concentration of fully ionized oxygen interstitials, O_i'', is proportional to $Po_2^{1/6}$ if O_i'' is the predominant defect in UO_{2+x}. A plot of log x for UO_{2+x} versus log Po_2 should have a slope of +1/6 in the region where fully ionized oxygen interstitials predominate. Similar sets of equations can be solved for all other crystal defects if each is independently assumed to predominate, and relations to Po_2 developed for each. Tallan et.al.[79] have performed computer solutions of equations similar to the above taking into account all possible crystal defects and also the effect of one major impurity. When relationships of the MO_2 defect concentrations to Po_2 have been determined, reference to the table will provide the neutrality relation of the predominating defect. Analysis of the possible neutrality conditions (several may have the same Po_2 dependence), and knowledge of other crystal behaviour will allow prediction of the predominant crystal defect structure.

Kofstad has also considered the case of an MO_2 which predominantly has oxygen interstitials at high oxygen pressures and oxygen vacancies at low oxygen pressures. Two conditions are considered at stoichiometry: intrinsic ionization predominates or internal disorder predominates. The relationships developed for x in $MO_{2\pm x}$ are:

$$[V_O^{\bullet\bullet}]\ n^2\ Po_2^{1/2} = K_v \tag{17a}$$

$$[O_i^{''}]\ p^2\ Po_2^{-1/2} = K_i \tag{17b}$$

$$n\ p = K_b \tag{18a}$$

$$[O_i^{''}]\ [V_O^{\bullet\bullet}] = K_f \tag{18b}$$

For large oxygen deficit or excess, the relationships are respectively,

$$[V_O^{\bullet\bullet}] = -x = (K_v/4)^{-1/3}\ Po_2^{-1/6} \tag{19}$$

$$[O_i^{''}] = +x = (K_i/4)^{1/3}\ Po_2^{1/6} \tag{20}$$

At stoichiometry, with intrinsic ionization predominating, p = n, and both are independent of Po_2 and

$$[V_O^{\bullet\bullet}] = -x = (K_v/K_b)\ Po_2^{-1/2} \tag{21}$$

$$[O_i^{''}] = +x = (K_i/K_b)\ Po_2^{1/2} \tag{22}$$

At stoichiometry, with internal disorder predominating, $[V_O^{\bullet\bullet}] = [O_i^{''}]$ and both are independent of Po_2, $n \propto Po_2^{-1/4}$ and $p \propto Po_2^{+1/4}$ respectively.

The two possible extreme results for these two cases are presented schematically in Figs. 1 and 2, which are plots of log x versus log Po_2. For predominant intrinsic ionization (Fig 1), the stoichiometric composition is seen to be at the midpoint of a curve proportional to $Po_2^{1/2}$. For predominant internal disorder (Fig 2), the stoichiometric composition occurs at the midpoint of a curve independent of Po_2. For measuring O/M as a function of Po_2 this latter case is more desireable, for in this case a very sharp change in the Po_2 will occur at stoichiometry.

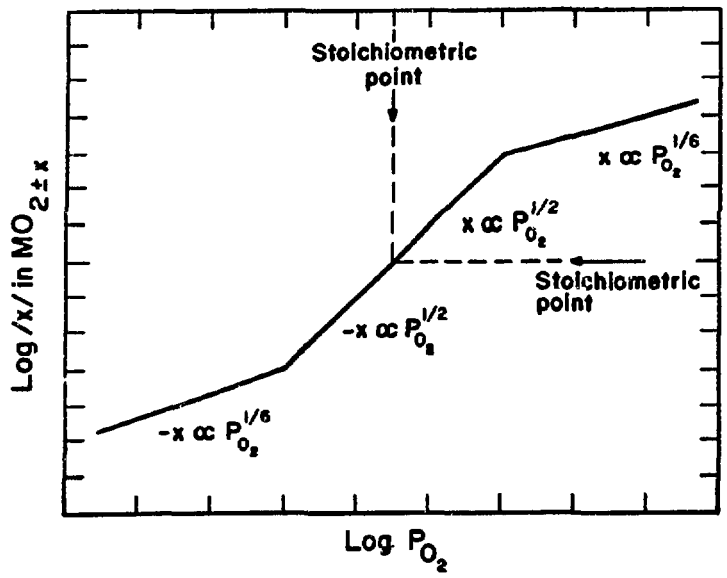

Figure 1.
Effect of predominant intrinsic ionization on oxide defect concentration.

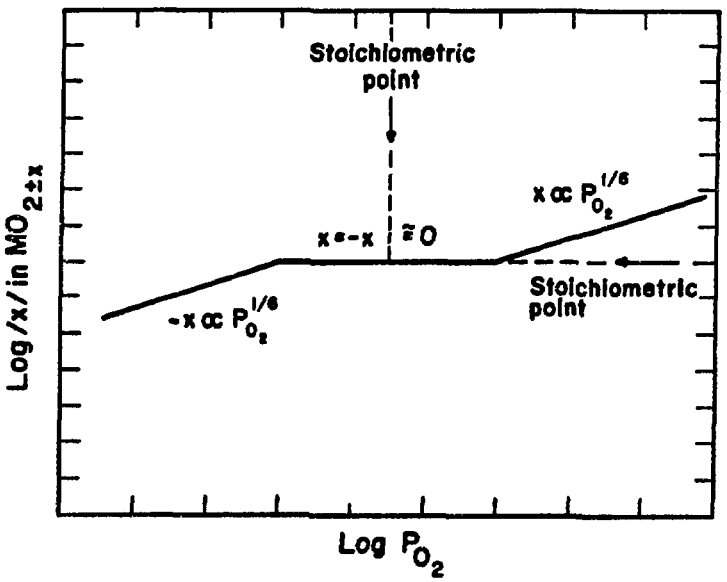

Figure 2.
Effect of predominant internal disorder on oxide defect concentration.

Solid-State Oxygen Electrochemical Cells

When doped with lower valence oxides, some high temperature oxides develop extensive oxygen ion defects within their crystal structures. Zirconium oxide stabilized with calcium oxide and thorium oxide doped with yttrium oxide are two such "oxygen-defective" oxides. The large concentration of oxygen vacancies in either oxide allows ionic conduction through the oxide lattice by jumping of oxide ions from vacancy to vacancy. A tube of such an oxide exposed to different oxygen partial pressures on the exterior and the interior surfaces develops an oxygen ion gradient through the lattice as each surface equilibrates to the oxygen potential it experiences. The $\mathcal{EMF}$ developed by the oxygen gradient is a measure of the difference between the oxygen potentials at the two surfaces, viz:

$$E = [(\Delta\bar{G}o_2' - \Delta\bar{G}o_2^\circ) - (\Delta\bar{G}o_2'' - \Delta\bar{G}o_2^\circ)]/4F \ , \qquad (23)$$

E is the measured $\mathcal{EMF}$ between cell interior and exterior, $\Delta\bar{G}o_2'$ and $\Delta\bar{G}o_2''$ are respectively the partial molar free energies of oxygen at the tube interior and exterior, and $\Delta\bar{G}o_2^\circ$ is the standard molar free energy of oxygen. Because, $\Delta\bar{G}o_2' = RT\ ln\ Po_2'$ and $\Delta\bar{G}o_2'' = RT\ ln\ Po_2''$, the $\mathcal{EMF}$ also relates the oxygen pressure between interior and exterior,

$$E = (RT/4F)\ ln\ (Po_2'/Po_2'') \ . \qquad (24)$$

Use of a reference with a known oxygen pressure at one side of the cell, allows determination of the Po_2 of a gas or solid at the other cell surface. Such cells constitute the oxygen responsive electrodes used to measure $\Delta\bar{G}o_2$ for UO_2, PuO_2, and $(U,Pu)O_2$ discussed in the introduction.

The preceeding relation of cell E to $\Delta\bar{G}o_2$ and Po_2 assumes that the sole electrolyte transporting charge was oxygen ions. In all cases, however, electrons and holes in the crystal are available to transport charge also. If the charge transported by either electrons or holes becomes significant the cell $\mathcal{EMF}$ is partially short circuited. Patterson[81] and Hardaway et.al.[82] have determined the electrolytic conduction regions for the two electrolyte systems CaO-ZrO_2, (CSZ), and Y_2O_3-ThO_2, (YDT). These regions are defined as those conditions of T and Po_2 for which the ionic transport

number, $t_{ion} \geq 99\%$. Use of either electrolyte outside the electrolytic domains shown in Fig 3, will cause a non-Nernstian $\mathcal{E}$ to develop due to the electronic or hole conduction. As shown in Fig 3 the YDT electrolyte is usable at higher temperatures and lower oxygen potentials than the CSZ electrolyte. Unfortunately, YDT is not usable with an air oxygen reference while CSZ is.

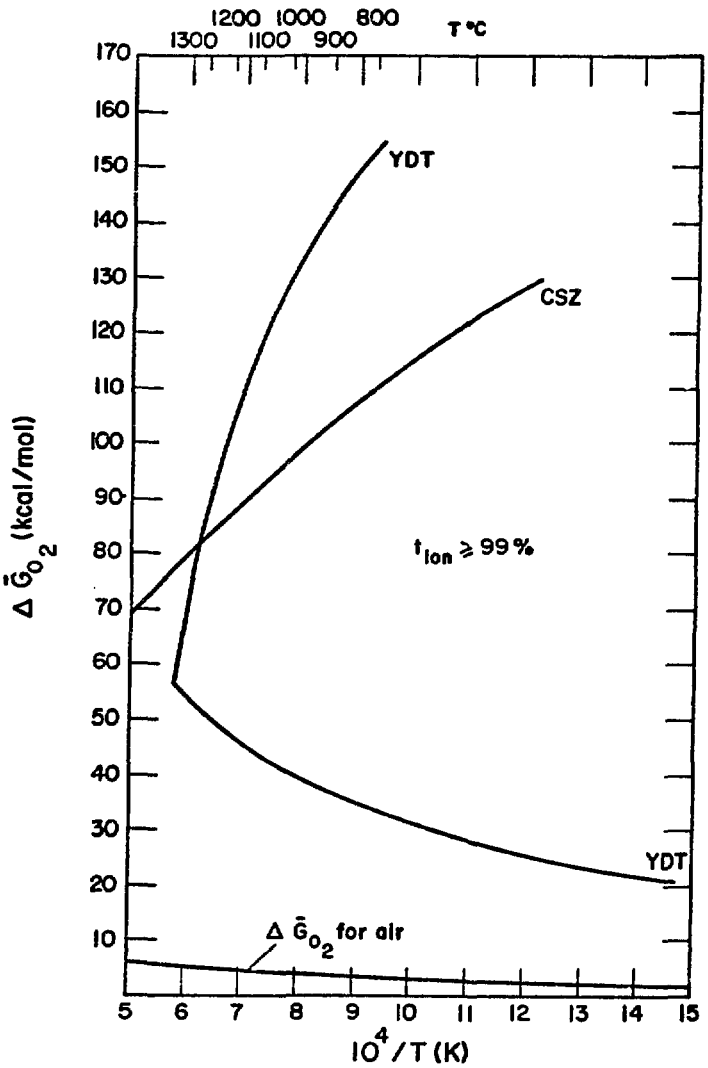

Figure 3.
Electrolytic conduction domains for YDT and CSZ.

Control of Gaseous Oxygen Potential

Experimentally the gaseous oxygen potential is determined by the ratio of water vapor to hydrogen gas. For the reaction:

$$H_2 + 1/2\ O_2 \leftrightarrows H_2O \tag{25}$$

an equilibrium constant may be determined,

$$K = (P_{H_2O})/(P_{H_2})(P_{O_2})^{1/2} \tag{26}$$

Solving for Po_2:

$$Po_2 = (P_{H_2O})^2/(P_{H_2})^2K^2 \tag{27}$$

Because K is a function only of temperature, the oxygen pressure is uniquely determined at constant temperature by the ratio H_2O/H_2. The equilibrium constant for this reaction has been determined by Wagman et.al.[82] from room temperature to 1500°K. The very low oxygen pressure determined by a given H_2O/H_2 ratio ($2x10^{-17}$ atmospheres for a H_2O/H_2 ratio of 10^{-3}) allows direct calculation of Po_2 without correction for the negligible amount of H_2O which dissociates to form the O_2. Any O_2 or other impurities present in the gas will be buffered by the H_2O and H_2 gases as long as the impurity level is small compared to those two gases.

EXPERIMENTAL

Apparatus, standards, and procedures have been developed to measure the O/M of UO_2, PuO_2, and $(U,Pu)O_2$ equilibrated with gases of known oxygen potential.

Apparatus

The apparatus used for the study of oxygen potential of oxides of varying O/M and temperatures consists of the thermobalance, the controlled-atmosphere generation system, and the oxygen potential measurement system. The thermobalance measures sample weight, measures and controls sample temperature, and records data in both analog and computer-reducible digital formats. The controlled-atmosphere system produces oxygen partial pressures spanning fourteen orders of magnitude. The oxygen potential measurement system independently measures the oxygen potentials of the atmospheres generated.

1. Thermobalance

The thermobalance system consists of a Mettler Recording Vacuum Thermoanalyzer attached to an alpha containment glove-box and interfaced to a digital data logging system (Fig. 4). The Mettler thermoanalyzer is composed of an electronic readout balance and control panel, a 1600°C furnace, temperature measurement and control panel, high vacuum system, vacuum measurement panel, six-channel multi-point recorder, power supply, and associated interconnections.

The balance is a rugged, electromagnetically compensated, substitution balance housed in a vacuum-tight stainless steel tank thermostatted at 25°C. Balance capacity is 16 grams, readability is ±5 μg, yielding a sensitivity at maximum load of 3×10^6. Vibrations, repeatability of release point, and other effects, however, reduce the precision to ~20 μg (s_i). The sample is weighed above the balance, supported on the thermocouple stick which also measures sample temperature. A set of mechanical compensation weights from 0.01 to 15 g are switched by vacuum tight controls, allowing mechanical weight changes under operating conditions.

The electronic output from the balance is amplified by the weight control panel which sends a 0

Figure 4.
Thermobalance for O/M measurements on uranium-plutonium oxides.

to 10 mv and a 0 to 100 mv signal to the multi-point recorder. The latter signal is automatically compensated by a precision voltage source so that both signals remain within the 10 mv recorder range. Three amplification ranges allow full scale output on the "1x" signal of 10 mg, 100 mg, and 1 g. An electronic tare allows uncalibrated adjustment of the weight signal.

The furnace which uses "Super-Kanthal" elements has a maximum temperature rating of 1600°C. Temperature is measured by a Pt/Pt-10% Rh thermocouple in contact with the sample crucible, and referred to a cold junction at 25°C. The thermocouple output is compared to a set point potential by the furnace controller. Temperature control is fully proportional and the controller has ten linear heating rates between 100°C/min and 0.5°C/min as well as controlled isothermal heating. The thermocouple signal is also fed to the multi-point recorder through an automatic 10 mv bucking potential which keeps the thermocouple signal on scale. The thermobalance furnace tube is Al_2O_3 as are all other components exposed to high temperature.

The vacuum system consists of a mechanical pump, two diffusion pumps, and a cold trap. The mechanical pump, which evacuates through the balance tank, is used to rapidly change the system atmosphere by evacuation and backfill. A differential manometer and a thermocouple gauge measure the system vacuum. A constant temperature bath provides the thermostatted 25°C water for circulation through the balance tank jacket and also maintains the thermocouple cold junction at 25°C. An immersion-type refrigerated coil provides the cooling to maintain the thermostat at 25°C.

The Mettler reactive gas inlet system is installed on the balance which allows direct introduction of the H_2O and H_2 gases to the sample. A stainless steel line enters the side of the sample chamber and carries the gases up an Al_2O_3 tube and vents them above the sample. The configuration inside the furnace tube is shown in Fig. 5. An Al_2O_3 gas deflector on the end of the reactive gas inlet tube diverts the gas flow directly into the sample crucible. The inner flow tube extending from the balance to just below the sample crucible, vents the Ar balance tank purge gas and prevents the reactive gas from entering the balance tank.

The six-channel multi-point recorder records the analog signals from all the thermobalance data-producing components. The source-signal stepping switch has been modified by addition of

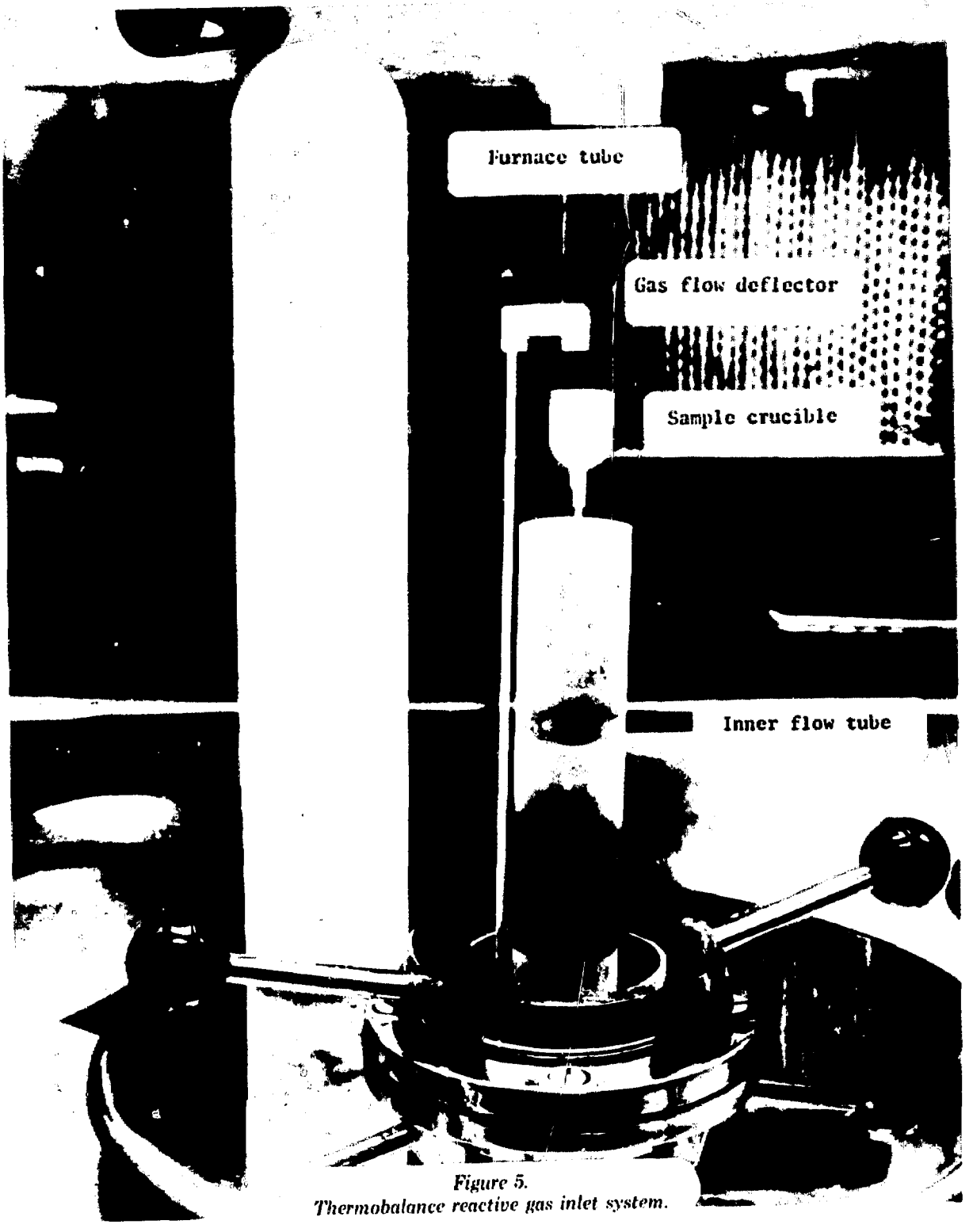

Figure 5.
Thermobalance reactive gas inlet system.

an extra switch plate and sensing switches to provide source switching and timing signals for the digital data logging system. The modifications do not affect the analog signal recording. The digital data logging system employs a Hewlett Packard 3480B autoranging digital voltmeter to convert analog voltages to a BCD signal fed through a Hewlett Packard 2575A bidirectional interface to a modified ASR-33 teletype. The teletype prints the data and punches a paper tape which is subsequently processed by an off-line computer. The multi-point recorder has a 27 sec. data recording cycle. To eliminate unnecessary redundancy of digital data and reduce the amount of paper tape punched, a timing interval board allows a continuously variable time delay up to 60 hours between each digital data record.

The electronic rack, shown in Fig. 4, contains the Mettler control panels, multi-point recorder, the digital voltmeter, bidirectional interface, and digital delay timer. It is mounted on wheels and connected to the thermobalance by a 3-m umbilical cord, which allows free movement for access to the panel and other components.

To contain the α-active materials handled in the thermobalance, a modified DB-100 glovebox has been attached to the thermobalance. Modifications to the glovebox and thermobalance were necessary to seal the glovebox to the thermobalance and provide sufficient filtered airflow to dissipate the furnace heat. Rubber gaskets seal the glovebox floor to the thermobalance sample compartment, furnace elevator, furnace guide, and cold trap. The furnace elevator is also enclosed in a pleated sleeve of polyvinyl chloride to contain any radioactive materials which might penetrate the sliding seal. Two 8-in square absolute air filters in the glovebox inlet and exhaust provide absolute air filtration at a flow rate sufficient to dissipate the furnace heat. A round airlock attached to the side of the glovebox conserves interior and exterior space and allows free passage of the absolute air filters and the furnace elements. The glovebox is supported by the heavy steel frame in which the thermobalance is mounted. Penetrations of the glovebox provide a vent inside the glovebox for the thermobalance gas flow and vacuum pump exhaust.

2. Controlled Atmosphere Apparatus

The oxygen potential of the atmosphere at the thermobalance sample crucible is controlled by mixing hydrogen gas and water vapor in an inert carrier gas and delivering the mixture to the

sample through the reactive gas inlet. The gas flow and blending apparatus is shown in Figs. 6 and 7. The hydrogen is added by flow mixing of tank gases, water vapor is produced by combination at a catalyst of H_2 and O_2 produced by electrolysis of water.

Inert carrier and purge gases are He and Ar purified by passing through U-metal turnings at 700°C followed by molecular sieve. The Ar purges the balance tank and the He carries the H_2 and the H_2O. The H_2 is added to the He either as pure gas or as premixed 1.8, 0.7, or 0.15% blends in He. The H_2 and H_2-He gases are purified by passing through copper wool at 750°C or 350°C followed by molecular sieve (Fig. 6). The hydrogen and impurities content of the gases prior to purification are listed in TABLE 1.

To assure accurate control of the thermobalance oxygen potential, the gas flow rates are carefully controlled. The He, H_2, and H_2-He gas flows are controlled by micrometer needle valves. The He flow is measured by a conventional flowmeter and the H_2 and H_2-He gas flows are measured by a Hastings Model DLF-100X thermal mass flowmeter. The Ar balance purge flow is controlled by the thermobalance needle valve and flowmeter. All gas flow measuring devices were calibrated at ambient conditions (580 torr, 25°C) with a soap bubble flowmeter. The flow calibration curves are shown in Figs 8, 9, and 10.

Controlled H_2O levels are added to the He carrier gas by electrolysis of water from 1N H_2SO_4. The H_2 and O_2 produced by electrolysis are swept past a liquid nitrogen-cooled trap which removes residual water vapor, and are recombined at a platinized-asbestos catalyst prior to entering the thermobalance. All gas flow lines between the electrolysis cell and the thermobalance are stainless steel and are heated to >100°C to prevent surface water sorption.

The electrolysis cell and trap (Fig. 11) are fabricated from borosilicate glass. The cell is fabricated from a gas-washing bottle with two Pt gauze semi-circular electrodes sealed in the base. The He carrier enters at the bottom of the solution through a coarse frit, sweeping from the solution the H_2 and O_2 produced. The liquid nitrogen-cooled trap is a 500-ml round bottom flask sealed within a 1000-ml round bottom flask. The trap is insulated by polyurethane foam and is gravity fed from a 5-gal liquid nitrogen reservoir insulated by polyurethane and polystyrene foams (shown on the side of the glovebox, Fig. 4) The glass neck connecting the cell and the cold

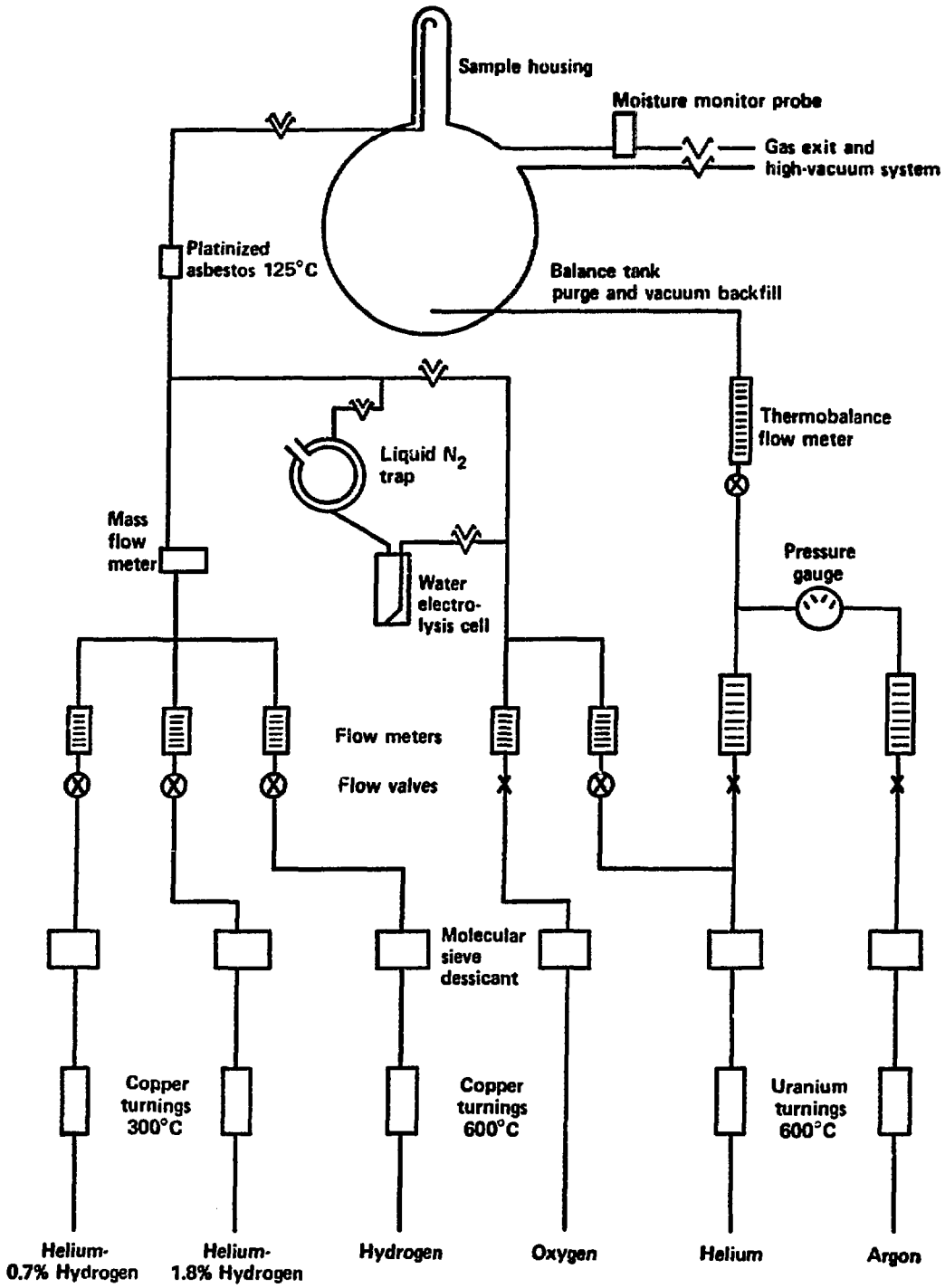

Figure 6.
Diagram of controlled-atmosphere gas flow system.

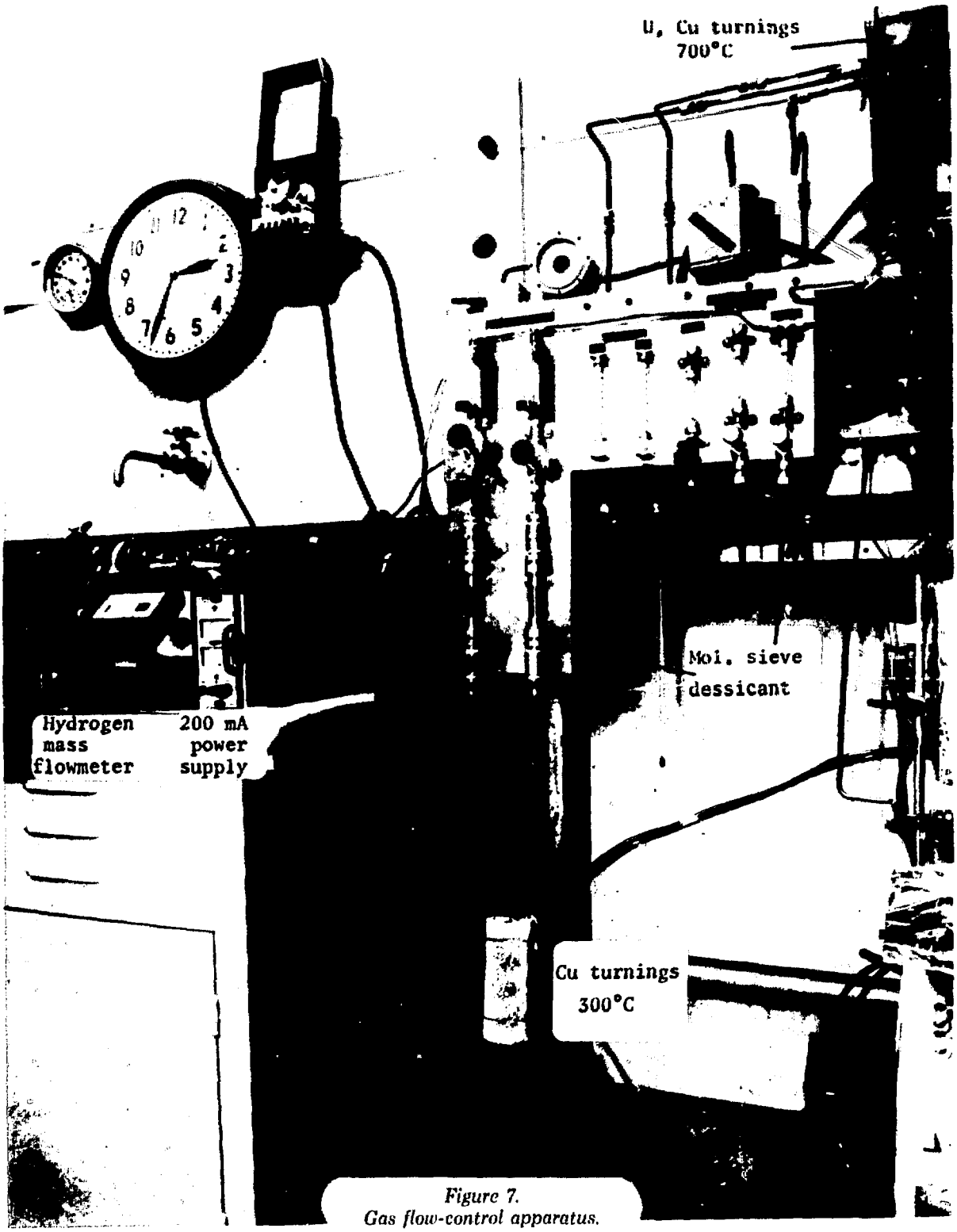

Figure 7.
Gas flow-control apparatus.

TABLE 1

HYDROGEN AND IMPURITY CONTENTS OF H_2 AND H_2-He PREMIXED GASES

	Determined Values			
	Pure	Nominal He Premix Values		
Component	H_2	2% H_2	0.5% H_2	0.1% H_2
H_2	100 mol%	1.8 mol%	0.7 mol%	0.15 mol%
He	*	98.2 mol%	99.3 mol%	99.85 mol%
O_2	*	<60vpm	<60vpm	*
CO	*	*	*	*
CO_2	*	<60vpm	*	*
N_2	*	<60vpm	<60vpm	*

*Not detected.

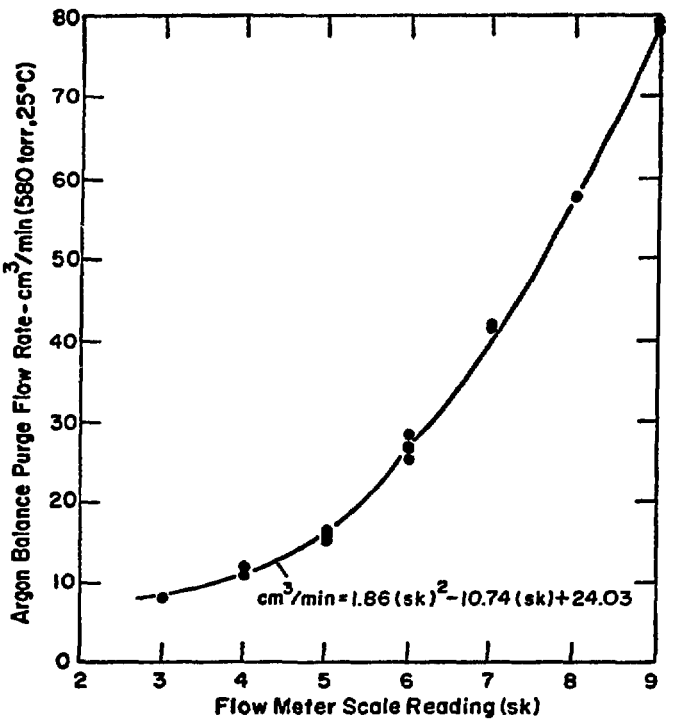

Figure 8.
Calibration curve for balance-purge argon gas flow.

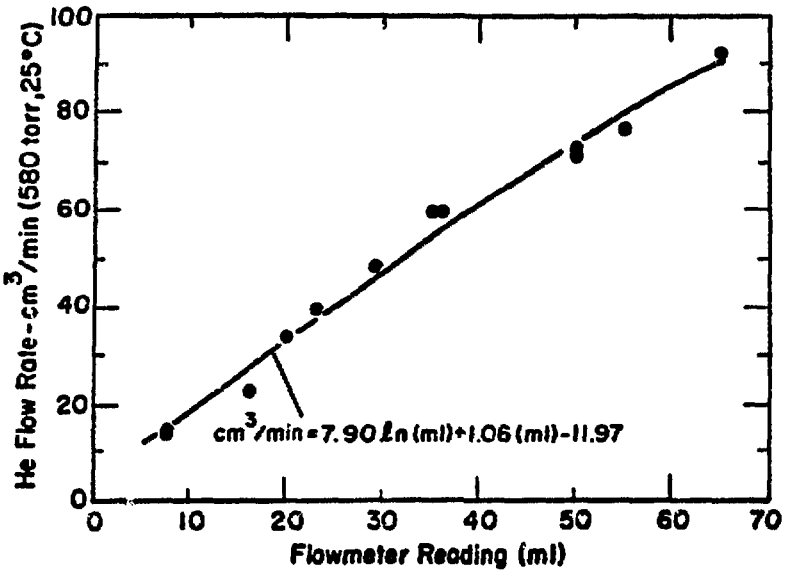

Figure 9.
Calibration curve for helium carrier gas.

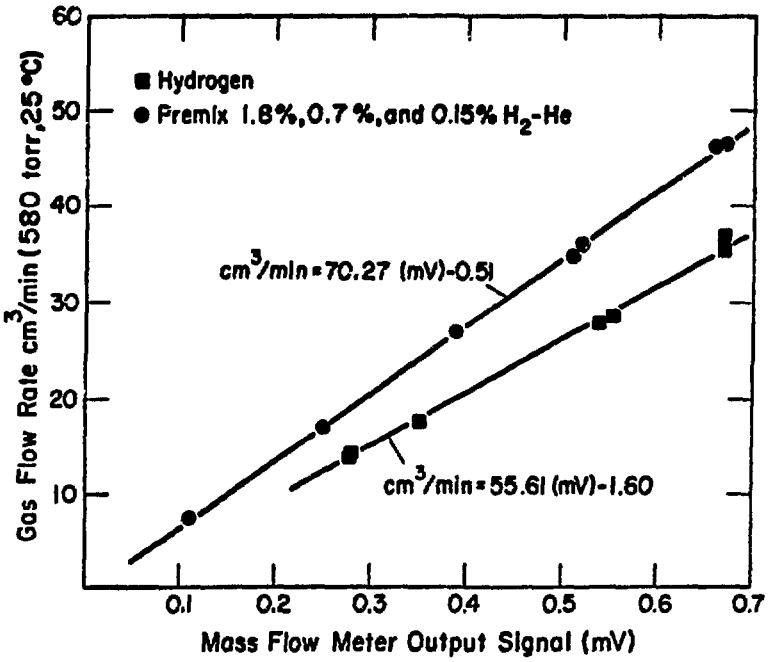

Figure 10.
Calibration curves for Hastings Mass Flowmeter, hydrogen and premixed hydrogen-helium gases.

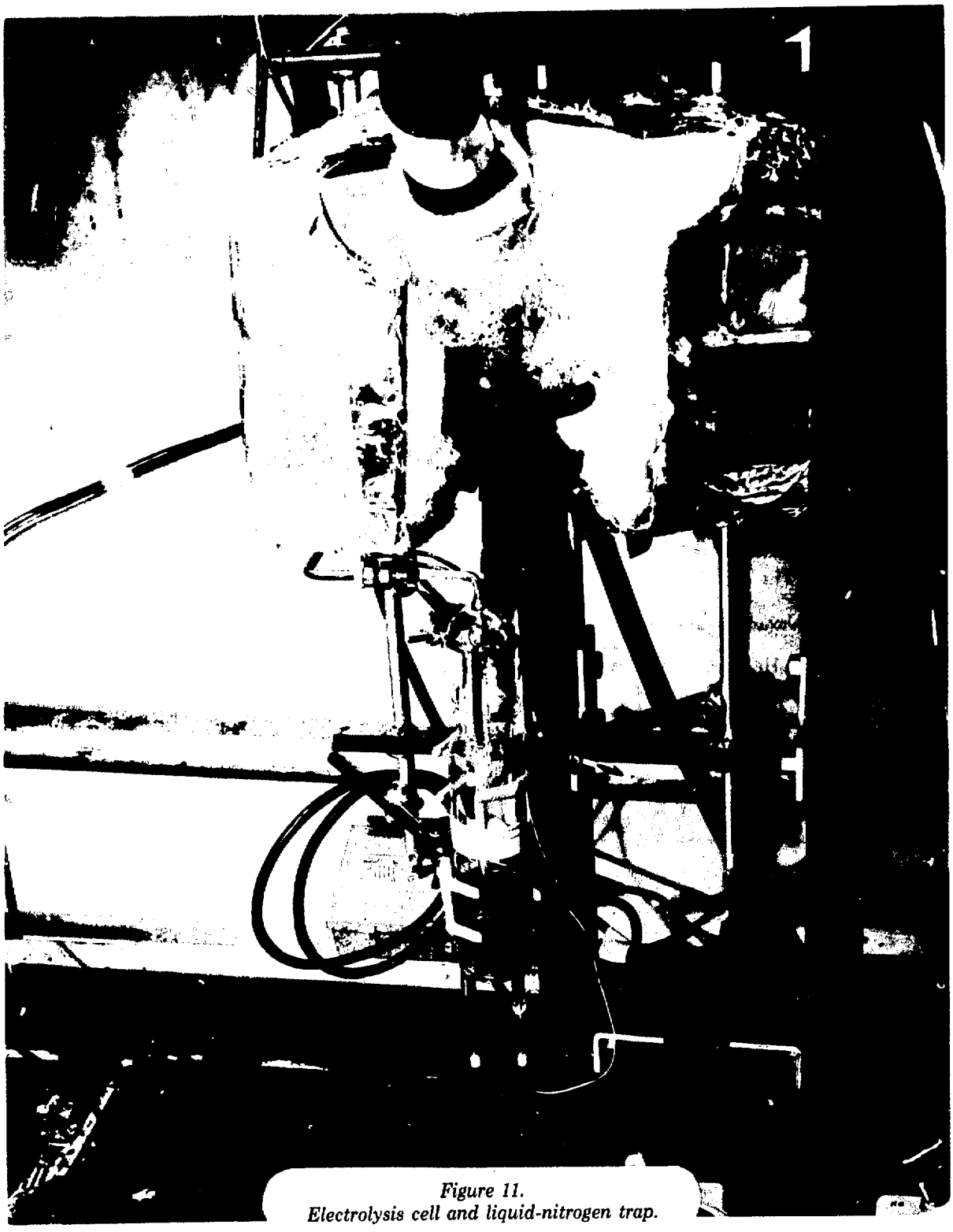

Figure 11.
Electrolysis cell and liquid-nitrogen trap.

trap is wound with copper wire and heated by heating tape to prevent plugging by ice formation. A 24-hr clock timer shuts off the heating tape each morning to cool the neck before liquid nitrogen is added.

The electrolysis current is supplied by either a Keithly 200-mA or a Hewlett Packard 500-mA constant current power supply. The 500-mA supply is manually controlled, the 200-mA supply is controlled by an external resistance network. The resistance network is programmed by a stepping switch and a 24-hr clock switch (shown partially in Fig. 7), allowing 24 hr control of the current levels as required by the experiment.

3. Oxygen Potential Measurement Systems

Two independent systems measure the oxygen potential of the thermobalance atmosphere. Flow of H_2 and H_2O into the thermobalance and moisture in the exiting gas are measured by one system. The other system is an oxygen potential electrode which measures the oxygen potential of the gas at the sample.

The digitally recorded output of the Hastings mass flowmeter and the electrolysis current measured across a precision resistor are used to calculate the partial pressures of H_2 and H_2O in the He carrier gas. The moisture level of the exit gas is measured by a Panametrics Model 2000 Moisture Monitor probe inserted into the cold trap cavity of the thermobalance. The oxygen potential at the sample is calculated from the sample temperature and the H_2 and H_2O partial pressures. Because the moisture monitor calibration is unstable, the moisture reading is only used to determine when the water level of the exit gas has equilibrated to changes in the electrolysis level.

A solid-state oxygen potential electrode was designed and fabricated for *in situ* measurement of gaseous oxygen potential at the sample. The electrode is fabricated from the ThO_2-15 mol% Y_2O_3 (YDT) discussed in the THEORETICAL chapter. The design (Fig. 12) incorporates several unique features necessitated by its use. The ceramic tube is fabricated to dimensions (6.3-mm o.d. x 250-mm long x 1-mm wall thickness) to allow fit between the thermobalance inner-flow tube and the furnace tube. The oxygen responsive area of the electrode is restricted to the tip,

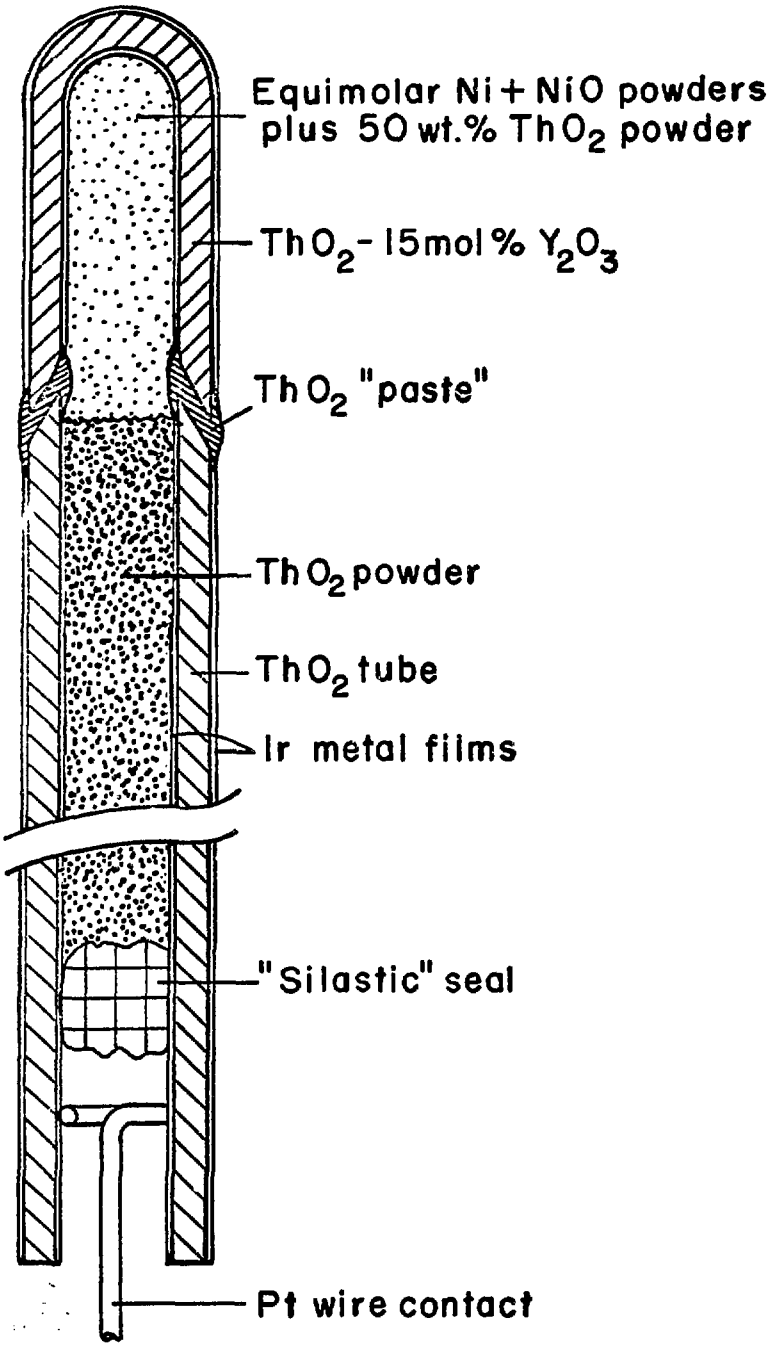

Figure 12.
Diagram of solid-state oxygen electrode.

because only the tip is in an isothermal region of the thermobalance. Non-Nernstian response may result if the oxygen responsive surface were in a thermal gradient.

The electrode was fabricated in two sections from YDT and pure ThO_2 prepared by the Los Alamos Scientific Laboratory (LASL) ceramics fabrication group using a slip cast process. Sources and purities of the ThO_2 and Y_2O_3 used are listed in TABLE 2. The ends of the two tube sections to be joined (the YDT was ~35-mm long) were ground to a common taper and were joined by a paste of the same ThO_2 used to prepare the tube body. Sintering at 1600°C produced a gas-tight joint between the two sections in two of four tubes fabricated.

The tubes were coated with a continuous Ir metal film by painting the interior and exterior surfaces with an iridium resinate solution (Engelhard No.A-1123). The Ir was reduced to metal by heating to 900°C in an Ar - 8% H_2 atmosphere. A tube fabricated from Al_2O_3 thermocouple sheath carried the gas into the YDT tube end to ensure reduction to metal on the interior surface. When a continuous film was formed on interior and exterior the open end of the tube was ground flat on No.400 carborundum paper to remove Ir metal bridging the two surfaces.

A Ni - NiO oxygen potential reference mixture was prepared by blending equi-molar amounts of Ni and NiO and combining on an equal weight basis with ThO_2. The ThO_2 prevents sintering of the Ni and the NiO, assuring a large surface area for setting the reference oxygen potential. The YDT section of the electrode was packed with the Ni - NiO reference and the remainder of the tube was packed with pure ThO_2. The base of the tube was sealed with Silastic compound and a Pt wire contact is placed in the end. The electrode fits within a special holder at the base of the thermobalance sample area, and the potential developed is measured by the digital voltmeter (input impedance = 10^{12} Ω) and recorded digitally.

Uranium and Plutonium Standard Materials

The O/M of uranium, plutonium, and mixed uranium-plutonium oxides was determined with reference to highly pure uranium and plutonium metals as starting materials. The two U metals used were NBS SRM-960 natural U metal and a highly-pure depleted ingot U metal prepared and

TABLE 2

IMPURITIES CONTENT OF Y_2O_3 AND ThO_2 SOURCE MATERIALS

	Determined Content, µg/g, As Received	
Element	ThO_2 Norton 900F	Y_2O_3 Michigan Chem, Keg #400
Li	<0.5	<3
Be	<0.5	<3
B	0.8	<3
Na	6	20
Mg	20	3
Al	<200, est 100	<10
Si	80	30
Ca	200	<10
Sc	-	<10
Ti	-	<10
V	<100	<100
Cr	20	<3
Mn	<2	<3
Fe	150	<10
Co	<5	<10
Ni	<5	<10
Cu	<2	<3
Zn	-	<100
Pb	<2	<10
Sr	-	<3
Nb	-	<100

TABLE 2 (cont.)

Nb	-	<100
Mo	-	<10
Cd	-	<3
Sn	-	<10
Ba	-	<30
La	-	<30
Ce	-	<100
Pr	-	<100
Nd	-	<100
Sm	-	<20
Eu	-	<3
Gd	-	<30
Tb	-	200
Dy	-	20
Ho	-	<30
Er	-	<10
Tm	-	<20
Yb	-	3
Lu	-	<100
Bi	-	<10
Th	-	<300

characterized at LASL. The Pu metal was NBS SRM-949 Pu metal which is also prepared and characterized at LASL for the NBS. Impurity contents of the LASL-prepared metals were determined by emmission spectrographic, radiochemical, and chemical analyses. Impurity content information for NBS SRM-960 was obtained from the National Bureau of Standards.[84] Impurity data for the three metals are listed in TABLES 3, 4, and 5.

The UO_2 and PuO_2 standards were prepared by direct oxidation of the metals in the thermobalance. The U metals were cleaned by filing with a new file surface or were chemically polished in ~8M HNO_3 followed by distilled water and acetone rinses. The Pu metal is received as 500-mg chunks sealed in an inert atmosphere and was used as received. After the metals were weighed into the thermobalance (see Procedure), they were heated to 250°C in an atmosphere of He saturated with H_2O. The oxide produced by this low temperature oxidation was a compact oxide scale with a very large surface area which should allow rapid equilibration of the oxide with the gas atmosphere.

The solid solution mixed oxide standard was to be prepared by melting together weighed portions of U and Pu in the thermobalance to form a U-Pu alloy. The melting is performed in the He carrier gas with the flow diverted around the electrolysis cell and trap. The alloy is then oxidized in the thermobalance to solid-solution oxide. Pu melts near 600°C, U melts near 1200°C, and the 3:1 U-Pu alloy melts at 1000°C.[85] The initial attempt to form the alloy by melting the metals in the Al_2O_3 crucible at 1300°C for 72 hr resulted in dissolution of the crucible (see RESULTS). Subsequent efforts to melt the metals together involved use of MgO and Y_2O_3 cups placed within the Al_2O_3 crucible, by heating initially to 1200°C then holding several hours at 1050°C. Oxidation of the alloy and measurements of the O/M were performed with the additional cup present.

Procedure

The basic experimental procedure involves weighing a metal into the thermobalance, converting it to oxide, weighing the oxide equilibrated with a series of determined gaseous oxygen potentials, and calculating the O/M for each equilibrated oxide weight. The O/M calculation includes corrections for buoyancy effects, impurity effects, and thermobalance drift.

TABLE 3

URANIUM AND IMPURITY CONTENTS OF NBS SRM-960

Impurity Element	Content (μg/g U)
Fe	42
Al	20
Ba	<10
C	11
Mg	9
Ni	13
Si	28
V	4

Sum of Measured Impurities = 137 μg/g U

NBS Certified Uranium Content = 99.975 ± 0.017 wt%

Sum of Impurities Calculated from Material Balance = 250 μg/g U

Difference Between Measured and Calculated Impurities = 113 μg/g U

TABLE 4

URANIUM AND IMPURITY CONTENTS OF LOT UR-1261 U METAL

Impurity Element	Content (µg/g U)
Mg	30
Al	5
Si	10
Ca	5
Cr	2
Mn	3
Fe	15
Ni	20
Cu	4
Ag	2
Pb	2
C	120
N	20

Sum of Measured Impurities = 238 µg/g U

Uranium Content Calculated from Material Balance = 99.9762 wt%

TABLE 5

PLUTONIUM AND IMPURITY CONTENTS OF NBS SRM-949 (LOT 7)

Impurity Element	Content (μg/g Pu)
Ni	3
Cr	2
Fe	2
Ta	10
Th	1
Np	12
C	10
H	10
O	10
Cl	3
F	0.5
U[a]	5
Am[b]	7.8

Sum of Measured Impurities = 76.3 μg/g Pu

Calculated ^{241}Am added by decay of ^{241}Pu = 61.6 μg/g Pu

Calculated U added by decay of ^{239}Pu and ^{240}Pu = 117.9 μg/g Pu

Calculated Sum of Impurities = 255.8 μg/g Pu

Plutonium Content Calculated[c] from Material Balance = 99.9744 wt%

---

[a]Date of analysis 2/7/73, ^{241}Am is produced at ∿ 28.5 ppm/yr.

[b]Date of analysis 3/14/73, U is produced at ∿ 54.6 ppm/yr.

[c]Plutonium content of this lot has not yet been certified.

The Al_2O_3 sample crucible was cleaned in 8M HNO_3 and heated to 1300°C in vacuum before a metal sample was loaded. The tare weight of the crucible is obtained after backfilling with Ar at 25°C in Ar flowing at 27 cm^3/min. The metal is added to the balance, the balance is evacuated and backfilled with Ar, and the metal is weighed under the same conditions as the crucible tare. The metal is heated to 250°C in He saturated with H_2O obtained by passing the He through the electrolysis cell with the liquid nitrogen trap warm. The metal is held at 250°C until oxidation is complete. The oxide is then equilibrated isothermally at 1300, 1200, 1100, 1000, 900, and 800°C with oxygen potentials determined by the H_2O-H_2-He flowing gas. Equilibration at a maximum of six different oxygen potentials is achieved per 24 hr isothermal "run". The oxide weight is recorded in the flowing gases at nominal total flow rate of 140 cm^3/min. The oxide weights are calculated with correction for buoyancy and thermal effects and thermobalance drift by comparison to a blank data file obtained under similar conditions with an empty Al_2O_3 crucible. Additional corrections are applied to convert all weights to *in vacuo* values calibrated against NBS weights. The metal and oxide weights are both corrected for impurities, different corrections are applied to the oxides than are applied to the metals to compensate chemical changes in the impurities. The impurity corrections applied to the oxides from the three metal sources are listed in TABLE 6.

The digital voltages recorded on paper tape are converted to scientific units using the FORTRAN program **PTAPE** which is run under the Control Data Corporation time share system KRONOS on a CDC 6600 computer. This program (see Appendix) calculates the time of day, temperature, weight, electrolysis current, H_2O partial pressure, H_2 partial pressure, moisture monitor reading, oxygen potential, and O_2 partial pressure for each recorded line of data. Further data reduction is performed by combining the oxide data file with the blank data file under control of the FORTRAN program **OMDATA**. The oxide weight is calculated, corrected for impurities and buoyancy, and the O/M is calculated. The O/M ratio is calculated from the measured oxygen content of the oxide and the theoretical oxygen content of the stoichiometric dioxide, calculated from the initial metal weight. The output from **OMDATA** is plotted by a

TABLE 6

IMPURITY CORRECTIONS APPLIED TO OXIDES PREPARED FROM U AND Pu

Impurity Element	Oxidation Product	Calculated Impurity Content (µg/g metal)		
		NBS SRM-960 U	Lot UR-1261 U	NBS SRM-949 Pu
Fe	FeO	54	19	3
Al	Al_2O_3	38	9	-
Ba	BaO	11	-	-
Ca	CaO	-	7	-
Cr	Cr_2O_3	-	3	3
Mn	MnO_2	-	5	-
Mg	MgO	15	50	-
Ni	Ni	13	20	3
Cu	Cu	-	4	-
Ag	Ag	-	2	-
Si	SiO_2	60	21	-
Pb	PbO	-	2	-
V	V_2O_5	7	-	-
Ta	Ta_2O_5	-	-	13
Th	ThO_2	-	-	1
Np	NpO_2	-	-	13
U	UO_2	-	-	139.4
Am	Am_2O_3	-	-	76.3
C	CO	0	0	0
N	N_2	-	0	-
H	H_2O	-	-	0
O	PuO_2	-	-	0

TABLE 6 (cont.)

Cl	HOCl	-	-	0
F	HF	-	-	0
Total Impurities µg/g metal		198	142	251.7

Zetaplotter to aid in interpreting equilibration data. Average O/M's at each equilibrated level and further data reduction for defect structure interpretation are performed by desk calculator.

Usually two or more 24-hr isothermal data runs were made at each temperature. The schedule for filling the liquid nitrogen reservoir was adjusted to allow the trap to defrost each morning before beginning another run. Oxygen potential was changed by step changes in electrolysis level and/or by change of the hydrogen gas source. Equilibrium was assumed after attainment of a constant weight following a change in the gaseous oxygen potential. Equilibration was generally attained by reduction from higher to lower O/M.

Calculations

The FORTRAN program **PTAPE** converts digital voltages to scientific units using several relationships developed specifically for this study, which are briefly presented here.

1. Temperature Calculation

To convert the Pt/Pt-10%Rh thermocouple potential to temperature a relationship was developed relating the data of the International Practical Temperature Scale-1968 (IPTS-68)[86] calculated for this thermocouple referred to a 25°C cold junction.[87] An equation relating temperature to thermocouple $\mathcal{EMF}$ was developed using an iterative approximation program on a CDC 7600 computer. The relation of absolute temperature to thermocouple $\mathcal{EMF}$ in millivolts is

$$T\ (^{\circ}K) = [\ 1 - exp(-1.908\ mv^{1.078})\ ] + 298.51 + 119.38\ mv - 2.573\ mv^2 + 0.05965\ mv^3 \qquad (28)$$

The temperatures calculated agree with the IPTS-68 to within ±0.5°K.

2. H_2O - H_2 - O_2 Equilibrium

The relationship to temperature of the equilibrium constant, K_{eq} for water, hydrogen, and oxygen was calculated from the data of Wagman et.al.[83] A least squares fit of a second order curve, yielded

$$\log_{10} K_{eq} = -3.037 + (13\ 242./T) - (144\ 575./T^2) \tag{29}$$

where T is the absolute temperature in degrees Kelvin.

3. Oxygen Potential from Oxygen Electrode $\mathcal{EMF}$

The oxygen potential of equi-molar Ni/NiO can be calculated from,[88]

$$\Delta Go_2(Ni/NiO) = -111\ 708. + 40.58(T^\circ K)\ cal/mol \tag{30}$$

Combining this relationship with Eq. 23 and solving for $\Delta Go_2''$, the oxygen potential of the exterior surface gives,

$$\Delta Go_2'' = -111\ 708. + 40.58\ T - 4 \cdot F \cdot E \tag{31}$$

where T is the absolute temperature, E is the measured $\mathcal{EMF}$ in volts and F is the Faraday equal to 96,485 Coul/mol[89] or 23,060 cal/volt equiv.

RESULTS

Apparatus

The modifications to the thermobalance, made to allow handling of α-radioactive materials, had no discernable effect on its operation. The gas flow deflector, added to the reactive gas inlet system (Fig. 5), would be expected to affect the apparent weight by momentum transfer from the gas impinging directly onto the Al_2O_3 crucible. To determine the gas flow effects, the Al_2O_3 crucible was weighed with the deflector in place with only He carrier and Ar purge gas flowing; He-0.7% H_2, He-1.8% H_2, and H_2 gases were then added to the He carrier gas and the weight recorded. The data, listed in TABLE 7, show an apparent weight increase of only 89 μg for a flow increase of nearly 100%.

TABLE 7

EFFECT OF THE REACTIVE GAS-CARRIER GAS FLOW RATE ON THE Al_2O_3 CRUCIBLE WEIGHT

Reactive Gas, Flow (cm^3/min)	Carrier Flow* (cm^3/min)	% Flow Increase	Weight (g)	Weight Change (μg)
None	60	0	3.148763	0
He-0.7%H_2 12	60	20	3.148790	27
He-1.8%H_2 13	60	22	3.148796	33
H_2 58	60	95	3.148852	89
H_2 12	60	20	3.148797	34
None	60	0	3.148772	9

*Argon balance-purge flow = 26 cm^3/min.

Tests of the controlled-atmosphere apparatus and thermobalance for leaks were conducted on a semi-routine basis. When first assembled, most of the gas flow components were tested by evacuating with a mass spectrometer leak detector while being sprayed with He. The thermobalance was routinely leak tested by evacuating with the high vacuum system and comparing the high vacuum attained with thermobalance specifications. The electrolysis cell-cold trap was leak tested by pressurizing the isolated cell-trap with He to 0.2 atm over ambiant, isolating from the He pressurization source for 2 hr, and repressurizing with He. A leak would be indicated by the He gas bubbling into the electrolysis solution when the cell was re-pressurized. As each test was performed any indicated leaks were resolved before additional data was taken.

A gas chromatographic-frontal analysis effect was observed for the H_2 and O_2 gases produced by the electrolysis cell. When electrolysis was initiated, a front of H_2-enriched gas reached the thermobalance, followed by the expected H_2O level, finally followed by an O_2-enriched peak when electrolysis was stopped. This effect was first observed when a UO_{2+x} sample equilibrated to a constant oxygen potential was to be oxidized to a higher stoichiometry by an increase in the H_2O electrolysis current. Instead of the expected oxidation, a rapid reduction occured indicative of a rather pure H_2 component in the gas, followed by the slow oxidation expected of the higher H_2O level.

That this was indeed a frontal analysis effect was confirmed when a UO_{2+x} sample was exposed to the products of the electrolysis cell with no H_2 gas flowing. When electrolysis was begun the oxide reduced sharply followed by slow oxidation as the H_2O level became constant. When electrolysis was stopped the oxide oxidized sharply then leveled to constant weight which was indicative of an overall oxidation of the sample. Repeating the experiment with the He carrier flow rate doubled produced the same qualitative effect with the reduction and oxidation occuring twice as rapidly.

The net effect of this phenomenon was to increase the time required to equilibrate samples to a constant oxygen potential. The time for a changed electrolysis rate to produce the changed H_2O level at the sample (from .5 to 1 hr) was directly added to the time required for equilibration. The

sample also sees an initial component which is opposite to the change desired, and thus the sample is always displaced away from the desired equilibration point, requiring more time to reach equilibrium.

Uranium Dioxide

The data for all of the oxides were obtained by equilibrating the samples isothermally to controlled oxygen potentials, a methodology based on initial non-isothermal studies on uranium oxide. A uranium oxide sample was programmed for a temperature ramp from 800°C to 1300°C back to 800°C with constant H_2O/H_2 ratio. Such data would allow evaluation of oxygen potentials and O/M ratios at any desired temperature between 800°C and 1300°C. The data are only useful, however, if the sample maintains an instantaneous equilibrium with the constantly changing temperature. Two curves run at 1°C/min and at 10°C/min with a constant H_2O/H_2 ratio are shown in Figs. 13 and 14. Neither curve indicates the desired attainment of instantaneous equilibrium. The 10°C/min curve shows O/M data values which, while appearing to be symmetrical with the temperature curve, changes much less than the 1°C/min O/M data. The 1°C/min O/M data is non-symmetric with the temperature curve, again indicating non-equilibration.

The generation of isothermal oxygen potential and O/M data for uranium and other oxides required the adoption of an operational definition of equilibrium, as it was impractical to approach equilibrium from both an oxidized and a reduced state. The operational definition of equilibrium comprises a set of three conditions which must be met before equilibrium is assumed. The first requirement is that the calculated oxygen potential of the gas must be constant. Since oxygen potential is calculated from measured H_2O electrolysis and H_2 flow rates, this condition requires both as well as sample temperature to be constant. The second condition is that the moisture level of the gas exiting the thermobalance (as measured by the Panametrics Moisture Monitor) must be relatively constant. This condition is subject to some leeway as a large amount of unheated surface is present between the sample and the moisture monitor which for large changes in

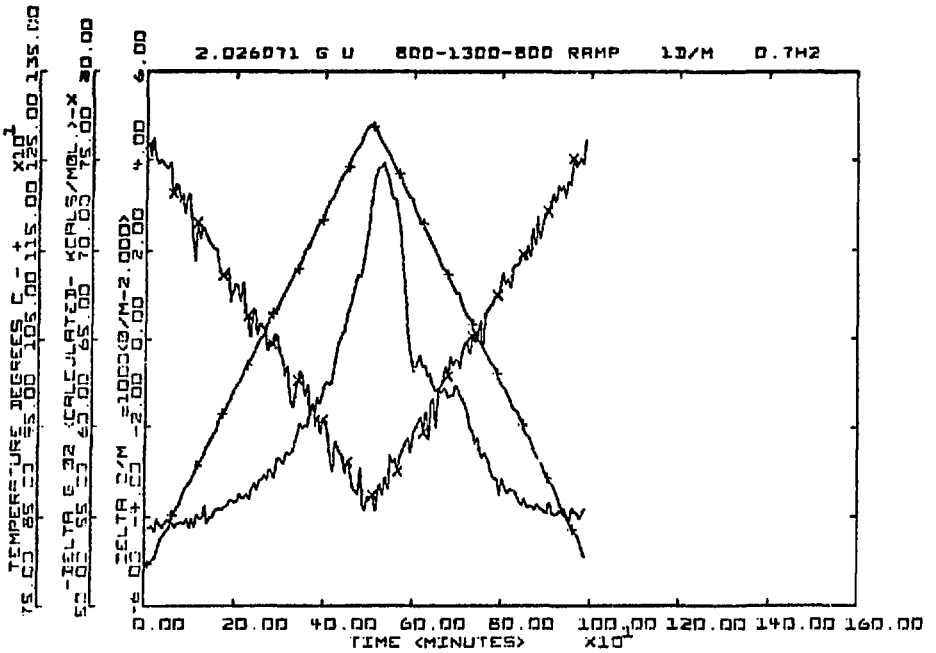

Figure 13.
O/M of uranium oxide for a 1°C/min temperature ramp.

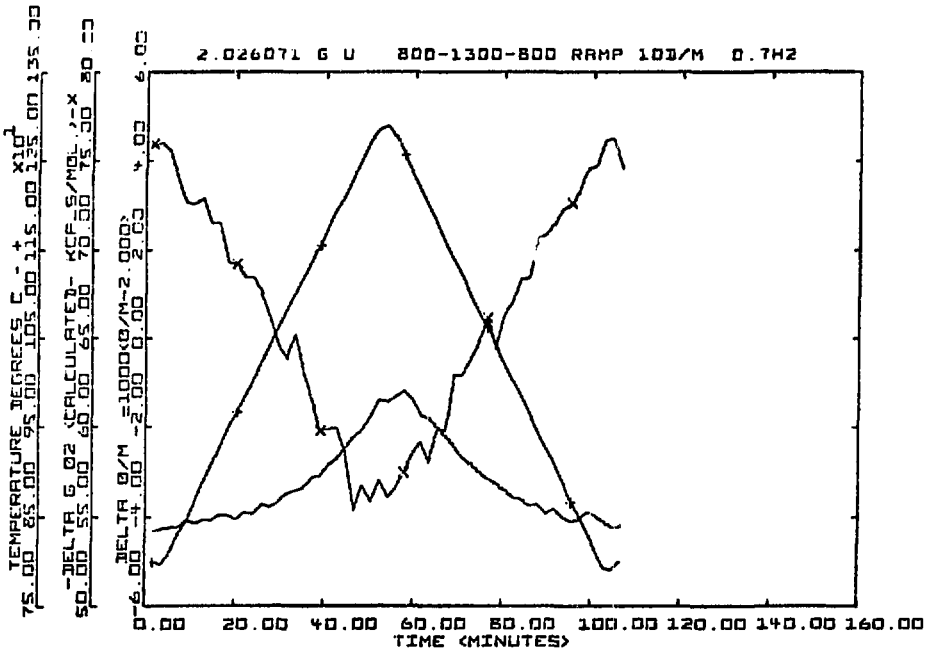

Figure 14.
O/M of uranium oxide for a 10°C/min temperature ramp.

moisture levels may delay equilibration at the moisture sensor. The third and most obvious condition is that the sample weight, as reflected in the calculated O/M, must also be constant for a significant period of time.

To aid in applying these conditions to the data generated in these studies, all of the data has been computer processed for plotting on a Zetaplotter. The calculated oxygen potential, O/M, and moisture monitor reading have been plotted as a function of time for each isothermal data file produced. The plots were examined visually for regions satisfying the above three conditions, the regions were marked and labeled, and the corresponding data were then averaged using a desk calculator. The plots used to evaluate all of the data presented in this dissertation are included in the appendices.

Two uranium oxide samples have been prepared from NBS SRM-960 U metal and LASL Lot UR-1261 U metal. The isothermal data for the oxygen potential, oxygen partial pressure, and O/M's of the two oxides are presented respectively in TABLEs 8 and 9. Also listed in the tables are references to the Zetaplot produced curves used in evaluating equilibrium. The reference code consists of two letters, two numbers, and a number and a letter. The initial letters designate the source metal used to prepare the oxide. UN is oxide prepared from SRM 960 and UL is oxide prepared from LASL U metal. The two digits are the nominal temperature at which the data was taken in hundreds of degrees C, ie. 08 = 800°C. The number and letter signify respectively the particular plot (1, 2, or 3) and the plot segment (a, b, c, etc.) which is assumed to demonstrate equilibrium

Examination of the data in TABLEs 8 and 9 shows that the values for the UN oxide are ~0.002 lower in O/M ratio than for the UL oxide. The difference may be attributable to the impurity correction applied to the UN oxide. As shown in TABLE 3, the information available for NBS SRM-960 does not account for 113 μg/g of impurities in the metal. The data are calculated assuming that the metal assay value assigned by the NBS is correct, and the oxide value is corrected only for the impurities known to be present, as listed in TABLE 6. This is equivalent to assuming that the unaccounted for impurities volatalize from the sample in the conversion from metal to oxide. This assumption may be in significant error.

TABLE 8

OXYGEN POTENTIAL, OXYGEN PARTIAL PRESSURE, AND O/M OF URANIUM OXIDE PREPARED FROM NBS SRM-960 U METAL

$\Delta\bar{G}o_2$ (kcal/mol)	Oxygen Pressure (atm)	O/M Ratio	Reference*
	1569°K 1296°C		
-68.5	3.0×10^{-10}	1.9999	UN-13-1a
-70.5	1.5×10^{-10}	1.9993	UN-13-1b
-73.5	5.5×10^{-11}	1.9990	UN-13-1c
-78.0	1.5×10^{-11}	1.9985	UN-13-1d
	1469°K 1196°C		
-73.0	1.5×10^{-11}	1.9984	UN-12-1a
-77.5	3.0×10^{-12}	1.9980	UN-12-1b
	1371°K 1098°C		
-62.0	1.5×10^{-10}	1.9999	UN-11-2a
-64.5	5.0×10^{-11}	2.0000	UN-11-2b
-68.5	1.0×10^{-11}	1.9996	UN-11-2c
-70.5	5.5×10^{-12}	1.9980	UN-11-1a
-72.0	3.5×10^{-12}	1.9979	UN-11-1b
-83.5	4.5×10^{-14}	1.9975	UN-11-1c
	1272°K 999°C		
-63.0	1.5×10^{-11}	1.9992	UN-10-2a
-65.5	5.0×10^{-12}	1.9982	UN-10-1a
-66.0	4.5×10^{-12}	1.9994	UN-10-2b
-67.0	3.0×10^{-12}	1.9981	UN-10-1b
-68.0	2.0×10^{-12}	1.9994	UN-10-2c
-69.0	1.5×10^{-12}	1.9980	UN-10-1c
-72.0	4.5×10^{-13}	1.9980	UN-10-1d

TABLE 8-cont.

	1173°K 900°C		
-70.0	9.0×10^{-14}	1.9980	UN-09-1a
-70.5	7.5×10^{-14}	1.9995	UN-09-2a
-72.0	4.0×10^{-14}	1.9979	UN-09-1b
-75.0	9.0×10^{-15}	1.9978	UN-09-1c
-80.0	1.0×10^{-15}	1.9999	UN-09-2b
-80.0	1.0×10^{-15}	1.9978	UN-09-1d
	1073°K 800°C		
-74.0	8.5×10^{-16}	1.9979	UN-08-1a
-75.0	5.0×10^{-16}	1.9982	UN-08-1b
-77.0	2.0×10^{-16}	1.9981	UN-08-1c
-80.0	5.0×10^{-17}	1.9980	UN-08-1d

*Refer to coded data plots in the Appendices.

TABLE 9

OXYGEN POTENTIAL, OXYGEN PARTIAL PRESSURE, AND O/M OF URANIUM OXIDE PREPARED FROM LASL LOT UR-1261 U METAL

$\Delta\bar{G}o_2$ (kcal/mol)	Oxygen Pressure (atm)	O/M Ratio	Reference*
	1569°K 1296°C		
-56.0	1.5×10^{-8}	2.0101	UL-13-2a
-60.5	4.0×10^{-9}	2.0058	UL-13-2b
-63.5	1.5×10^{-9}	2.0028	UL-13-3d
-65.0	8.5×10^{-10}	2.0023	UL-13-3c
-71.0	1.5×10^{-10}	2.0016	UL-13-1a
-74.0	5.0×10^{-11}	2.0011	UL-13-1b
-78.5	1.0×10^{-11}	2.0006	UL-13-1c
-84.0	2.0×10^{-12}	2.0001	UL-13-1d
-88.0	5.0×10^{-13}	1.9993	UL-13-3b
-118.0	3.5×10^{-17}	1.9988	UL-13-3a
	1469°K 1196°C		
-69.0	5.0×10^{-11}	2.0006	UL-12-1c
-70.0	3.5×10^{-11}	2.0006	UL-12-2a
-72.5	1.5×10^{-11}	2.0004	UL-12-2b
-75.0	7.0×10^{-12}	2.0003	UL-12-2c
-79.5	2.0×10^{-12}	2.0001	UL-12-2d
-89.0	6.0×10^{-14}	1.9991	UL-12-1b
-116.5	4.0×10^{-18}	1.9988	UL-12-1a
	1371°K 1098°C		
-69.0	9.5×10^{-12}	2.0003	UL-11-3b
-72.5	3.0×10^{-12}	1.9994	UL-11-2c

TABLE 9-cont.

	1371°K 1098°C		
-74.5	1.5×10^{-12}	1.9998	UL-11-1a
-76.5	6.0×10^{-13}	1.9995	UL-11-1b
-79.0	2.5×10^{-13}	1.9995	UL-11-1c
-94.0	1.0×10^{-15}	1.9989	UL-11-2b
-117.5	2.0×10^{-19}	1.9996	UL-11-3a
-120.0	8.5×10^{-20}	1.9991	UL-11-2a
	1272°K 999°C		
-68.5	2.0×10^{-12}	1.9995	UL-10-2c
-72.0	4.5×10^{-13}	1.9993	UL-10-2b
-72.5	3.5×10^{-13}	1.9999	UL-10-1b
-73.5	2.5×10^{-13}	1.9993	UL-10-2d
-76.0	8.0×10^{-14}	2.0002	UL-10-1c
-77.0	6.0×10^{-14}	1.9994	UL-10-2e
-80.5	1.5×10^{-14}	1.9995	UL-10-2f
-95.0	4.5×10^{-17}	1.9995	UL-10-1a
-96.5	2.5×10^{-17}	1.9989	UL-10-2a
	1073°K 800°C		
-73.5	1.0×10^{-15}	2.0024	UL-08-1a
-76.5	2.5×10^{-16}	2.0019	UL-08-1b
-77.0	2.0×10^{-16}	1.9994	UL-08-2d
-77.5	1.5×10^{-16}	1.9996	UL-08-2e
-82.0	2.0×10^{-18}	1.9994	UL-08-2c
-96.5	2.0×10^{-20}	1.9994	UL-08-2b
-117.0	1.5×10^{-24}	1.9994	UL-08-2a

*Refer to coded data plots in the Appendices.

The 1300°C and 1200°C oxygen potential data for the UL oxide are plotted in Fig. 15. It is apparent from the plot and the tabulated data for both oxides that conditions sufficient to produce significant departure from stoichiometry were only attained at 1300°C. Also, the data indicates that any method of analysis of O/M of UO_2 involving equilibration with a controlled oxygen potential will produce the stoichiometric dioxide in the oxygen potential range -70 to -120 kcal/mol between 800 and 1300°C.

A log-log plot of the 1300°C UL oxide data shows x in UO_{2+x} is proportional to $Po_2^{1/2.71}$ (Fig. 16). The uranium oxide data compilation of Kofstad (Ref. 46, p304) shows x in UO_{2+x} to be proportional to $Po_2^{1/2}$ which changes to $Po_2^{1/6}$ as temperature and defect concentration decrease. The defect structure close to stoichiometry is probably a variably ionized oxygen interstitial which becomes an ordered structure incorporating both oxygen interstitials and oxygen vacancies at higher defect concentrations.

Plutonium Oxide

The plutonium oxide produced by from NBS SRM-949 Pu metal (lot 7) was equilibrated with varying oxygen potentials at temperatures from 800 to 1300°C. The operational definition of equilibrium applied to the uranium oxide was also applied to the plutonium oxide. The plots used to evaluate equilibration are in Appendix 3, and the values of oxygen potential, oxygen partial pressure, and O/M are listed in TABLE 10. The oxygen potentials and O/M's are plotted in Fig. 17 for the temperature range 800 to 1300°C.

The defect concentration of plutonium oxide, as reflected by the O/M, is strongly dependent on both oxygen potential and temperature. At 1300°C the O/M deviates significantly from stoichiometry even at -70 kcal/mol. The nominal reference potential of -100 kcal/mol does produce a stoichiometric oxide at 800°C, however, significant reduction begins at that oxygen potential between 900 and 1000°C.

These plutonium data greatly expand and complement previous studies on oxygen potential and O/M of PuO_2, however, they do not fully agree with the results of those previous studies.

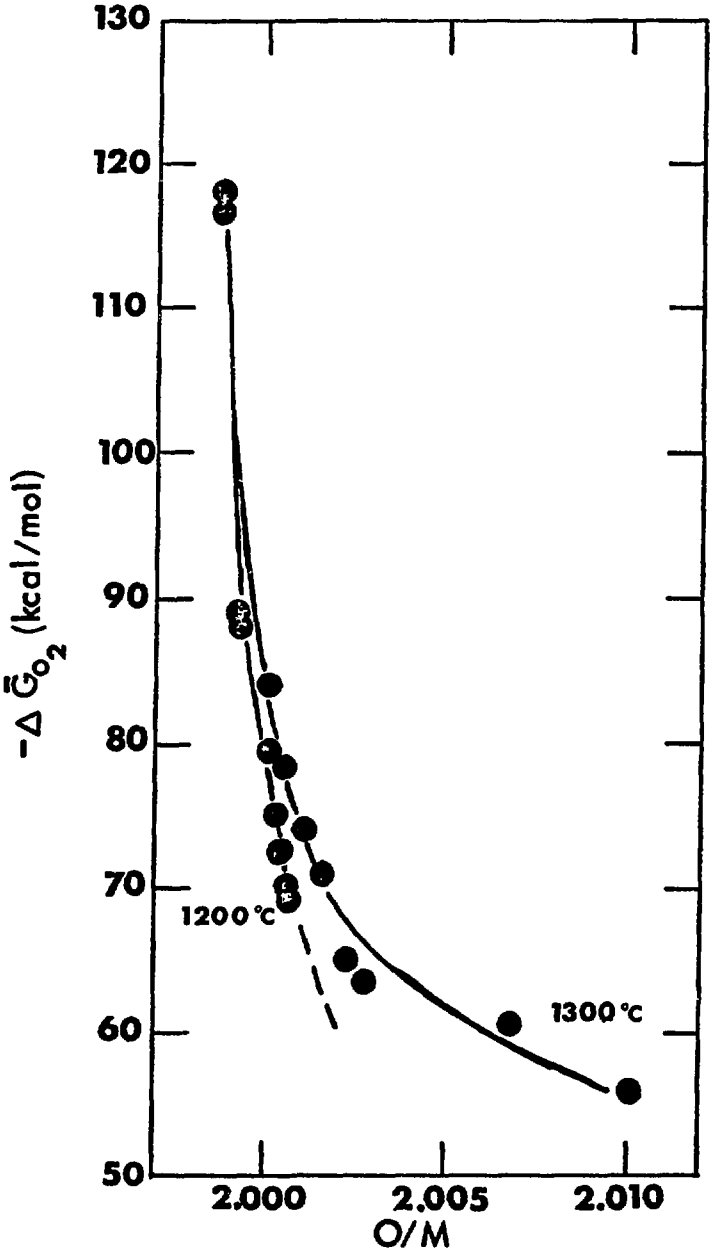

Figure 15.
Oxygen potential of uranium oxide (UL) at 1200°C and 1300°C.

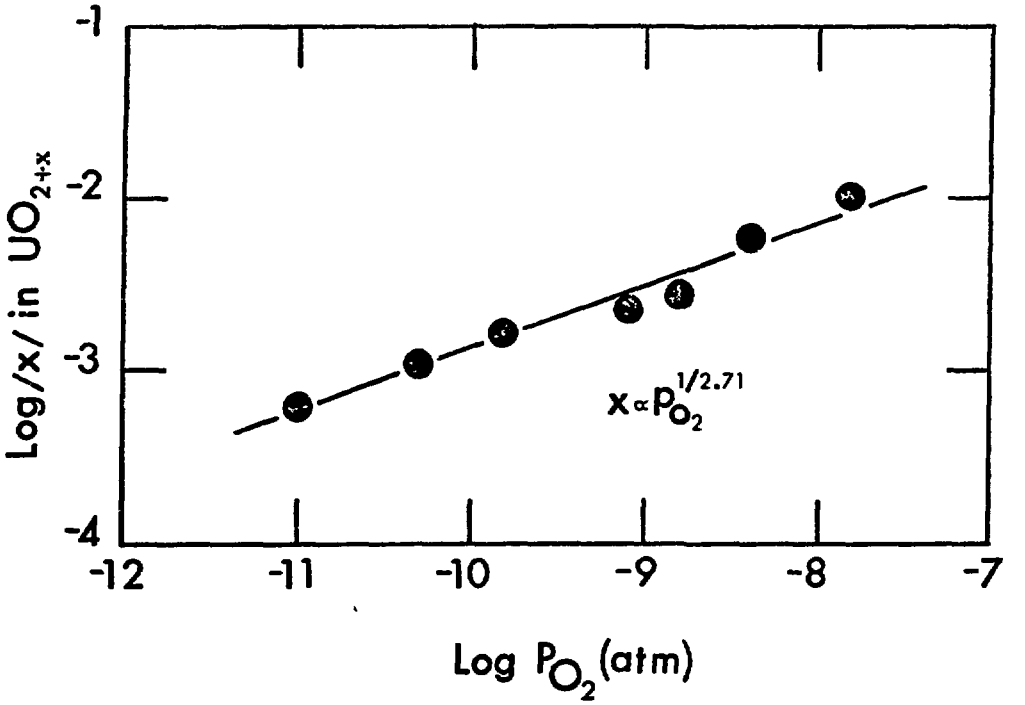

Figure 16.
Relationship of defect concentration in UO_{2+x} to oxygen pressure at 1300°C.

Atlas and Schlehman[56-57] determined the $\Delta\overline{G}_{O_2}$ for $PuO_{1.99}$ to be ~-97 kcal/mol at 1300°C whereas the present data indicate a much lower value of -84.5 kcal/mol. Markin et. al.[55] measured an oxygen potential of -114.3 kcal/mol for $PuO_{1.986}$ at 962°C using an electrochemical oxygen concentration cell. The present data extrapolates to an oxygen potential near -130 kcal/mol for this O/M at 960°C. Possible causes of these discrepancies are the reference conditions used in the previous studies. Markin et. al. referred their measurements to PuO_2 equilibrated in 10:1 CO/CO_2 at 850°C (an oxygen potential of -100 kcal/mol). The present data indicate this will produce a stoichiometric dioxide at equilibrium. Either equilibrium was not attained or the electrode system was non-Nernstian in its response. Atlas and Schlehman determined O/M by a gas reduction analysis, an error of ~0.005 in such an analysis would account for the discrepancy observed.

TABLE 10

OXYGEN POTENTIAL, OXYGEN PARTIAL PRESSURE, AND O/M OF PLUTONIUM OXIDE PREPARED FROM NBS SRM-949 Pu METAL (LOT 7)

$\Delta\bar{G}o_2$ (kcal/mol)	Oxygen Pressure (atm)	O/M Ratio	Reference*
	1569°K 1296°C		
-89.5	3.0×10^{-13}	1.9857	Pu-13-2f
-89.5	3.5×10^{-13}	1.9859	Pu-13-1c
-85.5	1.5×10^{-12}	1.9894	Pu-13-2e
-85.0	1.5×10^{-12}	1.9896	Pu-13-1b
-79.5	8.5×10^{-12}	1.9931	Pu-13-1d
-79.5	8.0×10^{-12}	1.9929	Pu-13-2d
-75.0	3.5×10^{-11}	1.9948	Pu-13-2c
-72.5	8.0×10^{-11}	1.9956	Pu-13-2b
-70.5	1.5×10^{-10}	1.9962	Pu-13-1a
-70.5	1.5×10^{-10}	1.9960	Pu-13-2a
	1469°K 1196°C		
-94.5	8.5×10^{-15}	1.9905	Pu-12-1b
-90.0	4.0×10^{-14}	1.9928	Pu-12-1a
-88.5	7.0×10^{-14}	1.9946	Pu-12-2e
-84.0	3.0×10^{-13}	1.9957	Pu-12-2d
-79.0	1.5×10^{-12}	1.9969	Pu-12-2c
-74.5	8.5×10^{-12}	1.9978	Pu-12-2b
-73.5	1.0×10^{-11}	1.9978	Pu-12-1c
-70.5	3.0×10^{-11}	1.9982	Pu-12-2a

TABLE 10-cont.

	1370°K 1097°C		
-115.5	3.5×10^{-19}	1.9839	Pu-11-1e
-111.5	1.5×10^{-18}	1.9839	Pu-11-1d
-107.5	7.5×10^{-18}	1.9884	Pu-11-1c
-103.0	3.5×10^{-17}	1.9919	Pu-11-1b
-99.5	1.5×10^{-16}	1.9955	Pu-11-2d
-95.5	5.5×10^{-16}	1.9951	Pu-11-1a
-87.0	1.5×10^{-14}	1.9979	Pu-11-2c
-82.0	8.5×10^{-14}	1.9983	Pu-11-2b
-74.5	1.5×10^{-12}	1.9992	Pu-11-2e
-74.5	1.5×10^{-12}	1.9988	Pu-11-2a
	1273°K 1000°C		
-120.5	2.0×10^{-21}	1.9873	Pu-10-1d
-115.5	1.5×10^{-20}	1.9918	Pu-10-1c
-112.0	5.5×10^{-20}	1.9939	Pu-10-1b
-109.0	2.0×10^{-19}	1.9951	Pu-10-1a
-108.5	2.5×10^{-19}	1.9960	Pu-10-2d
-103.0	2.0×10^{-18}	1.9974	Pu-10-2c
-96.5	2.5×10^{-17}	1.9983	Pu-10-2b
-95.5	4.0×10^{-17}	1.9985	Pu-10-2a
	1173°K 900°C		
-125.0	4.5×10^{-24}	1.9953	Pu-09-2f
-123.0	1.0×10^{-23}	1.9952	Pu-09-1c
-120.0	4.5×10^{-23}	1.9963	Pu-09-1b
-117.5	1.5×10^{-22}	1.9976	Pu-09-2e
-116.0	2.0×10^{-22}	1.9972	Pu-09-1a

TABLE 10-cont.

	1173°K 900°C		
-114.0	5.0×10^{-22}	1.9982	Pu-09-2d
-110.5	3.0×10^{-21}	1.9987	Pu-09-2c
-99.0	2.5×10^{-19}	1.9995	Pu-09-2b
-78.5	2.5×10^{-15}	1.9999	Pu-09-2a
	1073°K 800°C		
-131.0	1.5×10^{-27}	1.9985	Pu-08-3f
-125.5	2.5×10^{-26}	1.9992	Pu-08-3e
-123.0	9.0×10^{-26}	1.9996	Pu-08-3d
-123.0	9.0×10^{-26}	1.9983	Pu-08-2c
-120.5	3.0×10^{-25}	1.9987	Pu-08-2b
-119.0	5.0×10^{-25}	1.9999	Pu-08-3c
-116.5	2.0×10^{-24}	1.9989	Pu-08-2a
-114.5	4.0×10^{-24}	1.9984	Pu-08-1a
-113.0	9.0×10^{-24}	2.0001	Pu-08-3b
-84.0	7.0×10^{-18}	2.0002	Pu-08-3a

*Refer to coded data plots in the Appendices.

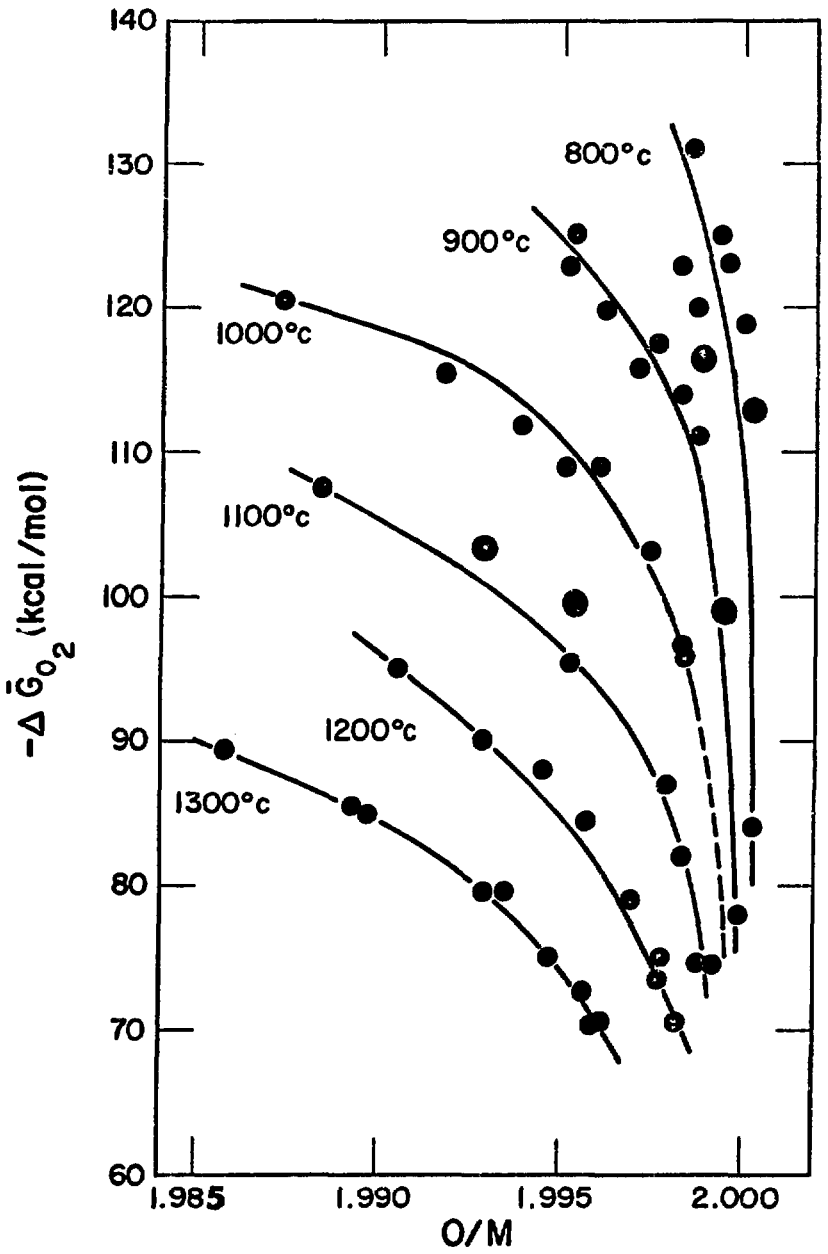

Figure 17.
Oxygen potential of plutonium oxide from 800°C to 1300°C.

The log of defect concentration in PuO_{2-x} is plotted in Fig. 18 versus log Po_2 for the 800°C to 1300°C data. The slope of the lines drawn through the data were calculated with a linear regression analysis. The relationship for the data from 900°to 1300°C are most nearly proportional to $Po_2^{-1/5}$. The data at 800°C are proportional to $Po_2^{-1/3.6}$. Possible defect structures which would display this relationship taken from the compilation of Tallan et. al.[80] are: a combination of $V_O^{\cdot\cdot}$ and $V_O^{\cdot}$ which respectively are proportional to $Po_2^{-1/6}$ and $Po_2^{-1/4}$, or $M_i^{\cdot\cdot\cdot\cdot}$ which is proportional to $Po_2^{-1/5}$, or a combination of $M_i^{\cdot\cdot\cdot\cdot}$ and $M_i^{\cdot\cdot}$ which are proportional respectively to $Po_2^{-1/5}$ and $Po_2^{-1/4}$. Atlas and Schlehman considered the most likely defect structure to be $M_i^{\cdot\cdot\cdot\cdot}$, since the fully ionized interstitial metal ions would satisfy the $Po_2^{-1/5}$ relationship. A combination of oxygen vacancies (partially ionized) and metal interstitials has been suggested by Kofstad (Ref. 46, p320) as the defect structures best accounting for the $Po_2^{-1/5}$ relationship which changes to $Po_2^{-1/4}$ at lower defect concentrations and temperatures.

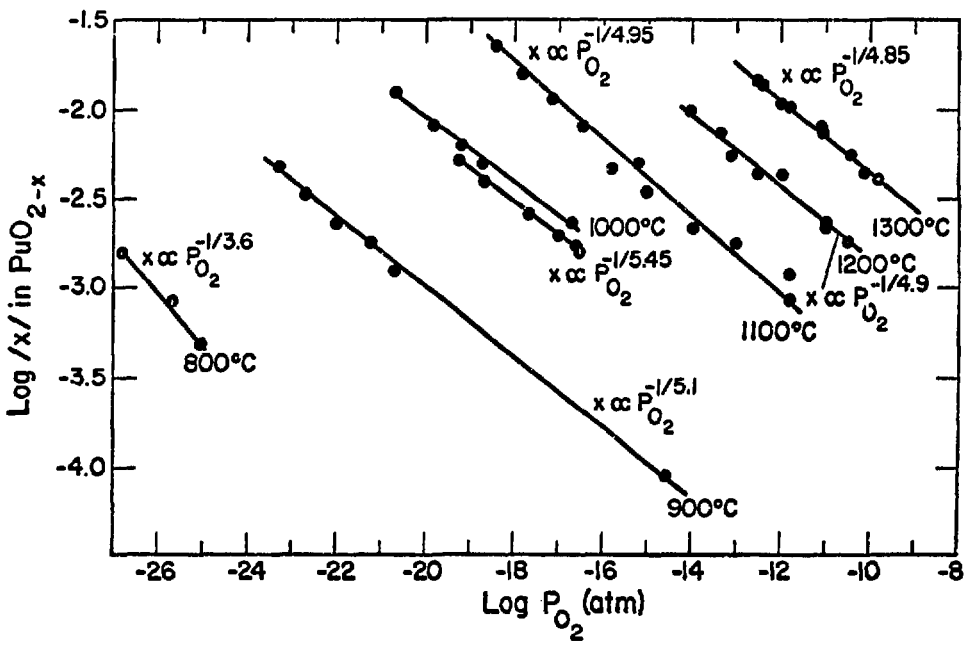

Figure 18.
Relationship of defect concentration in PuO_{2-x} to oxygen pressure, 800°C to 1300°C.

Solid Solution Uranium-Plutonium Oxide

1. Alloy Preparation

The initial effort to prepare the U-Pu alloy by melting the metals together in the Al_2O_3 crucible resulted in the dissolution of the crucible by the molten Pu. That the Pu had dissolved the crucible was confirmed by an electron microprobe examination of the metal ingot remaining. The U and Pu were uniformly distributed throughout the alloy, except for a few regions of high Pu content which also contained high Al levels. The probable reaction for the decomposition was,

$$3\ Pu + 2\ Al_2O_3 \leftrightarrows 3\ PuO_2 + 4\ Al \qquad (32)$$

The free energies of formation of PuO_2[57] and Al_2O_3[90] at 1300°C gives a calculated free energy for reaction 32 of -200 cal/mol. The negative free energy for the reaction explains the corrosive attack of the Al_2O_3 by the Pu.

A MgO liner was placed in the Al_2O_3 crucible to prepare the U-Pu alloy at 1200°C based on the free energy of the reaction,

$$Pu + 2\ MgO \leftrightarrows PuO_2 + 2\ Mg \qquad (33)$$

The calculated free energy for reaction 33 is +13.6 kcal/mol. This energy barrier was assumed sufficient to preclude reduction of the MgO by Pu. When the alloy preparation was attempted, a weight loss occurred. Visual examination of the liner and contents indicated decomposition of the MgO had occurred followed by volatilization of the Mg metal. Since Mg boils at 1107°C any metal formed at 1200°C would readily volatilize and provide a strong driving force for further decomposition despite the energy barrier. Further consideration also suggested the following reaction for the decomposition.

$$2\ Pu + 3\ MgO \leftrightarrows Pu_2O_3 + 3\ Mg \qquad (34)$$

Combining the data for the free energies of formation of Pu_2O_3[57] and MgO[90], the calculated free energy for reaction 34 is −4.4 kcal/mol.

Since Y_2O_3 is an oxide having one of the highest free energies of formation[90], its use for a crucible liner was considered. For the reaction,

$$2\ Pu + Y_2O_3 \leftrightarrows Pu_2O_3 + 2Y \qquad (35)$$

the calculated free energy change at 1200°C is +16.3 kcal/mol. This energy barrier should prevent reaction 35 from occuring to any significant extent. Also Y metal is rather refractory, having a melting point of 1400°C, so no volatilization of any Y metal formed should occur.

A Y_2O_3 crucible was obtained from the LASL ceramics-fabrication group and trimmed to fit within the Al_2O_3 crucible. The Y_2O_3 crucible was fabricated from a Y_2O_3 batch similar in purity to the material listed in TABLE 2. Uranium and plutonium metals (LASL lot UR-1261 and NBS SRM-949 lot 7) were weighed successively into the pre-tared Al_2O_3 crucible plus Y_2O_3 liner. The metals were alloyed together by heating in the highly purified He to 1200°C for 2hr followed by a soak at 1050°C for 6hr. The weight trace gave no indication of reaction between the molten metals and the Y_2O_3 liner.

2. Solid Solution Oxide

The U-Pu alloy (weight ratio, 77.5% U-22.5% Pu) was oxidized in the Y_2O_3 liner by heating ~30hr in He saturated with H_2O at 25°C. When the oxide reached constant weight, it was heated to 1300°C for equilibration with controlled oxygen-potential atmospheres.

The calculation used to compute O/M was changed to compensate the room temperature tare of the Y_2O_3 liner plus the added buoyancy effect. The data calculated in this manner for the solid solution oxide appeared to be biased by ~+0.005. A second Y_2O_3 crucible from the same fabrication batch as the first was equilibrated with extremes of oxygen potentials at 1300°C in the thermobalance. The second crucible showed an irreversible weight gain (~700 μg) when exposed to an oxidizing atmosphere and showed no additional weight changes when cycled through extremes of oxidizing and reducing atmospheres. A proportionate (but unmeasured) weight change was assumed to have occurred in the first Y_2O_3 liner containing the solid solution oxide, and a correction was applied to the O/M calculation. The oxygen potential, oxygen partial pressure,

and corrected O/M of the equilibrated solid solution oxide are listed in TABLE II. The computer-generated plots of the oxide thermograms are contained in the Appendices.

The O/M data at 1300°C show scatter which is easily seen in the plot of O/M vs. $\Delta\bar{G}_{O_2}$ in Fig. 19. Since the data at 1300°C were the first data accumulated, they probably reflect the effect of incomplete equilibration of the Y_2O_3 liner to the oxidizing atmospheres. This incomplete weight gain would cause a scatter among the data towards a lower O/M, which appears to be true for the 1300°C data. The data at 1200°C to 800°C appear to accurately reflect the behaviour of solid solution $(U_{.775},Pu_{.225})$ oxide.

Also plotted in Fig. 19 are curves for the calculated oxygen potential-O/M relationships of a 77.5% UO_2 - 22.5% PuO_2 mixture at 1300°C, 1200°C, and 1100°C. The curves were calculated by a weighted combination of the UO_2 and PuO_2 properties interpolated from Figs. 15 and 17. The experimental data at 1200°C and 1100°C are significantly displaced above the calculated curves, implying the solid solution oxide displays a wider oxygen potential range at stoichiometry than oxide mixtures.

The plot of the log of the defect concentration vs. the log of the oxygen partial pressure for the substoichiometric solid solution oxide at 1200°C is shown in Fig. 20. The linear regression analysis of the data gave a slope for the data proportional to $Po_2^{-1/5.9}$. This data disagrees with the evaluation by Kofstad (Ref 46, p322) of the data of Markin and McIver[52], which developed a relationship proportional to $Po_2^{-1/3}$. Markin and McIvers data only contains one point below x=0.05 for $(U,Pu)O_{2-x}$, and extrapolation to this point from data above x=0.05 is of doubtful validity. The −1/6 relationship found for the present data suggests the presence of fully ionized oxygen vacancies ($V_O^{\cdot\cdot}$) at these small deviations from stoichiometry. The defect structure probably changes as significant defect concentrations are formed to produce the −1/3 relationship above values of $X \geq 0.05$.

The solid solution oxide was examined by x-ray crystallography and emmission spectrography. The x-ray crystallographic results indicated the material was single phase (indicative of solid solution) with a lattice parameter between those of UO_2 and PuO_2. The emmission spectrographic analysis of impurities in the oxide did not detect Y at the 100 μg/g limit of detection, indicating no significant contamination of the oxide had occurred from the liner. The Y_2O_3

TABLE 11

OXYGEN POTENTIAL, OXYGEN PARTIAL PRESSURE, AND O/M

OF (77.5% URANIUM - 22.5% PLUTONIUM) OXIDE

PREPARED FROM LASL LOT UR-1261 U AND NBS SRM-949 Pu METALS

ΔGo_2 (kcal/mol)	Oxygen Pressure (atm)	O/M Ratio	Reference*
	1569°K 1296°C		
-105.5	2.0×10^{-15}	1.9948	U-Pu-13-2d
-101.0	8.5×10^{-15}	1.9948	U-Pu-13-2b
-95.0	6.0×10^{-14}	1.9974	U-Pu-13-2c
-88.5	4.5×10^{-13}	1.9968	U-Pu-13-2a
-78.5	1.0×10^{-11}	1.9974	U-Pu-13-3c
-70.0	2.0×10^{-10}	1.9976	U-Pu-13-3b
-67.5	4.0×10^{-10}	1.9994	U-Pu-13-1e
-64.5	9.0×10^{-10}	1.9994	U-Pu-13-1d
-64.0	1.5×10^{-9}	1.9983	U-Pu-13-3a
-63.0	1.5×10^{-9}	1.9993	U-Pu-13-1c
-60.5	4.0×10^{-9}	1.9994	U-Pu-13-1b
-58.5	7.5×10^{-9}	1.9995	U-Pu-13-1a
	1469°K 1196°C		
-111.0	3.0×10^{-17}	1.9967	U-Pu-12-1d
-101.5	8.0×10^{-16}	1.9984	U-Pu-12-1c
-94.5	9.5×10^{-15}	1.9986	U-Pu-12-1e
-92.5	1.5×10^{-14}	1.9990	U-Pu-12-1b
-63.5	3.5×10^{-10}	1.9998	U-Pu-12-1a

TABLE 11-cont.

	1371°K 1098°C		
-122.0	3.5×10^{-20}	1.9961	U-Pu-11-1e
-115.5	3.5×10^{-19}	1.9985	U-Pu-11-1d
-106.0	1.5×10^{-17}	2.0002	U-Pu-11-1c
-68.5	1.0×10^{-10}	2.0009	U-Pu-11-1b
-65.0	4.5×10^{-10}	2.0006	U-Pu-11-1a
	1273°K 1000°C		
-122.0	1.0×10^{-21}	1.9993	U-Pu-10-1c
-119.0	3.5×10^{-21}	1.9996	U-Pu-10-1b
-112.0	6.0×10^{-20}	1.9999	U-Pu-10-1a
	1173°K 900°C		
-122.5	1.0×10^{-23}	1.9999	U-Pu-09-1c
-101.0	1.5×10^{-19}	2.0000	U-Pu-09-1d
-100.5	2.0×10^{-19}	2.0003	U-Pu-09-1b
-71.5	5.0×10^{-14}	2.0002	U-Pu-09-1a
	1073°K 800°C		
-117.5	1.0×10^{-24}	2.0004	U-Pu-08-1b
-108.0	1.0×10^{-22}	2.0003	U-Pu-08-1c
-101.0	2.0×10^{-21}	2.0007	U-Pu-08-1a

*Refer to coded data plots in the Appendices.

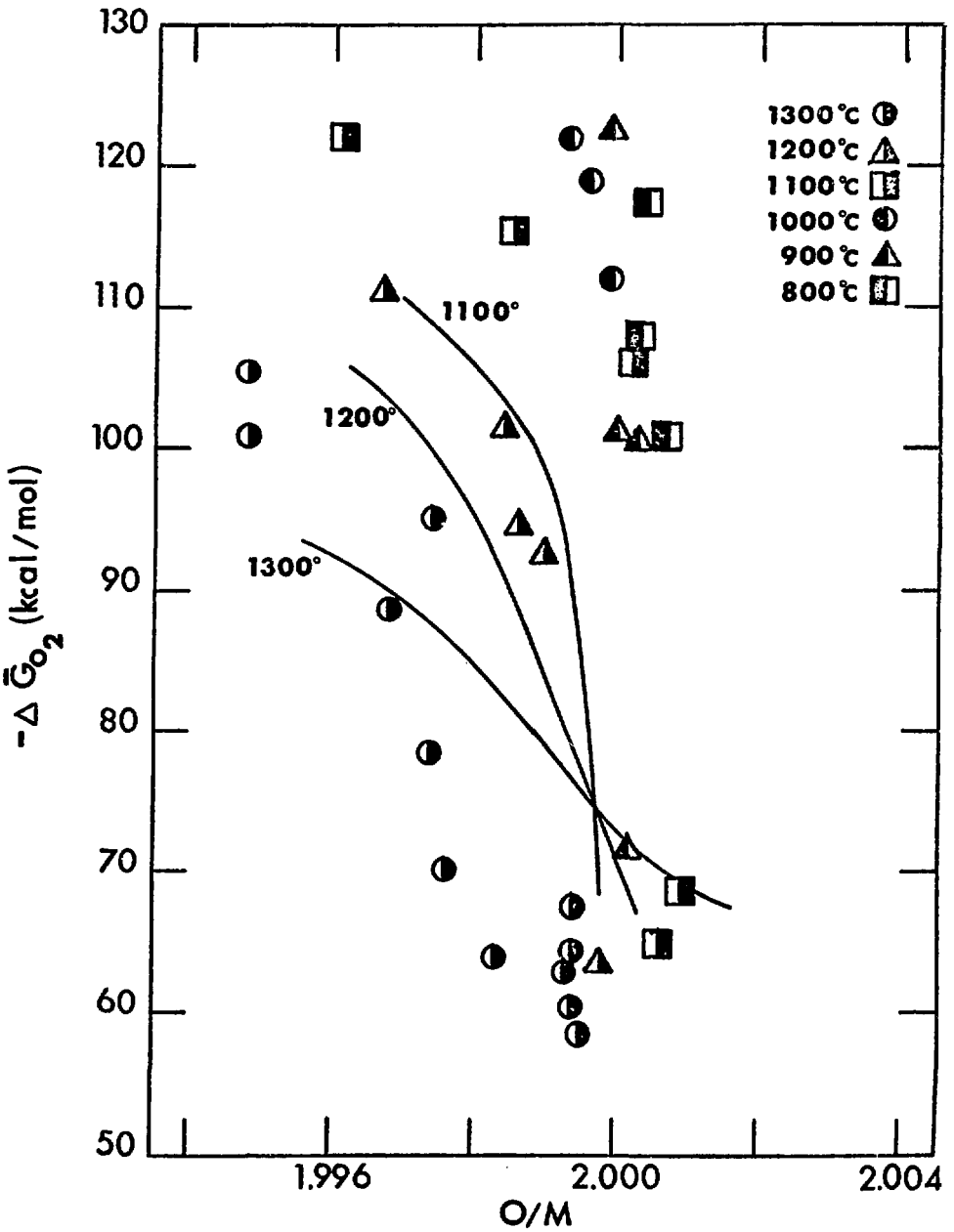

Figure 19.
Oxygen potential of $(U_{.775},Pu_{.225})$ oxide from 800°C to 1300°C.

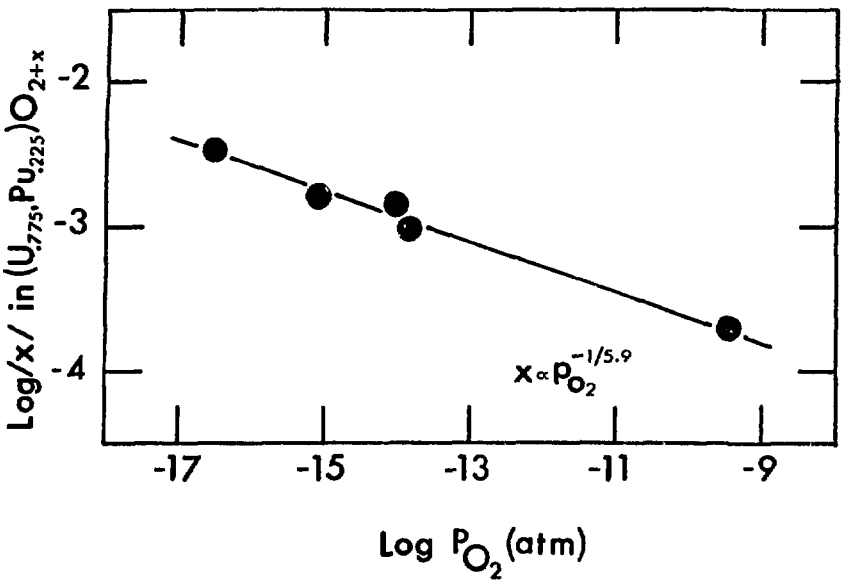

Figure 20.
Relationship of defect concentration in $(U_{.775},Pu_{.225})O_{2-x}$ to oxygen pressure at 1200°C.

liner surface which had been in contact with the molten alloy was discolored, probably due to (U,Pu)O_2 attached where the alloy melt had "wet" the Y_2O_3 surface.

Solid State Oxygen Electrode

Two oxygen electrodes were fabricated. The first was fabricated as described in the EXPERIMENTAL chapter, the electrolyte tube was filled with the Ni/NiO and ThO_2 powders in air and then sealed with "Silastic". The electrode failed to develop a stable *EMF* when placed in the balance and heated to 800°C. The varying *EMF* produced was more indicative of an air reference than the Ni/NiO. Heating the electrode at 1200°C reduced the still unstable *EMF* nearer to that expected of the Ni/NiO. Apparently the air entrapped within the powders in the interior set the initial reference, and at 1200°C the Ni gradually consumed the air.

The resistance of the internal Ir metal film which serves as both the sensing surface and contact to the electrode base was $\sim 10^4 \Omega$. This high internal resistance may have led to pickup of stray

signals from the thermobalance furnace elements which would have caused the instability in the electrode signal.

When the electrode was to be removed from the thermobalance for further study, the ceramic tube broke at the base. The silastic seal had apparently softened, flowed, and cemented the base; causing fracture when removal was attempted.

The second electrode fabrication was modified to avoid the problems displayed by the first electrode. The process for Ir metal coating the ceramic interior was modified to force the Ar-6% H_2 firing gas to flow the entire length of the tube interior. The firing furnace was also changed to allow more even heating of the ceramic tube length. The Ir metal film formed on the second tube interior had a resistance of only 200Ω. To avoid entrapment of air in the electrode the Ni/NiO and ThO_2 powders were added to the tube in an Ar-filled inert-atmosphere glovebox. The base of the electrode was then sealed, while in the inert atmosphere, by a high-vacuum, high-temperature epoxy ("Torr-Seal").

Before placing the electrode in the thermobalance a preliminary calibration using a tube furnace and controlled H_2O/H_2 gases was performed. The H_2O/H_2 ratio was controlled by saturating one of two premixed Ar-H_2 gas mixtures with H_2O at either 0°C or 20°C and by varying the tube furnace temperature. The $\mathcal{EMF}$ was converted to oxygen potential using Eq. 31 and compared to the oxygen potential calculated from the H_2O/H_2 ratio and temperature. The oxygen potential calculated from the electrode $\mathcal{EMF}$ was in general 10 to 15 kcal/mol more positive than the oxygen potential calculated from the H_2O/H_2 ratio and temperature. The $\mathcal{EMF}$ developed was, however, very stable.

When placed in the thermobalance and equilibrated to varying oxygen potentials at 800°C and at 1100°C the $\mathcal{EMF}$ produced by the oxygen electrode was again very stable. The oxygen potentials calculated from the electrode $\mathcal{EMF}$ were again, however, 5 to 30 kcal/mol more positive than the oxygen potentials calculated from the H_2O/H_2 ratios and temperature. Because of the lack of theoretical response, none of the electrode data was applied to the O/M - oxygen potential measurements.

DISCUSSION

Error Analysis

The random error of the O/M and oxygen potential measurements was readily estimated from the computerized data listings. The O/M random error was constant for all oxides, the pooled standard deviation for a single measurement is ±0.0001. The oxygen potential random error is also constant. The pooled standard deviation for a single measurement is ±0.5 kcal/mol.

The systematic error is more difficult to estimate. The O/M and oxygen potential calculations involve many parameters, the statistical distributions of which are unknown and can only be approximated. The estimated systematic error components of the O/M calculation for the two uranium and one plutonium oxide are listed in TABLE 12. Each error component has two values (expressed as O/M) associated with it, a maximum error and a probable error.

The maximum error is calculated assuming the error component is making its maximum contribution to total error and is totally uncompensated. The interpretation attached to these values is that for the materials used in this study these errors would be present if the effects of buoyancy corrections, hundred part-per-million impurity levels, and balance release errors were not calculated and corrected. Many of the studies referred to in the introduction do not indicate whether corrections were calculated for these or similar error sources. Lack of proper compensation may explain some of the discrepancies between these studies.

The probable errors listed are assumed standard deviations for the various error sources listed. The propogated total for the probable error values is an estimated standard deviation for the O/M ratio determined for each of the oxide sources. Because of the large number of parameters used in the O/M calculation the propogated systematic error contribution is much larger than the measured random error level for these O/M measurements.

The solid solution uranium-plutonium oxide has an additional error component to be considered beyond those listed in TABLE 12. The weight gain of the Y_2O_3 crucible, when uncorrected, contributed a systematic error of +0.005 to the calculated O/M. Because the correction is based on a measurement of another Y_2O_3 crucible, rather than the liner used, the standard deviation of the solid solution oxide O/M is estimated to be ±0.001.

TABLE 12

SYSTEMATIC ERROR COMPONENTS OF CALCULATED O/M

OF URANIUM AND PLUTONIUM OXIDES

	Maximum Error*			Probable Error*		
Error Component	UN	UL	Pu	UN	UL	Pu
Purity- Source Metal	0.0037	0.0035	0.0038	0.0008	0.0004	0.0003
Weight- Source Metal**	0.0005	0.0005	0.0005	0.0002	0.0002	0.0002
Buoyancy- Source Metal	0.0014	0.0014	0.0015	nil	nil	nil
Factor- Oxide Grav.	nil	nil	nil	nil	nil	nil
Purity- Metal Oxide	0.0092	0.0020	0.0038	0.0006	0.0002	0.0003
Weight- Metal Oxide**	0.0005	0.0005	0.0005	0.0002	0.0002	0.0002
Buoyancy- Metal Oxide	0.0027	0.0027	0.0027	0.0002	0.0002	0.0002
Propogated Total	0.0104	0.0051	0.0062	0.0011	0.0006	0.0005

*Error is expressed as effect on O/M ratio.
**Maximum weighing error is the range found for seven balance releases.

The error components of the calculated oxygen potentials are listed in TABLE 13. The major source is the error in the analysis of the premixed He-H_2 gases for H_2 concentration. The precision of these analyses was ±5 % RSD, however, since the lowest gas concentration used, 0.15% H_2, was near the limit of detection for the gas mass spectrometer, the maximum error was calculated assuming a 50 rel% error at that H_2 concentration. The probable error was calculated assuming the stated precision for the 0.7% H_2 gas analysis. The estimated standard deviation of a single measurement of the oxygen potential including random and systematic errors is ±0.7 kcal/mol.

TABLE 13

SYSTEMATIC ERROR COMPONENTS OF THE CALCULATED OXYGEN POTENTIALS*

Error Component	Maximum Error**	Probable Error**
Calibration- H_2 Flow	0.6	0.3
DVM Error- H_2 Flow	0.4	0.2
Barometric Pressure	nil	nil
Electrolysis Current	0.3	nil
Sample Temperature	nil	nil
Analysis- H_2 -He Gases	4.0	0.5
Calculation H_2O Equil. Const.	0.7	0.2
Flow- He Carrier Gas	nil	nil

*Calculated for nominal 1300°C.
**Error is calculated as kcal/mol.

Uranium Oxide

The data for the uranium oxides from both metal sources indicate high temperature and significantly oxidizing atmospheres are necessary for obtaining hyperstoichiometry. The isothermal data plots in the Appendices show that lengthy exposure to such conditions is necessary to achieve constant O/M. Cause of the extensive time required for equilibration may be a system artifact or slow kinetics or both. The highly oxidizing atmosphere required is obtained by a very large H_2O/H_2 ratio which is extremely sensitive to the amount of H_2 formed by H_2O oxidation of the oxide. The amount of H_2 formed by oxidation of $UO_{2.000}$ to $UO_{2.001}$ is equal to the total amount of H_2 flowing into the balance in 10 min. for He-0.15% H_2 flowing at 10 cm^3/min. Slow kinetics of bulk diffusion of the oxygen through the oxide may account for the longer equilibration times observed at the lower temperatures.

Such lengthy equilibration times suggest the desireability of using a UO_2 reference material to calibrate O/M methods for U rather than known oxygen potentials, since the conditions necessary to assure sample equilibration to the known oxygen potential cannot be predicted. A highly pure

U metal may be preferable as the metal source if it has been extensively characterized, since the data calculated for the oxide prepared from NBS SRM-960 indicate a bias probably due to the insufficient information available about its impurity contents. Whichever source is used, appropriate corrections for impurities and buoyancy effects must be applied.

Plutonium Oxide

The plutonium oxide data validate the use of a reference oxygen potential of −100 kcal/mol at 800°C for O/M analyses, subject to the same constraints applied to the uranium oxides. The reduction of PuO_2 appeared to occur much more readily than the oxidation of UO_2. This may be due to the more balanced H_2O/H_2 ratios used for equilibration or it may be due to faster kinetics of diffusion of the defect species in PuO_2. In addition to correction for impurities present in Pu metal used to prepare an O/M reference oxide, correction for the radionuclide daughters of ^{238}Pu, ^{239}Pu, and ^{240}Pu may be necessary as well as the normally corrected ^{241}Pu.

Uranium-Plutonium Oxide

Preparation of solid solution uranium-plutonium oxide O/M reference material from highly pure U and Pu metals has been demonstrated. The solid solution has been shown to display a much broader oxygen potential range at stoichiometry than the calculated range for a mixture of oxides. This broader oxygen potential range explains the discrepancy earlier discussed between the results of O/M studies for three different methods on solid solution oxides by Urie et. al.[77], and results for the same methods on oxide mixtures by Dahlby et. al.[18]. Since the three methods equilibrate to three different oxygen potentials the mixture would be expected to show a range of stoichiometries whereas the solid solution may not.

Use of the −100 kcal/mol reference oxygen potential for mixed oxide is validated by the present results for the solid solution oxide, subject to the same precautions as for UO_2 and PuO_2. Preparation of a solid solution oxide O/M reference material is recommended for calibration of those methods to be applied to solid solution oxides. Additional studies on the effects of parameters such as particle size, U/Pu ratio, gas composition, and temperature on the kinetics of equilibration are also recommended using such material.

The broad oxygen potential range of the solid solution oxide even at high temperatures suggests the use of higher temperatures (1100°C to 1200°C) to speed sample analysis. Use of low mass furnaces and high precision balances at such temperatures may significantly increase sample throughput by speeding both analyses and deadtime between analyses.

Solid State Oxygen Electrode

The lack of theoretical response from the oxygen electrode reflects the practical problems of construction of such a device. The $\mathcal{EMF}$ at any given oxygen potential and temperature was very stable and moderately reproducible. The cause of the non-theoretical nature of the response was not investigated. Construction of an independent system to calibrate the electrode $\mathcal{EMF}$ to gaseous oxygen potential would allow use of the electrode despite its lack of theoretical response.

ACKNOWLEDGEMENTS

I wish to express my gratitude to Glenn R. Waterbury and Nicholas E. Vanderborgh of the Los Alamos Scientific Laboratory, Analytical Chemistry Group, for their continued interest, advice, and encouragement throughout the course of this research. I also wish to thank Edward A. Walters of the University of New Mexico for his interest and support during the later stages of this work.

Excellent advice and materials were obtained from the Los Alamos Scientific Laboratory's Ceramics Fabrication Group, and I wish to particularly thank Steve Stoddard of that group for his interest and help. The uranium metal used in this research was obtained from the Los Alamos Scientific Laboratory's Uranium Metallurgy Group, whose contribution is gratefully acknowledged.

The text of this dissertation was prepared using the computer-phototypesetting facilities of the Los Alamos Scientific Laboratory's Technical Information Group, whose advice and assistance are very greatly appreciated and acknowledged.

REFERENCES

1. C. Sari, U. Benedict, and H. Blank, "A Study of the Ternary System UO_2 - PuO_2 - Pu_2O_3," J. Nucl. Mat. **35**, 267-277 (1970).

2. J. C. VanCraeynenst and J. C. Weilbacher, "Etude de la Conductibilite Thermique des Oxydes Mixtes d'Uranium et de Plutonium," J. Nucl. Mat. **26**, 132-136 (1968).

3. E. L. Zebroski, W. L. Lyon, and W. E. Baily, "Effect of Stoichiometry on the Properties of Mixed Oxide U-Pu Fuel," in *Proceedings of the Conference on Safety, Fuels, and Core Design in Large Fast Power Reactors*, David Okrent, Chairman, Argonne National Laboratory report ANL-7120, 374-389 (1965).

4. J. A. Christensen, "Non-Stoichiometry Effects on the Melting Heat Rating for UO_2-25wt% PuO_2 Fast Fuels - Interim Report," Batelle Northwest Laboratories report BNWL-CC-1490 (1968).

5. C. E. Johnson and G. E. Stahl, "Fission Product Distribution in Mixed Oxide Fuels," in *Chemical Engineering Division Fuels and Materials Chemistry Semiannual Report, January-June 1971*, Argonne National Laboratory report ANL-7822, 25 (1971).

6. H. R. Hoekstra and J. J. Katz, "The Chemistry of Uranium," in *The Actinide Elements*, G. T. Seaborg and J. J. Katz, Eds. (McGraw Hill, Inc., New York, 1954) pp. 130-188.

7. T. M. Florence, "A Review and Comparison of Methods for the Determination of Oxygen/Uranium Ratios in Uranium Oxides," in *Analytical Methods in the Nuclear Fuel Cycle*, Proc. Symp. Anal. Meth. in Nucl. Fuel Cycle, Vienna, November 29-December 3, 1971, pp. 45-56.

8. H. Kubota, "Determination of the Stoichiometry of Uranium Dioxide - Polarographic Determination of Uranium(VI) in Uranium Dioxide," Anal. Chem. **32**, 610-612 (1960).

9. R. W. Stromatt and R. E. Connally, "Determination of the Stoichiometry of Uranium Dioxide by Controlled Potential Coulometry," Anal. Chem. **33**, 345-346 (1961).

10. S. R. Dharwadkar and M. S. Chandrasekharaiah, "An Improved Titrimetric Method for the Determination of Uranium:Oxygen Ratios," Anal. Chim. Acta. **45**, 545-546 (1969).

11. E. A. Schaefer and J. O. Hibbits, "The Determination of Oxygen-to-Uranium Ratios in Hypo- and Hyperstoichiometric Uranium Dioxide and Tungsten-Uranium Dioxide," Anal. Chem. **41**, 254-259 (1969).

12. M. S. Chandrasekharaiah and S. R. Dharwadkar, "The Phase Equilibrium Composition of U_3O_8 and the O/U Analysis of the Urania Sample," Bhabna Atomic Research Center report B.A.R.C.-416 (1969).

13. R. J. Brouns and W. W. Mills, "The Preparation of Primary Standard U_3O_8," U.S. AEC report HW-39767 (1955).

14. E. A. Schaefer, M. R. Menke, and J. O. Hibbits, "The Determination of O/U Ratios in $UO_{2\pm x}$," General Electric Co. report GE-TM 66-4-0 (1966).

15. N. F. H. Bright, L. G. Ripley, and R. H. Lake, "The Determination of the Oxygen-Uranium Atomic Ratio in Non-Stoichiometric Uranium Dioxide and Other Oxides of Uranium," Canadian Department of Mines report MD-207 (1956).

16. K. T. Scott and K. T. Harrison, "Some Studies of the Oxidation of Uranium Dioxide," J. Nucl. Mat. 8, 307-319 (1963).

17. J. L. Drummond and V. M. Sinclair, "Some Aspects of the Measurement of the Oxygen-to-Metal Ratio in Solid Solutions of Uranium and Plutonium Dioxides," Proc. 6th Conf. Anal. Chem. in Nucl. Reactor Tech., Gatlinburg, Tenn, October 9-11, 1962, U.S. AEC report TID-7655, pp. 217-239.

18. J. W. Dahlby, T. K. Marshall, G. R. Waterbury, and G. C. Swanson, "Measurement of Oxygen-to-Metal Atom Ratios in Uranium and Plutonium Oxides" Los Alamos Scientific Laboratory report LA-5329 (1973).

19. L. E. J. Roberts and E. A. Harper, "The Determination of Oxygen in Uranium Oxides," Atomic Energy Research Establishment report A.E.R.E. C/R 885 (1952).

20. T. L. Marken, A. J. Walter, and R. J. Bones, "The Determination of Oxygen/Metal Ratios for Uranium, Plutonium, and (U,Pu) Oxides," Atomic Energy Research Establishment report AERE-R 4608 (1964).

21. H. Nickel, "Die Bestimmung des O/U-Verhaltnis in uberstoichimetrischem UO_{2+x}," Nukleonik 8, 366-372 (1966).

22. I. G. Jones, "The Determination of Oxygen-Metal Ratios in Uranium and Uranium-Plutonium Dioxides," Atomic Energy Research Establishment report AERE-R-6962 (1973).

23. B. D. Holt, "Rapid Macrodetermination of Oxygen in Uranium Oxides by Graphite Reduction," Anal. Chem. 45, 648-654 (1972).

24. C. S. MacDougall, M. E. Smith, and G. R. Waterbury, "Determination of Oxygen in Refractory Oxides," Anal. Chem. 41, 372-374 (1969).

25. H. R. Hoekstra and J. J. Katz, "Direct Determination of Oxygen in Less Familiar Metal Oxides," Anal. Chem. 25, 1608-1612 (1953).

26. T. L. Markin and R. J. Bones, "The Determination of Changes in Free Energy for Uranium Oxides Using a High Temperature Galvanic Cell-Part I," Atomic Energy Research Establishment report AERE-R 4042 (1962).

27. T. L. Markin and R. J. Bones, "The Determination of Some Thermodynamic Properties of Uranium Oxides With O/U Ratios Between 2.00 and 2.03 Using a High Temperature Galvanic Cell-Part II," Atomic Energy Research Establishment report AERE-R 4178 (1962).

28. C. Ferro, S. Moretti, and C. Patimo, "Nondestructive Method for the Determination of the Ratio O/U in Sintered Pellets," Los Alamos Scientific Laboratory translation LA-4160-TR (1970). Translation of Comitato Nazionale Energia Nucleare report CNEN Report RT/ING (67)7 (1967).

29. K. Kiukkola, "High Temperature Electrochemical Study of Uranium Oxides in the UO_2-U_3O_8 Region," Acta. Chemica. Scandanavia. 16, 327-345 (1962).

30. T. L. Markin and L. E. J. Roberts, "Thermodynamic Data for Uranium Oxides Between UO_2 and U_3O_8," in *Thermodynamics of Nuclear Materials*, (IAEA, Vienna, 1962) pp 693-711.

31. D. I. Marchidan and S. Matei, "Thermodynamic Data for Some Uranium Oxides with Nonstoichiometric Compositions," Rev. Rom. Chem. 17, 1487-1491 (1972).

32. S. Aronson and J. Belle, "Nonstoichiometry in Uranium Dioxide," J. Chem. Phys. 29, 151-158 (1958).

33. A. Companion and G. H. Winslow, "Diffuse Reflectance Measurements on Bulk Uranium Dioxide," J. Opt. Soc. Amer. 50, 1043-1045 (1960).

34. R. J. Ackerman, R. J. Thorn, and G. H. Winslow, "Visible and Ultraviolet Absorption Properties of Uranium Dioxide Films," J. Opt. Soc. Amer. 49, 1107-1112 (1959).

35. A. Arrott and J. E. Goldman, "Magnetic Analysis of the Uranium-Oxygen System," Phys. Rev. 108, 948-953 (1957).

36. P. Nagels, M. Denayer, and J. Devreese, "Electrical Properties of Single Crystals of Uranium Dioxide," Solid State Comm. 1, 35-40 (1963).

37. S. Ligenza, A. Murasik, J. Leciejewicz, and K. Solnicka, "On the Possibility of O/U Ratio Determination in UO_{2+x} Powder Samples by Neutron Diffraction," J. Nucl. Mat. 44, 345-346 (1972).

38. E. Aukrust, T. Forland, and K. Hagemark, "Equilibrium Measurements and Interpretation of Non-Stoichiometry in UO_{2+x}," in *Thermodynamics of Nuclear Materials* (IAEA, Vienna, 1962) pp 713-722.

39. T. L. Markin, V. J. Wheeler, and R. J. Bones, "High Temperature Thermodynamic Data for $UO_{2\pm x}$," J. Inorg. Nucl. Chem. 30, 807-817 (1968).

40. M. Tetenbaum and P. D. Hunt, "High Temperature Thermodynamic Properties of Oxygen Deficient Urania," J. Chem. Phys. 49, 4739-4744 (1968).

41. N. A. Javed, "Thermodynamic Study of Hypostoichiometric Urania," J. Nucl. Mat. 43, 219-224 (1972).

42. V. J. Wheeler and I. G. Jones, "Thermodynamic and Composition Changes in $UO_{2\pm x}$ ($x<0.005$) at 1950 K," J. Nucl. Mat. 42, 117-121 (1972).

43. K. Hagemark and M. Broli, "Equilibrium Oxygen Pressures over the Nonstoichiometric Uranium Oxides UO_{2+x} and U_3O_{8-z} at Higher Temperatures," J. Inorg. Nucl. Chem. 28 2837-2850 (1966).

44. R. J. Ackermann, E. G. Rauh, and M. S. Chandrasekharaiah, "A Thermodynamic Study of the Urania-Uranium System," J. Phys. Chem. 73 762-769 (1969).

45 A. Pattoret, J. Droward, and S. Smoes, "Etudes Thermodynamiques Par Spectrometrie de Masse sur le Systeme Uranium-Oxygene," in *Thermodynamics of Nuclear Materials 1967*, (IAEA, Vienna, 1968) pp 613-636.

46. P. Kofstad, *Nonstoichiometry, Diffusion, and Electrical Conductivity in Binary Metal Oxides*, (Wiley-Interscience, New York, 1972) p 319.

47. W. W. Mills, "Standardization of Plutonium Solutions by Ignition to the Oxide," U.S. AEC report HW-51822 (1957).

48. G. R. Waterbury, R. M. Douglas, and C. F. Metz, "Thermogravimetric Behaviour of Plutonium Metal, Nitrate, Sulfate, and Oxalate," Anal. Chem. **33**, 1018-1023 (1961).

49. M. J. Maurice and K. Bujis, "Some Considerations on the Gravimetric Determination of the Oxygen to Metal Ratio in Plutonium Oxides and Mixed Uranium-Plutonium Oxides," European Atomic Energy Community report EUR-4296-e (1969).

50. C. E. McNeilly and T. D. Chikalla, "Determination of Oxygen/Metal Ratios for Uranium, Plutonium, and (U,Pu) Mixed Oxides," J. Nucl. Mat. **39**, 77-83 (1971).

51. B. D. Holt and J. E. Stoessel, "Microdetermination of Oxygen in Metal Oxides by Inert Gas Fusion," Anal. Chem. **36**, 1320-1324 (1964).

52. T. L. Markin and E. J. McIver, "Thermodynamic and Phase Studies for Plutonium and Uranium-Plutonium Oxides with Application to Compatability Calculations," in *Plutonium, 1965*, A. E. Kay and W. B. Waldron, Eds., (Chapman and Hall, London, 1967) pp 845-857.

53. T. L. Markin and M. H. Rand, "Thermodynamic Data for Plutonium Oxides," in *Thermodynamics* **I**, Proc. Symp. Thermod. with Emphasis Nucl. Mat'l. and Atomic Transp't. in Solids, (IAEA, Vienna, 1966) pp 145-156.

54. T. L. Markin, R. J. Bones, and E. R. Gardner, "Thermodynamic Data for Plutonium Oxides," Atomic Energy Research Establishment report AERE-R4724 (1964).

55. L. M. Atlas and G. J. Schlehman, "Defect Equilibria of PuO_{2-x} 1100 to 1600°C," in *Thermodynamics* **II**, Proc. Symp. Thermo. with Emphasis Nucl. Mat. and Atomic Transp. in Solids, (IAEA, Vienna, 1966) pp 407-421.

56. L. M. Atlas and G. J. Schlehman, "Defect Equilibria of PuO_{2-x} 1945°C to 1545°C," in *Plutonium, 1965*, A. E. Kay and M. B. Waldron, Eds., (Chapman Hall, London, 1967) pp 838-844.

57. M. H. Rand, "Thermochemical Properties," in *Plutonium: Physico-Chemical Properties of its Compounds and Alloys*, Atomic Energy Review, **4**, 7-52 (1966).

58. C. Sari, U. Benedict, and H. Blank, "Metallographic and X-Ray Investigations in the Pu-O and U-Pu-O Systems," in *Thermodynamics of Nuclear Materials, 1967*, (IAEA, Vienna, 1968) pp 587-611.

59. W. L. Lyon, "The Measurement of Oxygen to Metal Ratio in Solid Solutions of Uranium and Plutonium Oxides," General Electric Co. report GEAP-4271 (1963).

60. I. R. McGowan, C. R. Johnson, and K. A. Swinburn, "Oxygen/Metal Ratios in Plutonium/Uranium Oxide Fuels A Study of Gravimetric Methods," in *Analytical Methods in the Nuclear Fuel Cycle*, Proc. Symp. Anal. Meth. Nucl. Fuel Cycle, (IAEA, Vienna, 1972) pp 3-21.

61. G. V. Gurumurthy, "Determination of Oxygen-to-Metal Ratios in Metal Oxide Nuclear Fuels," J. Appl. Chem. Biotechnol. **23**, 725-731 (1973).

62. N. E. Barring and G. Jonsson, "Controlled-Potential Coulometric Determination of the Oxygen-Metal Ratio in Mixed Uranium-Plutonium Oxides," Ana. Chim. Acta. **59**, 229-236 (1970).

63. N. H. Brett and A. C. Fox, "Oxidation Products of Plutonium Dioxide-Uranium Dioxide Solid Solutions in Air at 750°C," Atomic Energy Research Establishment report AERE-R 3937 (1963).

64. C. F. Metz, J. W. Dahlby, and G. R. Waterbury, "Measurement of the Oxygen to Heavy Metal Atom Ratio in Unirradiated Mixed-Oxide Fuels," in *Analytical Methods in the Nuclear Fuel Cycle*, Proc. Symp. Anal. Meth. in Nucl. Fuel Cycle, (IAEA, Vienna, 1972) pp 35-44.

65. N. Mostin and G. Valentini, "Gravimetric Determination of the Oxygen Content of Uranium-Plutonium Mixed Oxides," Euratom report EURAEC-818 (1963).

66. J. L. Drummond and H. Chapman, "Analytical Method for the Thermogravimetric Determination of the Oxygen/Metal Ratio of Uranium-Plutonium Oxides," United Kingdom Atomic Energy Authority report TRG Report 963(D) (1965).

67. R. H. Dodd, D. H. Schmitt, and R. C. Kochel, "Oxygen-to-Metal Ratio Measurement in Nuclear Fuels Using a Microthermogravimetric Technique," Presented at Thirteenth Conference on Analytical Chemistry in Nuclear Technology, Gatlinburg, TN, (October 1, 1969).

68. M. Ganivet and A. Benhamou, "Comparaison De Deux Methodes Du Rapport Oxygenne/Metal Dans Les Oxydes Mixtes D'Uranium Et De Plutonium," in *Analytical Methods in the Nuclear Fuel Cycle*, Proc. Symp. Anal. Meth. in Nucl. Fuel Cycle, (IAEA, Vienna, 1972) pp 23-33.

69. R. E. Woodley, "Equilibrium Oxygen Potential-Composition Relationships in $U_{0.75}Pu_{0.25}O_{2-x}$," Hanford Engineering Development Laboratory report HEDL-TME 72-85 (1972).

70. N. A. Javed, "Thermodynamic Behaviour of (U,Pu) Mixed Oxide Fuels," J. Nucl. Mat. 47, 336-344 (1973).

71. R. J. Bones and R. F. Carney, "A Galvanic Cell Technique for the Rapid Measurement of O/U Ratio in Oxide Fuel Pellets," Atomic Energy Research Establishment report AERE-R-6301 (1969).

72. I. Johnson, C. E. Johnson, C. E. Crouthamel, and C. A. Seils, "Oxygen Potential of Irradiated Urania-Plutonia Fuel Pins," J. Nucl. Mat. 48, 21-34 (1973).

73. M. H. Rand and T. L. Markin, "Some Thermodynamic Aspects of $(U,Pu)O_{2\pm}$ Solid Solutions and Their Use as Nuclear Fuels," in *Thermodynamics of Nuclear Materials 1967*, Proc. Symp. Thermo. Nucl. Mat. with Emphasis on Sol. Systems, (IAEA, Vienna, 1968) pp 637-650.

74. L. Jakesova, "Thermodynamic and Transport Properties in UO_2-PuO_2 and Related Systems," Czechoslovakia Nuclear Research Institute report PKP 19a/71 (1971). In Czechoslovakian.

75. "Chemical Engineering Division and Materials Chemistry Annual Report July 1973-June 1974," Argonne National Laboratory report ANL-8122 (1975). Other reports in this series include: ANL-8022, ANL-7977, ANL-7922, ANL-7877, and ANL-7822.

76. "A Thermodynamic Data Program Involving Plutonia and Urania at High Temperatures, Quarterly Report No. 23 February 1, 1973-April 30, 1973," General Electric Company report GEAP-12418 (1973), and preceeding reports.

77. M. W. Urie, M. C. Bert, and W. L. Delvin, "A Comparison of Thermogravimetric Methods Used to Determine Oxygen-to-Metal Ratios in Mixed Oxide Fuels," Hanford Engineering Development Laboratory report HEDL-TME- 72-56 (1972).

78. G. M. Barrow, *Physical Chemistry*, Second Ed, (McGraw Hill, New York, 1966) pp 211-229.

79. F. A. Kroger and H. J. Vink, "Relations Between the Concentrations of Imperfections in Crystalline Solids," in *Solid State Physics*, **3**, (Academic Press, New York, 1956) pp 310-438.

80. N. M. Tallan, H. C. Graham, R. W. Vest, and W. C. Tripp, "Relations Between Point Defects in the Compound MX_2," Aerospace Research Laboratories report ARL 68-0188 (1968).

81. J. W. Patterson, "Conduction Domains for Solid Electrolytes," J. Electrochem. Soc. **118**, 1033-1039 (1971).

82. J. B. Hardaway, III, J. W. Patterson, D. R. Wilder, and J. D. Schieltz, "Ionic Domain for Y_2O_3-Doped ThO_2 at Low Oxygen Activities," J. Amer. Ceram. Soc. **54**, 94-98 (1971).

83. D. D. Wagman, J. E. Kilpatrick, W. J. Taylor, K. S. Pitzer, and F. D. Rossini, "Heats, Free Energies, and Equilibrium Constants of Some Reactions Involving O_2, H_2, H_2O, C, CO, CO_2, and CH_4," J. Res. Nat'l. Bur. Standards, **34**, 143-161 (1945).

84. W. P. Reed, National Bureau of Standards, Personal Communication, May, 1975.

85. F. H Ellinger, C. C. Land, and K. A. Gschneidner, Jr., "Alloying Behaviour of Plutonium," in *Plutonium Handbook, A guide to the Technology*, O. J. Wick, Ed. (Gordon and Breach, New York, 1967) pp. 223-224.

86. "The International Practical Temperature Scale of 1968," Metrologia, **5**, 35-44 (1969).

87. The $\mathcal{E}_{113}$ for a Pt/Pt-10% Rh thermocouple with a 25°C cold junction was calculated by the Primary Standards Laboratory at Sandia Laboratories, Albuquerque, NM, using a National Bureau of Standards supplied computer program.

88. R. W. Headrick, "Design Criteria for Solid Electrolyte Electrochemical Cells," Lawrence Berkeley Laboratory report LBL-839 (1972).

89. E. R. Cohen, "Fundamental Constants Today," Research and Development, 32-38 (March, 1974).

90. C. E. Wicks and F. E. Block, "Thermodynamic Properties of 65 Elements Their Oxides, Halides, Carbides, and Nitrides," Bureau of Mines Bulletin 605 (U.S. Gov. Printing Off., Washington D.C., 1963).

APPENDIX A

FORTRAN Computer Program PTAPE

```
00100       PROGRAM PTAPE (INPUT,OUTPUT,TAPE6,TAPE8)
00110*
00120*      THIS PROGRAM READS A KRONOS FILE (TAPE8)
00130*      CREATED FROM THE THERMOBALANCE PUNCHED
00140*      PAPER TAPE. IT CONVERTS THE DIGITAL VOLTAGE
00150*      DATA TO SCIENTIFIC UNITS AND WRITES THE
00160*      CONVERTED DATA ONTO ANOTHER KRONOS FILE
00170*      (TAPE6) FOR FURTHER REDUCTION BY THE
00180*      PROGRAM GMDATA.
00190*
00200       DIMENSION GRAM(16), DGRAM(10), CGRAM(10)
00210       INTEGER FNAM
00220       REAL KEQ
00230*
00240*      VALUES USED TO CORRECT MECHANICAL WEIGHTS TO
00250*      NBS CALIBRATION ARE CREATED.
00260*
00270       DATA (GRAM(I),I=1,16)/0.0,0.999903,1.999922,2.999830,4.000195,
00280+      5.000103,6.000117,7.000025,8.000286,9.000144,10.000153,
00290+      11.000066,12.000041,13.000289,14.000358,15.000261/,
00300+      (DGRAM(J)J=1,10)/0.0,0.100068,0.200040,0.300111,0.400093
00310+      0.499996,0.600039,0.700044,0.800107,0.900094/,
00320+      (CGRAM(K),K=1,10)/0.0,0.010012,0.019993,0.029996,0.040018,
00330+      0.050048,0.060055,0.070027,0.080089,0.090061/
00340*
00350*      THE DATA COUNTER J IS INITIALIZED
00360*
00370    10 J=1
00380*
00390*      THE DATA FILE IDENTIFICATION IS READ.
00400*
00410       READ (8,370)FNAM,A1,A2,A3,A4,A5,A6
00420*
00430*      THE INPUT FILE IS TESTED FOR AN END-OF-FILE,
00440*      WHICH TERMINATES THE PROGRAM.
00450*
00460       IF (EOF,8) 360,20
00470    20 CONTINUE
00480*
00490*      THE FILE IDENTIFICATION IS WRITTEN ON
00500*      THE TIME-SHARE TELETYPE AND THE OUTPUT FILE.
00510*
00520       PRINT 400, FNAM,A1,A2,A3,A4,A5,A6
00530       WRITE (6,410)FNAM,A1,A2,A3,A4,A5,A6
00540*
00550*      THE FILE INITIAL DATA PARAMETERS ARE READ.
00560*      THE PARAMETERS ARE: BALANCE RANGE (MG),
00570*      THERMOCOUPLE TEMPERATURE RANGE, DATA START
00580*      TIME, DATA RECORDING TIME INTERVAL, BAROMETRIC
00590*      PRESSURE, ROOM TEMPERATURE, MOISTURE MONITOR
00600*      SCALE FACTOR, ARGON FLOWMETER READING,
00610*      HE-CARRIER GAS FLOWMETER READING, H2-MASS
00620*      FLOWMETER NOMINAL READING, HYDROGEN IN
00630*      THE REDUCING GAS, AND BALANCE MECHANICAL
00640*      WEIGHT SET VALUES.
00650*
00660       READ (8,230)RNG,ISENSE,TSTART,DTH,PRESS,TGAS,PPSK,ARP,ARCGI,H2FLOW
00670+      ,HCON,TARE
00680*
00690*      INITIAL CALCULATION OF PARAMETERS IS PERFORMED.
00700*
```

```
00710         GO TO 270
00720*
00730*        THE REPETITIVE DVH DATA IS READ.
00740*
00750      30 IDENT=-1
00760      40 READ (8,400)TEMP,WT,H2OI,H2OR,EXWT,H2MFM
00770*
00780*        THE REPETITIVE DATA IS TESTED FOR A CHANGE IN PARAMETERS.
00790*
00800         IF (TEMP.EQ.0.0.AND.WT.EQ.0.0.AND.H2OI.EQ.0.0.AND.H2OR.EQ.0.0.AND.
00810+        EXWT.EQ.0.0.AND.H2MFM.EQ.0.0) GO TO 120
00820*
00830*        TEMPERATURE IS COMPUTED FROM THE THERMOCOUPLE EMF.
00840*
00850         IF (ISENSE.EQ.0) ADV=0.000
00860         IF (ISENSE.EQ.1) ADV=0.010
00870         IF (J.NE.1) GO TO 50
00880         GO TO 80
00890*
00900*        INSERTION OF 10 MV BUCKING POTENTIAL IS TESTED.
00910*
00920      50 IF (TEMP.LT.0.002.AND.TH.GT.0.008.AND.ISENSE.EQ.0) GO TO 60
00930         IF (TEMP.GT.0.008.AND.TH.LT.0.002.AND.ISENSE.EQ.1) GO TO 70
00940         GO TO 80
00950      60 ADV=0.010
00960         ISENSE=1
00970         GO TO 80
00980      70 ADV=0.000
00990         ISENSE=0
01000      80 TH=TEMP
01010         THV=(TH+ADV)*1000.
01020*
01030*        IF THERMOCOUPLE OUTPUT IS NEGATIVE
01040*        TEMPERATURE IS SET TO 293.15 DEGREES K.
01050*
01060         IF (THV.LE.0.0) GO TO 90
01070*
01080*        TEMPERATURE IS CALCULATED FROM THERMOCOUPLE EMF.
01090*
01100         TEMP=25.62*(1.0-(EXP(-1.905*(THV**1.078))))+293.15+(119.38*THV)+(-
01110+        2.578*THV**2.)+(0.05965*THV**3.)
01120         GO TO 100
01130      90 TEMP=293.2
01140     100 CONTINUE
01150*
01160*        THE DATA TIME IS COMPUTED FROM START TIME, TIME INTERVAL, AND
01170*        THE DATA POINT NUMBER.
01180*
01190         IF (J.NE.1) GO TO 120
01200     110 TIME=TJTART
01210         GO TO 140
01220     120 KT=IFIX(TIM)
01230         TK=KT
01240         TR=TIM-TK
01250         TR=(100.*TR)+DTH
01260         IF (TR.GE.60.) GO TO 130
01270         TIME=TK*(TR/100.)
01280         GO TO 140
01290     130 TR=TR-60.
01300         TK=TK+1.
01310         IF (TK.GE.25.) TK=TK-24.
01320         TIME=TK*(TR/100.)
01330     140 TIM=TIME
01340         IF (IDENT.EQ.0) GO TO 30
01350*
01360*        THE WEIGHT IS CALCULATED FROM DIGITAL VOLTAGES
01370*        AND CORRECTED MECHANICAL WEIGHTS.
01380*
01390         AA=1000.*WT
01400         K=IFIX(AA)
```

```
01610         B=K
01620         AA=AA-B
01630         IF (AA.GT.0.75.AND.EXWT.LT.0.002) B=B+1
01640         IF (AA.LT.0.25.AND.EXWT.GT.0.007) B=B-1
01650         B=B*RNG*0.0001
01660         EXWT=EXWT*RNG*0.01
01670         WT=TARE+B+EXWT
01680*
01690*        H2O AND H2 PARTIAL PRESSURES ARE COMPUTED
01700*        FROM H2O ELECTROLYSIS CURRENT AND H2 FLOW.
01710*        THE OXYGEN PARTIAL PRESSURE AND OXYGEN
01720*        POTENTIAL ARE ALSO CALCULATED.
01730*
01740         H2OI=H2OI*10.
01750         IF (H2OI.LT.0.) H2OI=-H2OI
01760         IF (H2OI.EQ.0.) H2OI=0.001
01770*
01780*        H2O FLOW IS CALCULATED FROM ELECTROLYSIS CURRENT.
01790*
01800         H2OFL=0.000960*H2OI
01810*
01820*        H2 MASS FLOWMETER OUTPUT IS TESTED FOR
01830*        MEANINGFUL VALUES.
01840*
01850         IF (H2MFM.LT.0.00303.OR.H2MFM.GT.0.00500) GO TO 160
01860*
01870*        H2 FLOW CALIBRATION EQUATION IS DETERMINED BY
01880*        HYDROGEN GAS CONCENTRATION.
01890*
01900         IF (H2SCN.LT.0.) GO TO 150
01910         H2F=-1.599*(53.618*1000.*H2MFM)
01920         GO TO 170
01930    150  H2F=(70.27*1000.*H2MFM)-0.51
01940         GO TO 170
01950    160  H2F=H2FL
01960    170  CONTINUE
01970*
01980*        GAS FLOWS ARE SUMMED.
01990*
02000         GASFL=(H2OFL+H2F+ALGF+ARFF)*(PRESS/520.)*((273.15+TGAS)/298.15)
02010         H2F=(H2SCN/100.)*H2F
02020*
02030*        H2O PARTIAL PRESSURE IS CALCULATED.
02040*
02050         H2OATM=(0.760*H2OFL)/GASFL
02060*
02070*        H2 PARTIAL PRESSURE IS CALCULATED.
02080*
02090         H2ATM=(0.760*H2F)*(PRESS/520.)*((273.15+TGAS)/298.15))/(GASFL)
02100         TKEL=TEMP
02110*
02120*        H2O EQUILIBRIUM CONSTANT IS CALCULATED.
02130*
02140         EXPKO=-0.0363+(103.72/TKEL)-(144575.34/(TKEL**2.))
02150         KEQ=10.0**EXPKO
02160*
02170*        OXYGEN PARTIAL PRESSURE IS CALCULATED.
02180*
02190         PO2=(H2OATM**2.)/((H2ATM**2.)*(KEQ**2.))
02200*
02210*        DEFAULT OXYGEN PARTIAL PRESSURE IS ASSIGNED.
02220*
02230         IF (H2OI.LT.0.05.OR.H2FL.EQ.0.) PO2=0.0
02240         PO=1.0
02250         IF (PO2.NE.0.0) PO=PO2
02260*
02270*        OXYGEN POTENTIAL IS COMPUTED,
02280*        (KCAL/MOL AND KJOUL/MOL).
02290*
02300         DGO2=(1.9879*TKEL)*(ALOG(PO))
02310         SIDGO2=(0.01441*TKEL)*(ALOG(PO))
```

```
C
C     MOISTURE MONITOR READING IS COMPUTED.
C
      PPSK=FLOAT(PPSK)
      H2OR=PPSK*H2OR*10.0
C
C     ALL COMPUTATIONS ARE NOW COMPLETE.
C     THE DATA IS WRITTEN ONTO THE KRONOS OUTPUT FILE,
C     AND A NEW LINE OF DATA IS READ.
C
      WRITE (6,410)TIME,TEMP,WT,H2O1,H2OATM,H2ATM,H2OR,DG02,P02
      J=J+1
      GO TO 40
C
C     FOR CHANGES IN INITIAL PARAMETERS,
C     THE IDENTIFIER OF THE CHANGED PARAMETER IS READ.
C
  120 READ (5,420)IDENT
      IF (IDENT.EQ.0) GO TO 190
      IF (IDENT.EQ.1) GO TO 200
      IF (IDENT.EQ.2) GO TO 210
      IF (IDENT.EQ.3) GO TO 220
      IF (IDENT.EQ.4) GO TO 230
      IF (IDENT.EQ.5) READ (5,420)PPSK
      IF (IDENT.EQ.6) READ (5,390)TGAS
      IF (IDENT.EQ.7) READ (5,390)PRESS
      IF (IDENT.EQ.8) READ (5,390)DTH
      IF (IDENT.EQ.9) GO TO 240
      IF (IDENT.EQ.10) READ (5,420)ISENSE
      IF (IDENT.EQ.11) READ (5,390)RNG
      IF (IDENT.EQ.12) GO TO 250
C
C     AN END OF FILE IS SIGNIFIED BY IDENT=99.
C
      IF (IDENT.EQ.99) GO TO 260
      GO TO 40
C
C     ALPHANUMERIC COMMENTS ARE READ AND PRINTED ON
C     THE TIME-SHARE TELETYPE.
C
  190 READ (5,430)C1,C2,C3,C4,C5,C6,C7
      PRINT 430, C1,C2,C3,C4,C5,C6,C7
      GO TO 40
C
C     A NEW MECHANICAL WEIGHT SET VALUE IS READ.
C
  200 READ (5,390)TARE
      GO TO 220
C
C     A NEW NOMINAL H2 FLOW VALUE IS READ.
C
  210 READ (5,390)H2FLOW
      GO TO 200
C
C     A NEW H2-CARRIER FLOW VALUE IS READ.
C
  220 READ (5,390)ARGG1
      GO TO 220
C
C     A NEW ARGON FLOW VALUE IS READ.
C
  230 READ (5,390)ARP
      GO TO 240
C
C     A NEW DATA RESTART TIME IS READ.
C
  240 READ (5,390)TSTART
      GO TO 110
C
C     A NEW PREMIX HYDROGEN CONCENTRATION IS READ.
```

```
02820*
02830     250 READ (3,390)HCON
02840         GO TO 290
02850*
02860*        AN END OF FILE IS WRITTEN.
02870*        A TEST IS MADE FOR AN ADDITIONAL DATA FILE.
02880*
02890     260 END FILE 6
02900         GO TO 10
02910     270 CONTINUE
02920*
02930*        NONREPETITIVE CALCULATIONS FROM INITIAL (J=1)
02940*        AND CHANGED (J>1) PARAMETERS ARE PERFORMED.
02950*
02960*        MECHANICAL WEIGHT CORRECTIONS ARE MADE BASED
02970*        ON HCS CALIBRATIONS.
02980*
02990     280 IGH=IFIX(TARE)
03000         GH=IGH
03010         IGH=IGH+1
03020         DGH=TARE-GH
03030         DGH=(DGH*10.)+.02
03040         IDGH=IFIX(DGH)
03050         DGH3=IDGH
03060         IDGH=IDGH+1
03070         CGH=DGH-DGH3
03080         CGH=CGH*10.
03090         ICGH=IFIX(CGH)
03100         ICGH=ICGH+1
03110         TARE=GRAM(IGH)+DGRAM(IDGH)+CGRAM(ICGH)
03120         IF (J.NE.1) GO TO 40
03130*
03140*        H2 PARAMETERS (FLOW AND PREMIX CONCENTRATION)
03150*        ARE CALCULATED.
03160*
03170     290 IF (HCON.LT.25.) H2SIGN=-1.0
03180*
03190*        H2SIGN SELECTS THE FLOW CALIBRATION USED.
03200*
03210         H2FL=+1.962*H2FLOW
03220         IF (HCON.GE.25.) GO TO 300
03230         GO TO 310
03240     300 H2SIGN=1.0
03250         IF (H2FLOW.EQ.0.0) H2FL=0.0
03260         IF (H2FLOW.EQ.0.0) GO TO 310
03270         H2FL=-1.809+(1.567*H2FLOW)
03280     310 CONTINUE
03290         IF (J.NE.1) GO TO 40
03300*
03310*        HE CARRIER GAS FLOW IS CALCULATED.
03320*
03330     320 IF (ARCGI.EQ.0.0) ARCF=0.0
03340         IF (ARCGI.EQ.0.0) GO TO 330
03350         ARCF=(-11.97)+(1.065*ARCGI)+(7.097*(ALOG(ARCGI)))
03360     330 IF (J.NE.1) GO TO 40
03370*
03380*        ARGON PURGE GAS FLOW IS CALCULATED.
03390*
03400     340 IF (ARP.EQ.0.0) ARPF=0.0
03410         IF (ARP.EQ.0.0) GO TO 350
03420         ARPF=(24.027)+(-10.737*ARP)+(1.853*(ARP**2.))
03430     350 IF (J.NE.1) GO TO 40
03440*
03450*        ALL NON-REPETITIVE CALCULATIONS ARE COMPLETED.
03460*
03470         GO TO 40
03480     360 STOP
03490*
03500     370 FORMAT (2X,I8,6A10)
03510     380 FORMAT (F9.0,/,I3,4(/,F9.0),/,I3,5(/,F9.0))
03520     390 FORMAT (F9.0)
```

```
03530     400 FORMAT (6E11.0)
03540     410 FORMAT (I8,/,6A10)
03550     420 FORMAT (1X)
03560     430 FORMAT (10X,I8, ',6A10)
03570     440 FORMAT (9E14.7)
03580     450 FORMAT (7A10)
03590         END
```

APPENDIX B

FORTRAN Computer Program OMDATA

```
      PROGRAM OMDATA (INPUT,OUTPUT,TAPE2,TAPE4,TAPE6)
C
C     THIS PROGRAM CALCULATES O/H VALUES FROM A KRONOS
C     O/H DATA FILE (TAPE4) AND A KRONOS BLANK DATA
C     FILE (TAPE2). THE O/H DATA ARE OUTPUT TO KRONOS
C     DATA FILE TAPE6.
C
C     THE INITIAL METAL WEIGHT, OXYGEN WEIGHT IN THE
C     THEORETICAL DIOXIDE, CORRECTION FOR CRUCIBLE TARE,
C     RECORDING FILE INTERVAL, AND A CORRECTION FOR
C     BUOYANCY AND IMPURITY EFFECTS ARE REQUESTED
C     THROUGH THE TIME-SHARE TERMINAL.
C
      PRINT,*ENTER METAL WT, THEO O2 WT, DTARE  , DELTA TIME, DWEIGHT*
      PRINT,*/          //          //          //          //          /*
      READ 120, UWT,O2WT,DTARE,DLTH,DWT
      J=1
      I=1
C
C     IDENTIFICATION IS READ FROM BLANK AND DATA
C     FILES AND WRITTEN ONTO THE TELETYPE AND
C     THE OUTPUT FILE.
C
      READ (2,100)JNAM,A1,A2,A3,A4,A5,A6
      READ (4,100)JNAM,B1,B2,B3,B4,B5,B6
      WRITE (6,140)JNAM,INAM
      PRINT 150, JNAM, INAM
      WRITE (6,160)B1,B2,B3,B4,B5,B6
      PRINT 160, B1,B2,B3,B4,B5,B6
   10 CONTINUE
C
C     THE DATA LINES ARE READ FROM EACH FILE.
C     THE BLANK FILE IS TO BE SYNCHRONIZED TO
C     THE DATA FILE BY TIME OF DAY. SYNCHRONY
C     IS TESTED, AND THE BLANK FILE IS POSITIONED
C     AS NECESSARY FOR SYNCHRONIZATION.
C
      READ (2,170)TIM,B1,WT1,B2,B3,B4,B5,B6,B7
      IF (EOF,2) 100,20
   20 READ (4,170)TIM,TEMP,WT2,W1,WA,HA,WR,BG02,P02
      IF (EOF,4) 120,30
   30 CONTINUE
      DTH=ABS(TIM-TIH)
      IF (DTH.GT.(.75*DLTH/100.)) GO TO 60
C
C     WHEN THE FILES ARE SYNCHRONIZED, THE
C     WEIGHT OF THE OXIDE IS CALCULATED FROM
C     THE DATA FILE SAMPLE WEIGHT, BLANK WEIGHT,
C     AND BUOYANCY PLUS IMPURITY CORRECTION.
C
      UOX=WT2+DWT-(WT1+DTARE)
C
C     THE MEASURED OXYGEN WEIGHT IS THE DIFFERENCE
C     BETWEEN THE OXIDE WEIGHT AND THE METAL WEIGHT.
C
      OX=UOX-UWT
C
C     THE O/H RATIO IS CALCULATED AS TWICE THE
C     RATIO OF MEASURED TO THEORETICAL OXYGEN WEIGHTS.
C
      OH=2.*(OX/O2WT)
```

```
00720*
00730*      THE CHANGE IN O/M IS ALSO CALCULATED.
00740*
00750       IF (J.EQ.1) GO TO 40
00760       DOM=OM-OMPST
00770       OMPST=OM
00780       GO TO 50
00790   40  DOM=0.0
00800       OMPST=OM
00810*
00820*      THE DATA WRITTEN ONTO THE KRONOS OUTPUT FILE
00830*      FOR FURTHER PROCESSING INCLUDE:
00840*      TIME OF DAY, TEMPERATURE, O/M, OXYGEN
00850*      POTENTIAL, OXYGEN PARTIAL PRESSURE, O/M
00860*      CHANGE, ELECTROLYSIS CURRENT, AND MOISTURE
00870*      MONITOR READING; ALL CALCULATED FROM THE
00880*      OXIDE DATA FILE.
00890*
00900   50  WRITE (6,100)TIM,TEMP,OM,DG02,P02,DOM,WI,WR
00910       J=J+1
00920       GO TO 10
00930*
00940*      THIS SECTION POSITIONS TAPE2 AS NECESSARY
00950*      TO SYNCHRONIZE IT TO TAPE4.
00960*
00970   60  IF (TIM.LT.TI) GO TO 80
00980       IF (TIM.GT.S.15.AND.TM.LT.S.15) GO TO 90
00990   70  READ (2,130)TM,D1,WT1,D2,D3,D4,D5,D6,D7
01000       IF (EOF,2) 100,80
01010   80  IF (TIM.LT.S.15.AND.TM.GT.S.15) GO TO 70
01020   90  BACKSPACE 2
01030       BACKSPACE 2
01040       GO TO 70
01050  100  REWIND 2
01060       K=K+1
01070*
01080*      IF TAPE2 IS REWOUND 3 TIMES IN AN EFFORT
01090*      TO SYNCHRONIZE IT TO TAPE4, TAPE6 IS
01100*      ENDFILED AND THE PROGRAM IS TERMINATED.
01110*
01120       IF (K.GE.4) GO TO 110
01130       READ (2,130)K,A1,A2,A3,A4,A5,A6
01140       GO TO 70
01150       PRINT 210, TIM
01160  120  END FILE 6
01170       STOP
01180*
01200  130  FORMAT (I8,/,6A10)
01210  140  FORMAT (2X,I8,2X,I8)
01220  150  FORMAT (  3,16H EVALUATED VERSUS ,I8)
01230  160  FORMAT (2X,6A10)
01240  170  FORMAT (20H IS EVALUATED VERSUS,/,2X,6A10)
01250  180  FORMAT (9E14.7)
01260  190  FORMAT (8E14.7)
01270  200  FORMAT (40H  BLANK FILE REWOUND THREE TIMES,       )
01280  210  FORMAT (20H  AT A DATA FILE TIME OF      ,F7.3)
01290  220  FORMAT (5F12.8)
01300       END
```

APPENDIX C

Uranium Oxide O/M Zetaplots

The data plotted are:

O/M Ratio, Solid Line, Unmarked

Oxygen Potential, Solid Line, Marked by "X"

Moisture Monitor Reading, Solid Line, Marked by "+"

The plots are coded in the lower right corner as follows:

Two letters specifying U metal source used,

UN = Uranium oxide prepared from NBS SRM-960 U metal.

UL = Uranium oxide prepared from LASL Lot UR-1261 U metal.

Two digits specifying nominal temperature x 100°C.

08 = 800°C etc.

One digit signifying a plot sequence number at each temperature.

The bracketed regions of the O/M curves, labeled with lower case letters, delineate regions used to calculate the data listed in TABLES 8 and 9.

UN-13-1
2.026071 G U 1300 DEG 1.8H2
a
b
c
d
DELTA G 02 <CALCULATED- KCALS/MOLE>-X
50.00 65.00 80.00 95.00 110.00 125.00 140.00
MOISTURE MONITOR READING-+
0.00 0.20 0.40 0.60 0.80 1.00 1.20
DELTA 0/M =1000<0/M-2.000>
-15.00 -10.00 -5.00 0.00 5.00 10.00 15.00
0.00 20.00 40.00 60.00 80.00 100.00 120.00 140.00 160.00
TIME <MINUTES>
X10

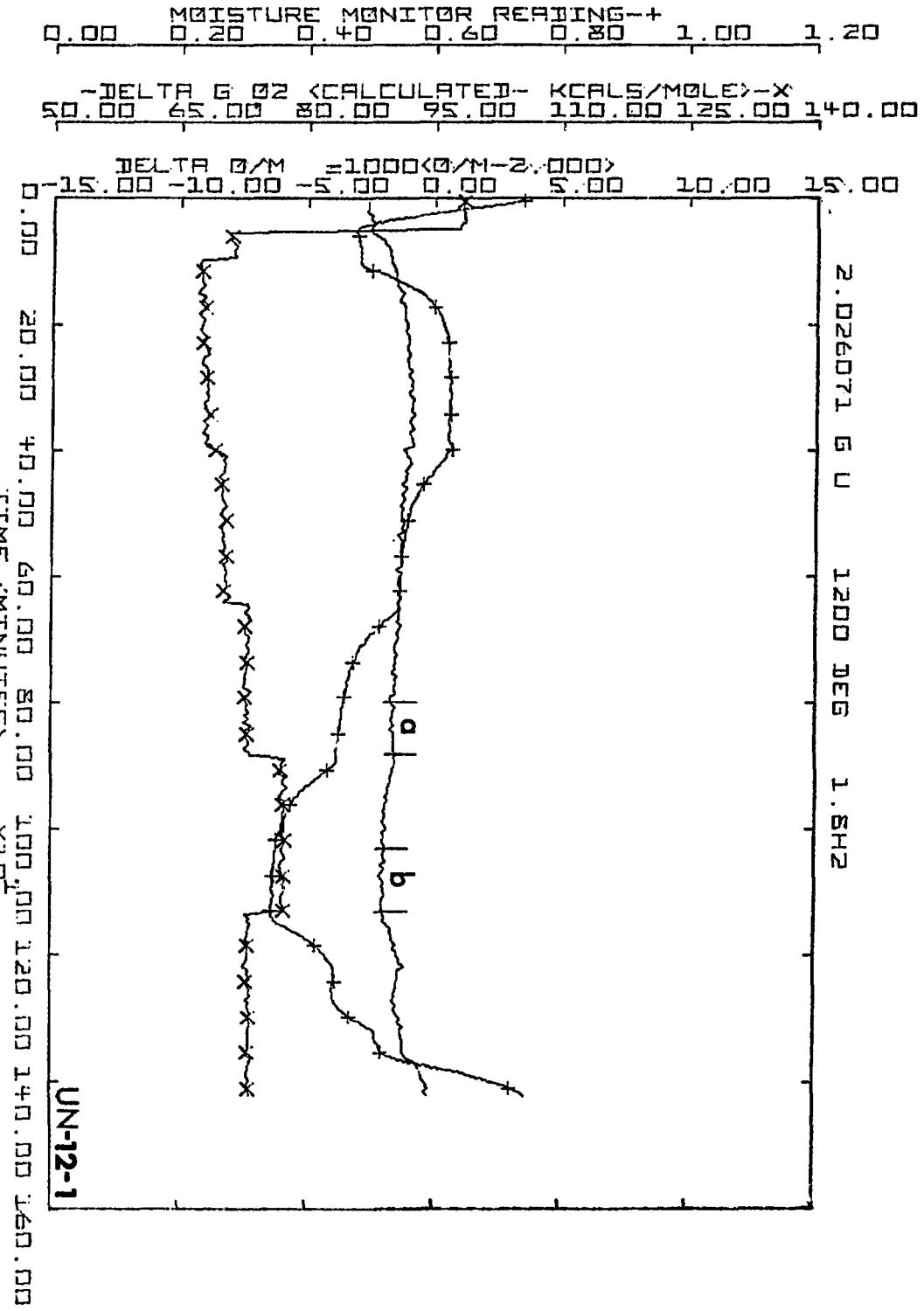
MOISTURE MONITOR READING-+
0.00 0.20 0.40 0.60 0.80 1.00 1.20
-DELTA G 02 (CALCULATED)- KCALS/MOLE)-X
50.00 65.00 80.00 95.00 110.00 125.00 140.00
DELTA Ø/M =1000(Ø/M-2.000)
-15.00 -10.00 -5.00 0.00 5.00 10.00 15.00
TIME (MINUTES)
0.00 20.00 40.00 60.00 80.00 100.00 120.00 140.00 160.00
X10
a
b
UN-12-1
2.026071 G U 1200 DEG 1.5H2

UN-11-1
a
b
c
TIME <MINUTES>
DELTA G/M =1000(G/M-2.000)
MOISTURE MONITOR READING-+
-DELTA G G2 (CALCULATED- KCAL5/MOLE)-X

UN-11-2
a
b
c
TIME <MINUTES>
DELTA G 02 <CALCULATED- KCALS/MOLE>-X
DELTA O/M =1000<O/M-2.000>
MOISTURE MONITOR READING-+
2.026017 G U 1100 DEG 0.1H2

UN-10-1
2.026071 B U 1000 DEG 0.7H2
MOISTURE MONITOR READING-+
0.00 0.20 0.40 0.60 0.80 1.00 1.20
-DELTA G 02 <CALCULATED- KCALS/MOLE>-X
50.00 65.00 80.00 95.00 110.00 125.00 140.00
DELTA 0/M =1000<0/M-2.000>
-15.00 -10.00 -5.00 0.00 5.00 10.00 15.00
0:00 20.00 40.00 60.00 80.00 100.00 120.00 140.00 160.00
TIME <MINUTES>
X10
a
b
c
d

UN-10-2
2.026071 S U 1000 DEG 0.1H2
MOISTURE MONITOR READING-+
-DELTA G 02 (CALCULATED- KCALS/MOLE)-X
DELTA 0/M =1000(0/M-2.000)
TIME (MINUTES) X10^1
a
b
c

UN-09-1
2.026071 G U 900 DEG 0.7HZ
DELTA G/M =1000(G/M-2.000)
-15.00 -10.00 -5.00 0.00 5.00 10.00 15.00
0.00 20.00 40.00 60.00 80.00 100.00 120.00 140.00 160.00
TIME (MINUTES)
X10
a
b
c
d
-DELTA G O2 (CALCULATED- KCALS/MOLE)-X
50.00 65.00 80.00 95.00 110.00 125.00 140.00
MOISTURE MONITOR READING-+
0.00 0.20 0.40 0.60 0.80 1.00 1.20

MOISTURE MONITOR READING-+
0.00 0.20 0.40 0.60 0.80 1.00 1.20
-DELTA G 02 (CALCULATED- KCALS/MOLE)-X
50.00 65.00 80.00 95.00 110.00 125.00 140.00
DELTA O/M =1000(O/M-2.000)
-15.00 -10.00 -5.00 0.00 5.00 10.00 15.00
TIME (MINUTES)
00.00 20.00 40.00 60.00 80.00 100.00 120.00 140.00 160.00
XIO
2.026071 G U 900 DEG 0.1HZ
UN-09-2
a
b

UN-08-1
2.026071 G U 800 DEG 0.7H2
DELTA O/M =1000(O/M-2.000)
TIME (MINUTES)
MOISTURE MONITOR READING-+
-DELTA G O2 (CALCULATED- KCALS/MOLE)-X
a
b
c
d

UI-13-1
2.686994 G U, 1300 DEG, 1.8 PCNT H2
a
b
c
d
DELTA D/M =1000(D/M-2.000)
-15.00 -10.00 -5.00 0.00 5.00 10.00 15.00
TIME (MINUTES)
0.00 20.00 40.00 60.00 80.00 100.00 120.00 140.00 160.00
MOISTURE MONITOR READING-+
0.00 0.20 0.40 0.60 0.80 1.00 1.20
-DELTA G O2 (CALCULATED- (CALS/MOLE)-X
50.00 65.00 80.00 95.00 110.00 125.00 140.00

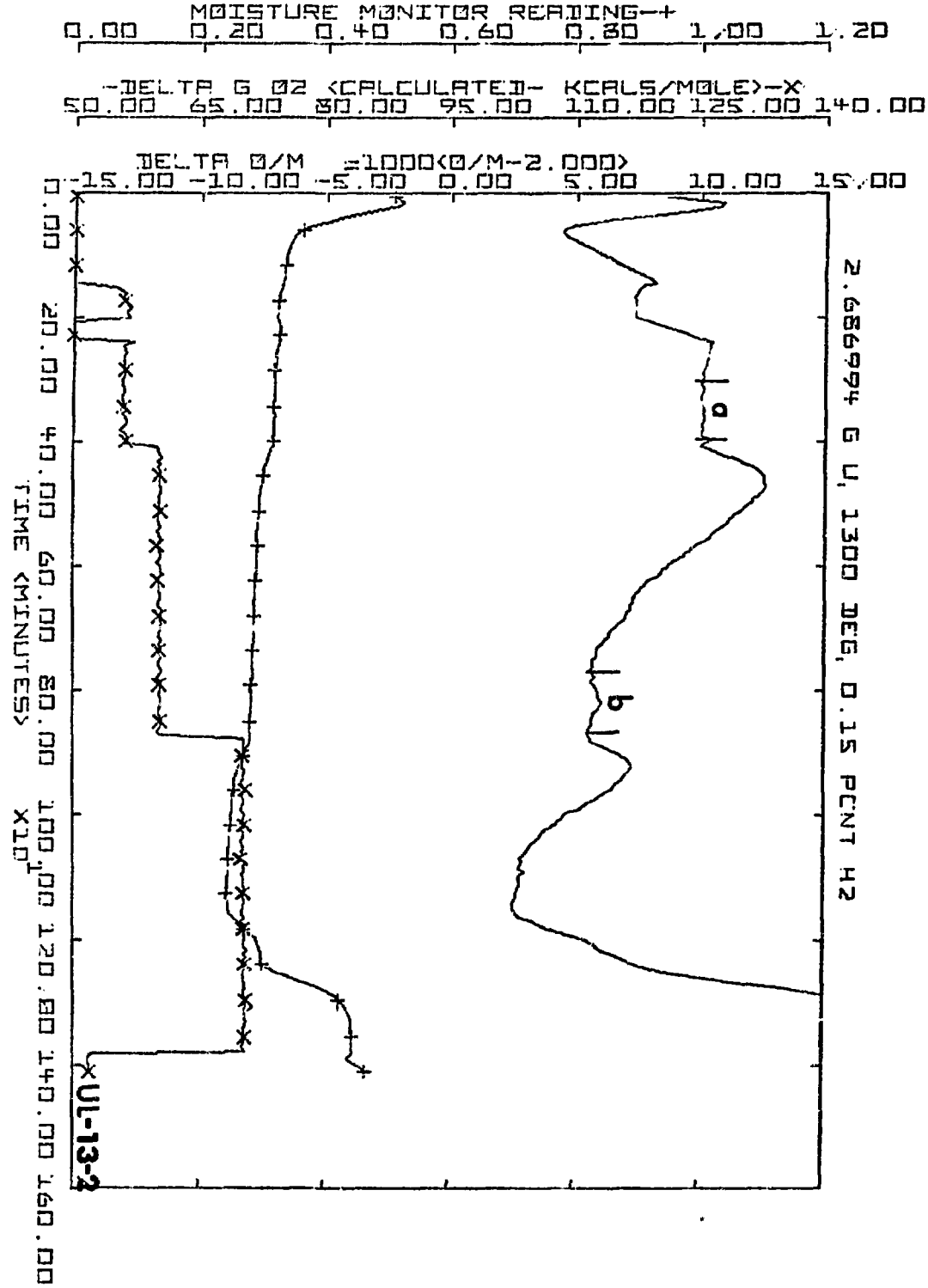
MOISTURE MONITOR READING-+
0.00 0.20 0.40 0.60 0.80 1.00 1.20
-DELTA G 02 (CALCULATED)- KCALS/MOLE)-X
50.00 65.00 80.00 95.00 110.00 125.00 140.00
DELTA 0/M =1000(0/M-2.000)
-15.00 -10.00 -5.00 0.00 5.00 10.00 15.00
TIME (MINUTES)
0.00 20.00 40.00 60.00 80.00 100.00 120.00 140.00 160.00
UI-13-2
a
b
2.688694 G U, 1300 DEG, 0.15 PCNT H2

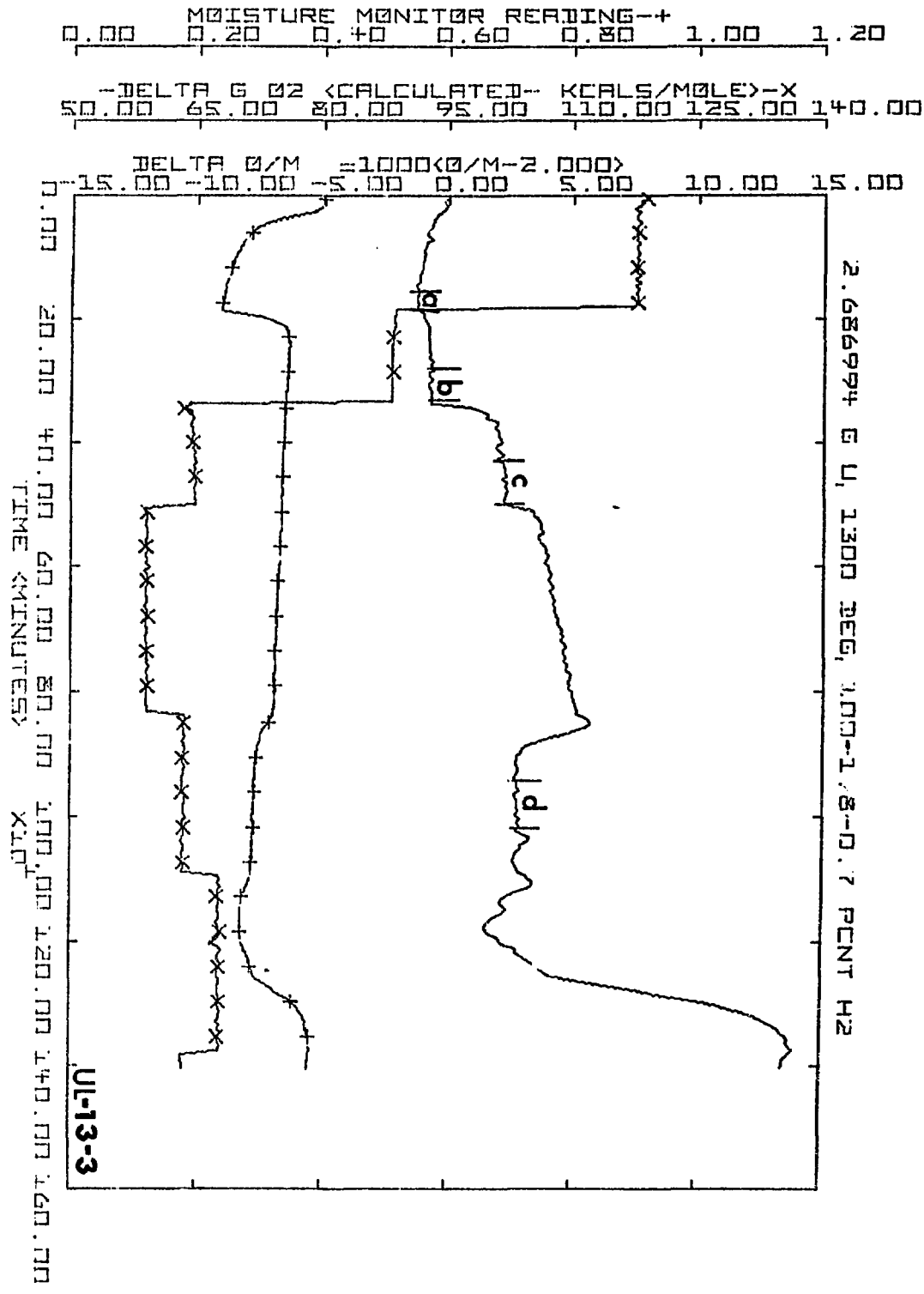
MOISTURE MONITOR READING-+
0.00 0.20 0.40 0.60 0.80 1.00 1.20
-DELTA G 02 <CALCULATED- KCALS/MOLE>-X
50.00 65.00 80.00 95.00 110.00 125.00 140.00
DELTA O/M =1000<O/M-2.000>
-15.00 -10.00 -5.00 0.00 5.00 10.00 15.00
2.686694 G U, 1300 DEG, 100-1.8-0.7 PCNT H2
UI-13-3
a
b
c
d
TIME (MINUTES)
0.00 20.00 40.00 60.00 80.00 100.00 120.00 140.00 160.00
X10

UL-12-1
2.686994 G U, 1200 DEG, 100, 1.8, 0.7 PCNT H2
DELTA G/M =1000(G/M-2.000)
-15.00 -10.00 -5.00 0.00 5.00 10.00 15.00
a
b
c
TIME (MINUTES) x10
0.00 20.00 40.00 60.00 80.00 100.00 120.00 140.00 160.00
-DELTA G O2 (CALCULATED- KCALS/MOLE)-X
50.00 65.00 80.00 95.00 110.00 125.00 140.00
MOISTURE MONITOR READING-+
0.00 0.20 0.40 0.60 0.80 1.00 1.20

MOISTURE MONITOR READING-+
0.00 0.20 0.40 0.60 0.80 1.00 1.20
-DELTA G 02 (CALCULATED)- KCALS/MOLE)-X
50.00 65.00 80.00 95.00 110.00 125.00 140.00
DELTA 0/M =1000(0/M-2.000)
-15.00 -10.00 -5.00 0.00 5.00 10.00 15.00
2.686994 G U, 1200 DEG, 0.15 PCNT H2
a
b
c
d
UI-12-2
TIME (MINUTES)
XLOT

UL-11-1
2.686994 G U, 1100 DEG, 100, 1.8, 0.15 PCNT H2
a
b
c
DELTA G/M =1000(G/M-2.000)
-15.00 -10.00 -5.00 0.00 5.00 10.00 15.00
TIME <MINUTES> X10^0
0.00 20.00 40.00 60.00 80.00 100.00 120.00 140.00 160.00
-DELTA G 02 (CALCULATED- KCALS/MOLE)-X
50.00 65.00 80.00 95.00 110.00 125.00 140.00
MOISTURE MONITOR READING-+
0.00 0.20 0.40 0.60 0.80 1.00 1.20

UL-11-2
2.686994 G U, 1180 DEG, 100, 1.8, 0.7 PCNT H2
DELTA D/M =1000(D/M-2.000>
-15.00 -10.00 -5.00 0.00 5.00 10.00 15.00
0.00 20.00 40.00 60.00 80.00 100.00 120.00 140.00 160.00
TIME <MINUTES> X10
MOISTURE MONITOR READING-+
0.00 0.20 0.40 0.60 0.80 1.00 1.20
-DELTA G 02 <CALCULATED- KCALS/MOLE>-X
50.00 65.00 80.00 95.00 110.00 125.00 140.00

UL-11-3
2.686994 G U, 1100 DEG, 100, 1.8, 0.7 PCNT H2
MOISTURE MONITOR READING-+
0.00 0.20 0.40 0.60 0.80 1.00 1.20
-DELTA G O2 <CALCULATED- KCALS/MOLE>-X
50.00 65.00 80.00 95.00 110.00 125.00 140.00
DELTA O/M =1000<O/M-2.000>
-15.00 -10.00 -5.00 0.00 5.00 10.00 15.00
0.00 20.00 40.00 60.00 80.00 100.00 120.00 140.00 160.00
TIME <MINUTES>
X10⁴

MOISTURE MONITOR READING-+
0.00 0.20 0.40 0.60 0.80 1.00 1.20
-DELTA G 02 (CALCULATED)- KCALS/MOLE)-X
50.00 65.00 80.00 95.00 110.00 125.00 140.00
DELTA 0/M =1000(0/M-2.000)
-15.00 -10.00 -5.00 0.00 5.00 10.00 15.00
0.00 20.00 40.00 60.00 80.00 100.00 120.00 140.00 160.00
TIME (MINUTES)
XLO
UL-10-1
a
b
c
2.689694 G U, 1000 MCG, 100, 1.8, 0.11 PCNT H2

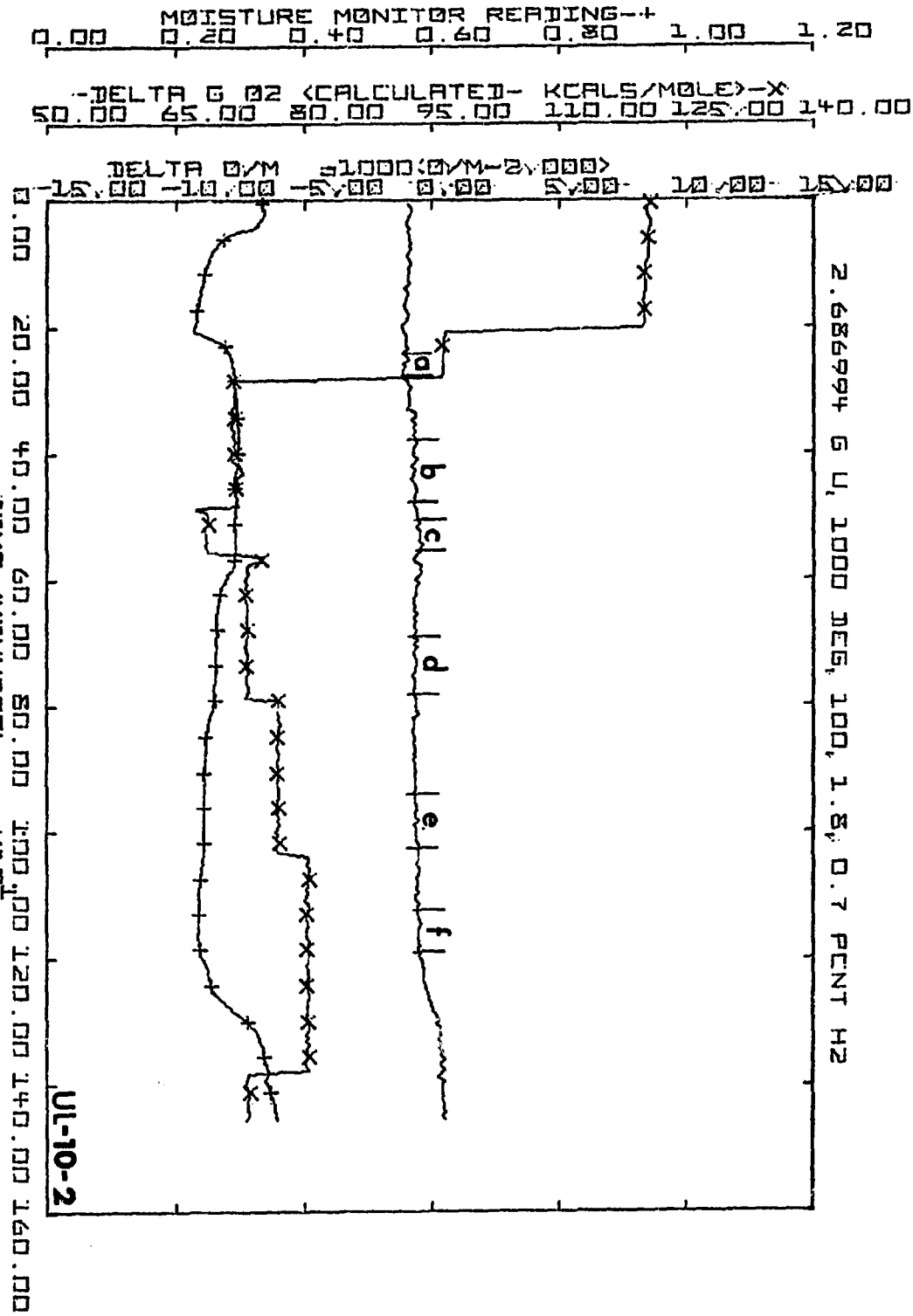
MOISTURE MONITOR READING-+
0.00 0.20 0.40 0.60 0.80 1.00 1.20
-DELTA G 02 (CALCULATED- KCALS/MOLE)-X
50.00 65.00 80.00 95.00 110.00 125.00 140.00
DELTA D/M =1000(D/M-2.000)
-15.00 -10.00 -5.00 0.00 5.00 10.00 15.00
TIME (MINUTES)
0.00 20.00 40.00 60.00 80.00 100.00 120.00 140.00 160.00
XLO
UL-10-2
a
b
c
d
e
f
2.688694 G U, 1000 DES, 1000, 1.8, 0.7 PCNT H2

UL-08-1
2.636994 G U, 800 DEG, 0.15 PCNT H2
a
b
TIME <MINUTES> X10¹
0.00 20.00 40.00 60.00 80.00 100.00 120.00 140.00 160.00
DELTA D/M =1000(D/M-2.000)
-15.00 -10.00 -5.00 0.00 5.00 10.00 15.00
-DELTA G O2 <CALCULATED- KCALS/MOLE>-X
50.00 65.00 80.00 95.00 110.00 125.00 140.00
MOISTURE MONITOR READING-+
0.00 0.20 0.40 0.60 0.80 1.00 1.20

MOISTURE MONITOR READING-+
0.00 0.20 0.40 0.60 0.80 1.00 1.20
-DELTA G 02 (CALCULATED)- KCALS/MOLE)-X
50.00 65.00 80.00 95.00 110.00 125.00 140.00
DELTA 0/M =1000(0/M-2.000)
-15.00 -10.00 -5.00 0.00 5.00 10.00 15.00
TIME (MINUTES)
0.00 20.00 40.00 60.00 80.00 100.00 120.00 140.00 160.00
XIO
UL-08-2
2.686994 G U, 800 DEG, 100, 1.8, 0.7 PCNT H2

APPENDIX D

Plutonium Oxide O/M Zetaplots

The data plotted are:

O/M Ratio, Solid Line, Unmarked

Oxygen Potential, Solid Line, Marked by "X"

Moisture Monitor Reading, Solid Line, Marked by "+"

The plots are coded in the lower right corner as follows:

Two Letters, Pu, specifying plutonium oxide prepared from NBS SRM-949 Pu metal (lot 7).

Two digits specifying nominal temperature x 100°C.

08 = 800°C etc.

One digit signifying a plot sequence number at each temperature.

The bracketed regions of the O/M curves, labeled with lower case letters, delineate regions used to calculate the data listed in TABLE 10.

Pu-13-1
2.225903 G PU 1300 DEG 1.8 O/O H2
DELTA O/M =1000<O/M-2.000>
MOISTURE MONITOR READING-+
-DELTA G O2 <CALCULATED- KCALS/MOLE>-X
TIME <MINUTES>
X10^1
a
b
c
d

MOISTURE MONITOR READING-+
DELTA G 02 <CALCULATED- KCALS/MOLE>-X
DELTA 0/M =1000<0/M-2.000>
2.225903 G PU 1300 DEG 1.8 O/O H2
Pu-13-2
TIME <MINUTES>
X10^1
a
b
c
d
e
f

Pu-12-1
2.225903 G U 1200 DEG 1.8 0/0 H2
DELTA 0/M =1000(0/M-2.000)
-15.00 -10.00 -5.00 0.00 5.00 10.00 15.00
TIME (MINUTES)
0.00 20.00 40.00 60.00 80.00 100.00 120.00 140.00 160.00
X10^1
a
b
c
-DELTA G 02 (CALCULATED- KCALS/MOLE)-X
50.00 65.00 80.00 95.00 110.00 125.00 140.00
MOISTURE MONITOR READING-+
0.00 0.20 0.40 0.60 0.80 1.00 1.20

Pu-12-2
2.225903 G PU 1200 DEG 1.8 O/O H2
MOISTURE MONITOR READING-+
DELTA G O2 <CALCULATED- KCALS/MOLE>-X
DELTA O/M =1000<O/M-2.000>
TIME <MINUTES>
X10^1
a
b
c
d
e

Pu-11-1
2.225903 G PU 1100 DEG 100 0/0 H2
DELTA 0/M =1000(0/M-2.000)
-15.00 -10.00 -5.00 0.00 5.00 10.00 15.00
MOISTURE MONITOR READING-+
0.00 0.20 0.40 0.60 0.80 1.00 1.20
-DELTA G 02 (CALCULATED- KCALS/MOLE)-X
50.00 65.00 80.00 95.00 110.00 125.00 140.00
0.00 20.00 40.00 60.00 80.00 100.00 120.00 140.00 160.00
TIME (MINUTES)
X10
a
b
c
d
e

Pu-11-2
2.225903 G PU 1100 DEG 1.8 O/O H2
DELTA O/M =1000(O/M-2.000)
-15.00 -10.00 -5.00 0.00 5.00 10.00 15.00
TIME (MINUTES) X10^1
0.00 20.00 40.00 60.00 80.00 100.00 120.00 140.00 160.00
a
b
c
d
e
MOISTURE MONITOR READING
0.00 0.20 0.40 0.60 0.80 1.00 1.20
-DELTA G O2 (CALCULATED- KCALS/MOLE)-X
50.00 65.00 80.00 95.00 110.00 125.00 140.00

Pu-10-1
2.225903 G PU 1000 DEG 100 0/0 H2
MOISTURE MONITOR READING-+
-DELTA G @2 <CALCULATED- KCALS/MOLE>-x
DELTA @/M =1000(@/M-2.000>
TIME <MINUTES>
x10^1
a
b
c
d

Pu-10-2
2.225903 G PU 1000 DEG 100 D/D H2
DELTA D/M =1000(D/M-2.000)
TIME (MINUTES) X10^1
DELTA G O2 (CALCULATED- KCALS/MOLE)-X
MOISTURE MONITOR READING-+
a
b
c
d

MOISTURE MONITOR READING-+
0.00 0.20 0.40 0.60 0.80 1.00 1.20
-DELTA G O2 (CALCULATED- KCALS/MOLE)-X
50.00 65.00 80.00 95.00 110.00 125.00 140.00
DELTA O/M =1000(O/M-2.000)
-15.00 -10.00 -5.00 0.00 5.00 10.00 15.00
TIME (MINUTES)
X10
0.00 20.00 40.00 60.00 80.00 100.00 120.00 140.00 160.00
2.225601 G PU 900 DEG 100 PCNT H2
a
b
c
Pu-09-1

Pu-09-2
2.225903 G PU 900 DEG 1.8-100 O/O H2
DELTA O/M =1000(O/M-2.000)
TIME (MINUTES) X10^1
-DELTA G O2 (CALCULATED- KCALS/MOLE)-X
MOISTURE MONITOR READING-+
a
b
c
d
e
f

Pu-08-1
2.225903 G PU 800 DEG 100 PCT H2
DELTA 0/M =1000(0/M-2.000)
-15.00 -10.00 -5.00 0.00 5.00 10.00 15.00
0.00 20.00 40.00 60.00 80.00 100.00 120.00 140.00 160.00
TIME (MINUTES) X10
MOISTURE MONITOR READING-+
0.00 0.20 0.40 0.60 0.80 1.00 1.20
-DELTA G 02 (CALCULATED- KCALS/MOLE)-X
50.00 65.00 80.00 95.00 110.00 125.00 140.00

Pu-08-2
2.225903 G PU 800 DEG 100 PCNT H2
MOISTURE MONITOR READING-+
-DELTA G 02 <CALCULATED- KCALS/MOLE>-X
DELTA 0/M =1000<0/M-2.000>
TIME <MINUTES> X10^1
a
b
c

Pu-08-3
2.225903 G PU 800 DEG 1.8 100 0/0 H2
DELTA 0/M =1000(0/M-2.000)
TIME (MINUTES) X10^1
-DELTA G 02 (CALCULATED- KCALS/MOLE)-X
MOISTURE MONITOR READING-+
a
b
c
d
e
f

APPENDIX E

Solid Solution Uranium-Plutonium Oxide O/M Zetaplots

The data plotted are:

O/M Ratio, Solid Line, Unmarked

Oxygen Potential, Solid Line, Marked by "X"

Moisture Monitor Reading*, Solid Line, Marked by "+"

The plots are coded in the lower right corner as follows:

Three letters, U-Pu, specifying solid solution (U,Pu) oxide prepared from LASL lot UR-1261 U and NBS SRM-949 (lot 7) Pu metals.

Two digits specifying nominal temperature x 100°C.

08 = 800°C etc.

One digit signifying a plot sequence number at each temperature.

The bracketed regions of the O/M curves, labeled with lower case letters, delineate regions used to calculate the data listed in TABLE 11.

---

*Moisture monitor data are ommitted from plots U-Pu-11-1, U-Pu-09-1, and U-Pu-08-1.

U-Pu-13-1
1.746747 G U+PU, 1300 DEG, 0.7 PCNT H2
DELTA G/M =1000<G/M-2.000>
MOISTURE MONITOR READING
-DELTA G O2 <CALCULATED- KCALS/MOLE>-X
TIME <MINUTES>
X10
a
b
c
d
e

MOISTURE MONITOR READING-+
0.00 0.20 0.40 0.60 0.80 1.00 1.20
-DELTA G 02 <CALCULATED- KCALS/MOLE>-X
50.00 65.00 80.00 95.00 110.00 125.00 140.00
DELTA O/M =1000<O/M-2.000>
-6.00 -4.00 -2.00 0.00 2.00 4.00 6.00
1.746747 G U+Pu, 1300 DEG, 100 PCNT H2
TIME <MINUTES>
X10
0.00 20.00 40.00 60.00 80.00 100.00 120.00 140.00 160.00
a
b
c
d
U-Pu-13-2

U-Pu-13-3
1.746747 G U+Pu, 1300 DEG, 1.8 PCNT H2
DELTA O/M =1000(O/M-2.000)
TIME (MINUTES)
X10^1
MOISTURE MONITOR READING
-DELTA G O2 (CALCULATED- KCALS/MOLE)-X
a
b

1.746747 G U+PU, 1200 DEG, 0.7, 100 PCNT H2
U-Pu-12-1
DELTA D/M =1000(D/M-2.000)
TIME <MINUTES>
x10
MOISTURE MONITOR READING
-DELTA G O2 (CALCULATED- KGRLS/MOLE)-x
a
b
c
d
e

U-Pu-11-1
1.746747 G U+PU; 1100 DEG, 0.7-100 PCNT H2
DELTA G/M =1000<G/M-2.000>
DELTA G O2 <CALCULATED- KCALS/MOLE>-X
MOISTURE MONITOR READING-+
TIME <MINUTES>
X10
a
b
c
d
e

U-Pu-10-1
1.746747 G U+PU, 1000 DEG, 0.7-100 PCNT H2
DELTA G/M =1000<G/M-2.000>
TIME <MINUTES>
X10^1
MOISTURE MONITOR READING
-DELTA G 02 <CALCULATED- KCALS/MOLE>-X
a
b
c

U-Pu-09-1
1.746747 G U+Pu, 900 DEG, 0 7, 100 PCNT H2, 02 ELEC.
MOISTURE MONITOR READING-+
0.00 0.20 0.40 0.60 0.80 1.00 1.20
-DELTA G 02 <CALCULATED- KCALS/MOLE>-X
50.00 65.00 80.00 95.00 110.00 125.00 140.00
DELTA 0/M =1000<0/M-2.000>
-6.00 -4.00 -2.00 0.00 2.00 4.00 6.00
0.00 20.00 40.00 60.00 80.00 100.00 120.00 140.00 160.00
TIME <MINUTES>
X10+1
a
b
c

☆ U.S. GOVERNMENT PRINTING OFFICE: 1975—677-343/32